Stony Brook University

DOCK7 interacts with TACC3 to regulate interkinetic nuclear migration and genesis of neurons from cortical neuronal progenitors

A Dissertation Presented

by

YUTING R. YANG

to

The Graduate School

in Partial Fulfillment of the

Requirements

for the Degree of

Doctor of Philosophy

in

Molecular and Cellular Biology

Stony Brook University

August 2012

Stony Brook University

The Graduate School

YUTING R. YANG

We, the dissertation committee for the above candidate for the

Doctor of Philosophy degree, hereby recommend

acceptance of this dissertation.

Linda Van Aelst, Ph.D. – Dissertation Advisor
Professor, Cold Spring Harbor Laboratory

Styliani-Anna E. Tsirka, Ph.D. - Chairperson of Defense
Professor, Department of Pharmacological Sciences

Alea A. Mills, Ph.D.
Professor, Cold Spring Harbor Laboratory

Joshua Dubnau, Ph.D.
Associate Professor, Cold Spring Harbor Laboratory

Glenn Turner, Ph.D.
Associate Professor, Cold Spring Harbor Laboratory

This dissertation is accepted by the Graduate School

Charles Taber
Interim Dean of the Graduate School

Abstract of the Dissertation

DOCK7 interacts with TACC3 to regulate

interkinetic nuclear migration

and genesis of neurons from cortical neuronal progenitors

by

YUTING R.YANG

Doctor of Philosophy

in

Molecular and Cellular Biology

Stony Brook University

2012

The six-layered mammalian neocortex derives from a pseudostratified neuroepithelium by a series of cell divisions of neuronal progenitors, neuroepithelial and radial glial cells. Neurogenesis, a major event in the developing neocortex, relies on the ability of radial glial cells (RGCs) to switch from proliferative self-expanding to differentiative neuron-generating/progenitor self-renewing divisions. However, the molecular mechanisms that control this switch in a correct temporal manner are not well understood. In this thesis, I demonstrated that the DOCK180 family member DOCK7, an activator of Rac GTPases, plays an important role in the regulation of RGC proliferation versus differentiation. Silencing of DOCK7 in RGCs of developing mouse embryos hampers neuronal differentiation and maintains cells as cycling

progenitors. Conversely, DOCK7 overexpression promotes RGC differentiation into basal progenitors and neurons. Using different approaches, including live-cell imaging experiments, I obtained evidence that DOCK7 influences RGC fate and neurogenesis by controlling the apically directed interkinetic nuclear migration (INM) process of RGCs. Importantly, DOCK7 exerts its effects on INM and neurogenesis independently of its GEF activity towards Rac, but instead does so by antagonizing the microtubule growth-promoting function of the centrosome-associated protein TACC3. Taken together, DOCK7 interacts with TACC3 to control INM, as such governing RGC fate and genesis of neurons during cortical development.

Table of Contents

List of Figures

List of Abbreviations

NEs	Neuroepithelial cells
VZ	ventricular zone
SVZ	subventricular zone
CP	cortical plate
PP	preplate
IZ	intermediate zone
MZ	marginal zone
SP	subplate
RGCs	radial glial cells
INM	interkinetic nuclear migration
IPCs	intermediate progenitor cells
BPs	basal progenitor cells
bFGF2	basic fibroblast growth factor-2
MT	microtubule
ap-to-bl	apical to basal
bl-to-ap	basal to apical
DH	Dbl-homology

PH	Pleckstrin-homology
GEF	guanine-nucleotide exchange factor
DHR2	Dock Homology Region 2
DHR1	Dock Homology Region 1
SH3	SRC Homology 3
shRNA	short hairpin RNA
UTR	untranslated region
BrdU	5-bromo-2'-deoxyuridine
PH3	phospho-histone H3
TACC	transforming acidic coiled-coil protein
ASPM	Abnormal spindle-like microcephaly-associated protein
DISC1	Disrupted in schizophrenia 1
MTOC	microtubule organizing center
SGZ	subgranular zone
DG	dentate gyrus
RMS	rostral migratory stream

Acknowledgements

I am heartily thankful to my advisor, Dr. Linda Van Aelst, for her continued encouragement, guidance and support from the initial to the final level, enabled me to make this project possible. Her enthusiasm, inspiration, as well as her academic experience has been invaluable to me. I would like to thank my lab members who provided a stimulating and fun environment, gave great advice and listened to my work through these years that helped me to learn and grow. I am indebted to my committee members, Dr. Stella Tsirka, Dr. Alea Mills, Dr. Josh Dubnau and Dr. Glenn Turner for all their support and advice. Special thanks to Dr. Chia-Lin Wang for collaborating with me to accomplish this fascinating project. I wish to thank Justyna Janas for her support, friendship and all of her help over the years. Lastly, and most importantly, I wish to thank my family in Taiwan. Thanks to my parents, they have been a constant source of love and support. Thanks to my brother, he has always cheered me on. Thanks to my family in law for their continued prayer for my family in the U.S. And great thanks to my husband, my boy and little girl; they have been, always, my pillar, my joy and my guiding light. To them I dedicate this thesis.

Publications

Yu-Ting Yang, Chia-Lin Wang and Linda Van Aelst (2012). DOCK7 interact with TACC3 to regulate interkinetic nuclear migration and cortical neurogenesis. *Nature Neuroscience*. In press.

CHAPTER ONE

Introduction

1.1 Development of neocortex

The cerebral cortex, the outer layer of the cerebrum, is a highly specialized brain region derived from the dorsal telencephalon. It is the major information processing unit of the brain responsible for higher functions from sensory perception and generation of motor commands to cognition, including attention, memory, producing and understanding language, solving problems, and making decisions. The cerebral cortex is a laminar structure consisting of six-layers of postmitotic neurons generated through a strictly regulated sequence of proliferation, differentiation and migration, which are named layer I to layer VI (with VI being the innermost and I being the outermost)[1,2]. (Figure 1.1)

The development of the neocortex commences at a layer composed of proliferating neuroepithelial cells (NEs) that are lining the lateral ventricles, described as ventricular zone (VZ) (Figure 1.2a). The radially orientated NEs make contact with the ventricular lumen and the cerebral pial surface. The first neuronal layer to appear during cortical histogenesis, the preplate, forms above the VZ (Figure 1.2b). The subventricular zone (SVZ) is subsequently formed as a second proliferative layer between the VZ and the preplate. While cortical neurogenesis continues, the newly generated neurons move radially out of the proliferative zones using radial glial processes and infuse themselves into the preplate. These newborn neurons separate the preplate into an outer marginal zone and an inner subplate layer. Between the marginal zone and the subplate is the cortical plate (CP), where new born neurons consequently construct a new laminar architecture[3,4] (Figure 1.2c).

Figure 1.1

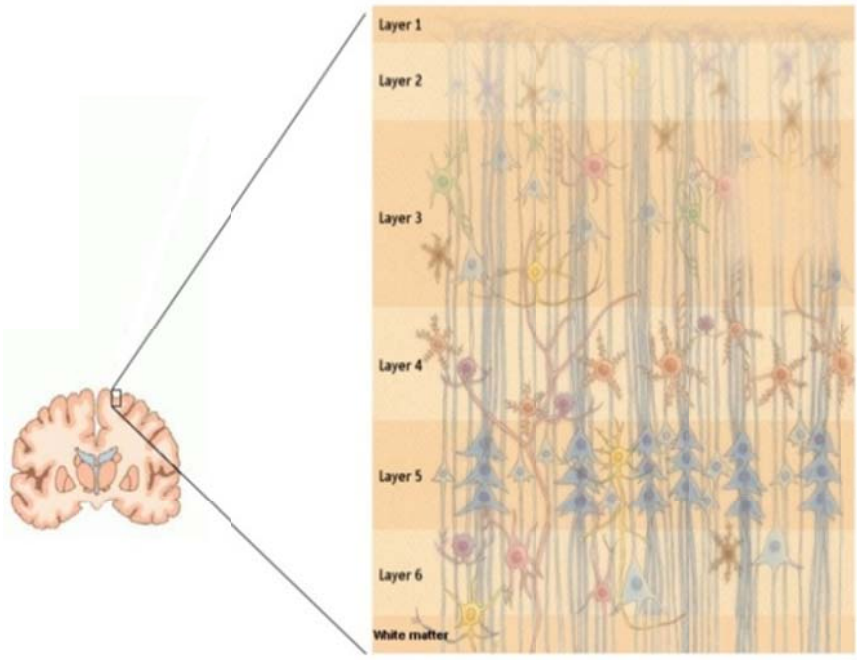

Figure 1.1. The six-layered structure of the cerebral cortex. A schematic view of the cerebral cortex. Cerebral cortex consists of six layers with the outermost being layer 1 and the innermost layer 6. (adapted from T.Hosoya[5])

Figure 1.2

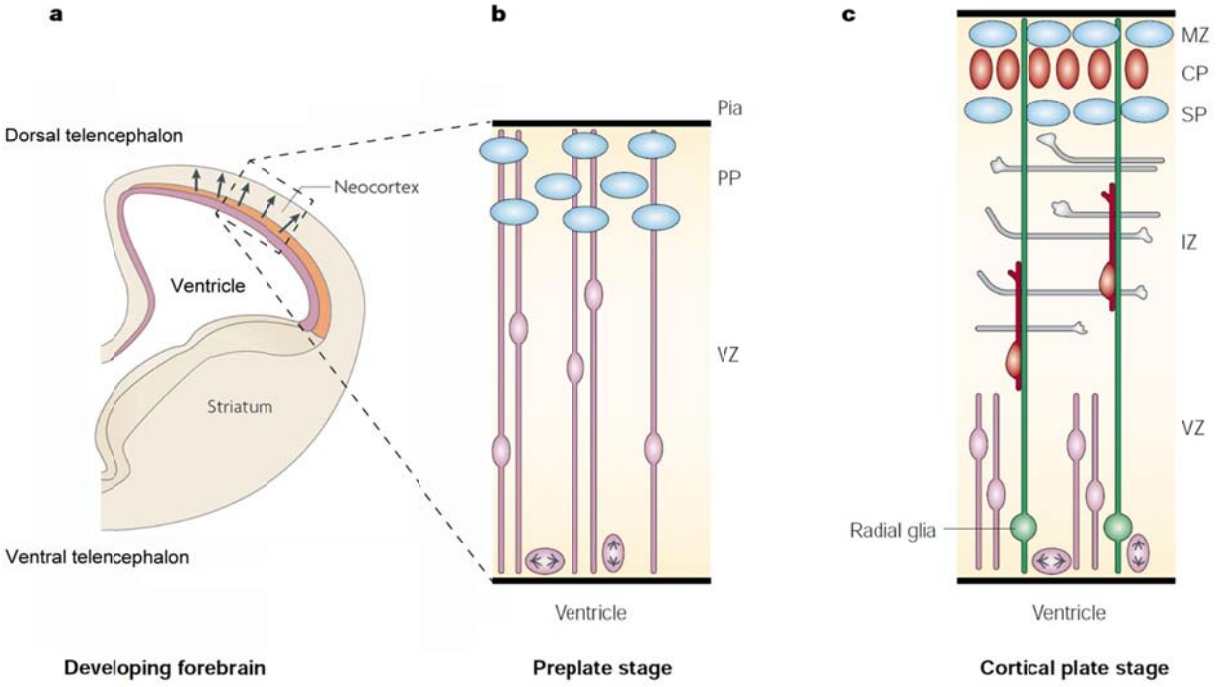

Figure 1.2. Neocortical development. **(a)** A schematic view of a coronal section of mouse cerebral brain Pyramidal neurons generated in the cortical VZ (pink) and SVZ (orange) that migrate radially to the cortical plate (black arrows)(adapted from C. Dehay et al[6]) **(b)** In the dorsal forebrain, neuronal migration begins when the first cohort of postmitotic neurons moves out of the ventricular zone (VZ) to form the preplate (PP). **(c)** Subsequent cohorts of neurons migrate, aided by radial glia, through the intermediate zone (IZ) to split the PP into the outer marginal zone (MZ) and inner subplate (SP). CP, cortical plate (adapted from B.Nadarajah et al[7]).

The newly generated cortical pyramidal neurons derive directly from the radial glial cells in the VZ or indirectly from intermediate progenitors in the SVZ of the dorsal telencephalon[8-11]. These newly differentiated neurons undergo a complex process involving several stringently coordinated stages, including a) cell cycle exit of progenitors, b) the commitment of multi-potent cells to the fate as a neuron, c) the formation of axons and dendrites and d) the migration of nascent neurons from the germinal zone into a particular layer in the cortical plate[12,13]. Of note, they migrate radially along the laminar structure made by radial glia into the underlying cortical plate in a so-called “inside-out” fashion. That is, early-born neurons form inner layers (layer VI and V) and later-born neurons migrate past them to form more outer layers (layer IV to I)[12,14]. By performing time-lapse imaging, several groups have demonstrated that late-born neurons generated in the cortical proliferative zones undergo distinct stages of migration characterized by drastic changes in many aspects, including cell morphology, direction and speed of movement as they migrate[9,11,15].

In the early stage of corticogenesis, the neuroepithelium, a tissue composed of multi-potent cortical progenitor cells, occupies the whole region of the telencephalon. The NEs, like other epithelial cells, are highly polarized along their apical – basal axis. Each of these NEs spans the entire thickness of the epithelium and has a spindle-shape soma with thin apical and basal processes extending to the neural tube lumen (apical side) and the basal lamina, respectively[2,16]. NEs are connected to each other with tight junctions and adherens junctions, largely dependent upon the conserved Par6 polarity complex, at the most apical end of the lateral plasma membrane and they present receptors for the basal lamina component at the basal side of plasma membrane[2,17]. The centrosome of NEs is localized near the apical surface with cilium extending into the ventricular lumen, and microtubules extending basally from the centrosome to the nucleus[18,19]. Two remarkable features of NEs are 1) pseudostratification, which refers to a single layer of cells with their nuclei positioned at various positions along its apical-basal axis resulting in a multilayer appearance, and 2) interkinetic nuclear migration

(INM), which refers to the nuclei of these cells changing position along the apical-basal axis during the progression of cell cycle (see more details in section 1.3)[20-23]. Therefore, the pseudostratified appearance is the consequence of INM. Notably, during development, the NEs undergo symmetric proliferative division to produce two identical self-renewing NEs and later on exponentially amplifying their population to extend the tangential size of the cerebral cortex until the initiation of neurogenesis[24].

Before onset of neurogenesis (around embryonic day 9-10 in mice), NEs transform into neuronal progenitors termed radial glial cells (RGCs) residing at the most apical region of the telencephalon, henceforth referred to as the ventricular zone. The morphology of RGCs is very similar to their precursors. RGCs are highly polarized pseudostratified cells, like NEs, with an apical process extending from their cell body that inserts into ventricular surface. However, the soma of RGC locates only within VZ and its long thin basal process reaches the pial surface throughout the neural layers[25,26]. When development of the neocortex is proceeding, the radial thickness of the telencephalon increases as new born neurons migrate into the cortical plate; the basal process of RGCs extends along with increasing thickness of the neocortex[4]. Akin to NEs, RGCs also undergo INM with migrating along the ap – bl axis during cell cycle progression. Because RGCs and NEs undergo mitosis at the ventricular surface, they are also commonly referred to as apical progenitors (APs). Notably, RGCs are the major type of neuronal progenitors in the developing neocortex which produce most of the cortical pyramidal neurons[2].

Prior to the peak of neurogenesis (around embryonic day 11-13 in mouse), RGCs divide mostly symmetrically and generate two identical daughter cells to amplify the progenitor pool. However, when cortical development start to reach the peak of neurogenesis (around embryonic day 13-18), the RGCs undergo mostly asymmetrical differentiative division to generate two different daughter cells: one is a “self-renewing” radial glial cell retaining its radial fiber while the other is giving rise to either a neuroblast, which then differentiates into a neuron,

or an intermediate/basal progenitor cell (IPC/BP)[9,11,27-29]. The BPs further migrate to the SVZ where they produce via symmetric divisions either two neurons, or much less frequently two BPs. The later subsequently produce 4 neurons. These neurons will establish the superficial layers of the cortex[2,3,10,11](Figure 1.3). Notably, unlike RGCs, BPs do not display apical-basal polarity nor INM[10,15,30,31]. While the new-born neurons migrate away from the VZ/SVZ along the radial glial fibers of the RGCs and build the cortical plate underneath the pial surface, the renewing precursors (APs) remain in the VZ for subsequent divisions[2,32,33](Figure 1.2c).

1.2 Cellular mechanisms controlling progenitor fate/behavior

The production of the precise number of neurons is fundamental for the neuronal development of the neocortex. Abnormalities in the precise number of neurons is associated with several neurological and neuropsychiatric disorders, such as microcephaly, lissencephaly and schizencephaly[34,35]. As mentioned in section 1.1, RGCs divide either symmetrically to generate two RGCs to amplify the progenitor pool or asymmetrically to generate one RGC and one postmitotic neuron or one intermediate progenitor cell (IPC/BP). While newly generated neurons migrate away from the VZ to build the cortical plate, the renewing radial glial progenitor cells remain in the proliferative VZ, which ensure the maintenance of sufficient progenitors to produce later born neurons and glial cells[2,32,33]. Thus, the self-renewability of RGCs must be tightly regulated for the proper development of the neocortex[36]. To date, the cellular mechanism(s) that control self-renewal versus neuronal differentiation are still under intense investigation[2,32,33,37,38]. Recent studies suggest that cellular parameters, including cell polarity, cell cycle kinetics, programmed cell death and interkinetic nuclear migration (INM) influence the balance between neurogenesis and progenitor pool maintenance[6,22,23,39-44].

1.2.1 Apical-basal polarity

Similar to other epithelium cells, the structural layout of the RGCs is orchestrated with adherens junctions at the edge of their apical processes, which are critical for the formation of

Figure 1.3

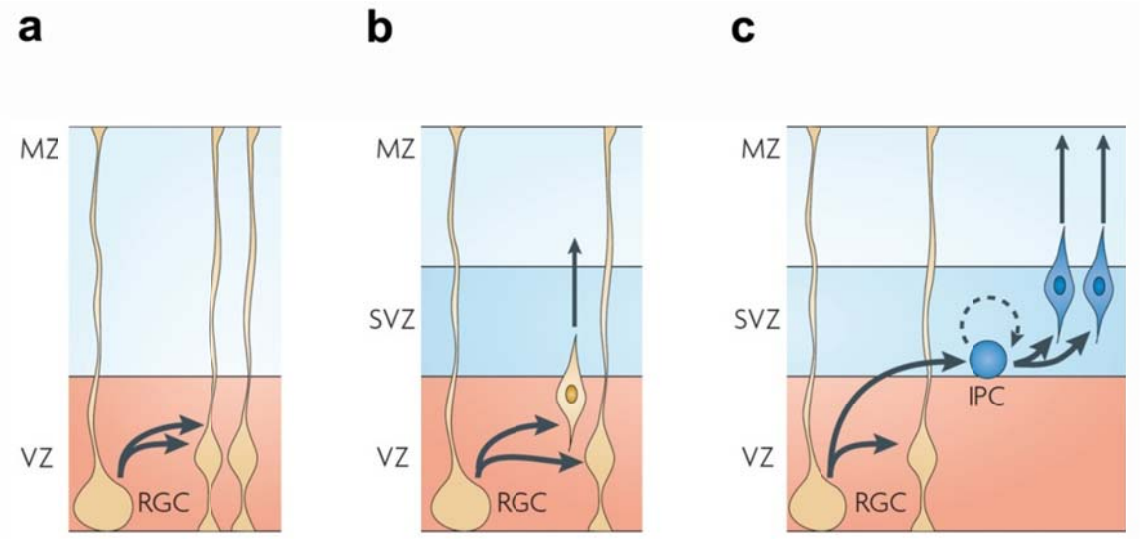

Figure 1.3. The proliferative behavior and progeny of cortical progenitors. Schemas of rodent cortex. Cortical pyramidal neurons are generated from radial glia cells (RGC) and intermediate progenitor cells (IPC). **(a)** RGCs undergo symmetrical divisions in the VZ to expand the progenitor pool at early embryonic stages i.e. around E13. **(b)** RGCs undergo asymmetrical divisions in the VZ to generate one neuron and one self-renewing progenitor. **(c)** Through asymmetrical divisions, RGCs give rise to IPCs that migrate to and divide in the SVZ. IPCs have been reported to undergo mostly neurogenic divisions with a small fraction undergoing symmetrical proliferative divisions (as indicated by the dotted circular arrow) (adapted from C. Dehay et al[6])

the cerebral cortex. The apical-basal polarity and adhesion of RGCs, in large, are depend on cadherin-based adherens junctions with the apical end-feet of adjacent RGCs anchoring to each other at the ventricular surface[2,19]. Several lines of evidence suggest that adherens junction components including Par complex proteins function by controlling cell polarity and thereby influencing progenitor cell fate and behavior[45].

Expression of β-catenin, a signal-transducing adherens junction component, was shown to cause an expansion of the progenitor pool in a transgenic mouse model expressing stabilized β-catenin, which then leads to the production of enlarged brains with dramatic effects on the overall brain architecture[46]. In addition, deletion of *αE-catenin* exclusively in nestin-positive neuronal progenitors in mice leads to more rapid proliferation than those of wild-type mice, resulting in cortical hyperplasia[47].

The Cdc42 GTPase, a Par complex regulator, together with Par3, Par6 and aPKC is found at the apical cell cortex, which is the region underneath the apical plasma membrane, including the adherens junctions, of the developing neocortex. Depletion of *Cdc42* in neural progenitors of mice has been reported to cause several defects, including loss of apical adherens junctions and the Par complex, increased delamination of progenitor cells by loss of apical processes, INM disruption and an overall conversion of the APs to BPs[48]. Similarly, inactivation of aPKCλ during late neurogenesis generates phenotypes as seen in *Cdc42*-null mice[49]. The Par complex proteins, Par-3 and Par-6, have also been shown to promote self-renewing proliferative divisions of APs in the developing neocortex[41,45]. Thus, Cdc42 and the Par complex were suggested to be important to maintain cells in a proliferative state. Taken together, these reports indicate the possibility that those apically-located adherens junction molecules are required to maintain cell polarity and thereby regulate the maintenance of distinct populations of proliferative neural progenitors.

1.2.4 Cell cycle progression

In eukaryotes, the cell cycle can be divided into four consecutive phases: G1, S, G2 (collectively known as interphase) and mitosis (M). Cells grow, accumulate material for mitosis, and replicate DNA during interphase, then enter mitosis to divide into two daughter cells and completely separate by cytokinesis. The transition of each phase is tightly controlled by cyclin-CDK (cyclin-dependent kinase) protein complexes which ensure the proper progression and completion of the previous phase[50].

During cortical development, determination of the precise number of neurons is largely dependent on the rate of cell-cycle progression, all cell cycle length, and the tight regulation of cell-cycle re-entry and exit of cortical progenitors[51]. While proliferative divisions generate two progenies that re-enter the cell-cycle, differentiative divisions result in at least one daughter cell withdrawing from the cell cycle to undergo differentiation. The mode of division is correlated to the length of G1-phase. In fact, the G1 phase is a crucial stage, allowing responses to environmental cues, to determine either commitment to a further round of cell division or withdrawal from the cell cycle (G0) to enter into a differentiation pathway[6,50].

During mouse corticogenesis, the rate of cell-cycle progression is gradually slowing down concomitant with an increase in frequency of differentiative divisions and neuron production as development proceeds. This change in cell-cycle kinetics is mainly due to a lengthening of the G1 phase which has been observed in cortical regions with a higher ratio of neurogenic division such as neocortex[24,52]. In addition, an increase in G1 phase duration has also been observed in cortical progenitors treated with the differentiation promoting factor, neurotrophin 3, while on the other hand treatment with mitogenic factors such as bFGF2 reduced G1 length[53]. Moreover, Cdk4/CyclinD1 was found to regulate the duration of the G1 phase in mouse cortical progenitors. Overexpression of Cdk4/CyclinD1 in the mouse neocortex, which prevents G1 lengthening, was shown to inhibit neurogenesis. Conversely, using

Cdk4/CyclinD1-RNAi to deplete protein expression caused the opposite effects. Specifically, knockdown of Cdk4/CyclinD1 resulted in G1 lengthening and increase in neuron production[40].

1.2.3 Apoptosis

During the development of multicellular organism, cells proliferate vigorously to increase the population and therefore expand the dimension of the organism. Meanwhile, cells are also actively involved in programmed cell death to control the precise number of progeny so as to build a normal size and functional organism[54,55]. The proliferative zone of the neocortex, VZ and SVZ, was shown to have a higher incidence of cell death than other regions of the developing cortex during the period of neurogenesis, which suggested that programmed cell death, or apoptosis, is prominent in the proliferating neural progenitors[56]. Moreover, manipulation of this process can greatly alter cortical size[44,57]. For example, reducing apoptosis in the cerebral progenitor by knockout of caspase 3[58] or caspase 9[59] lead to vast overgrowth and folding of the neocortex.

In addition to the canonical apoptosis pathway, signaling pathways and proteins that are important for cell-fate decision, axon guidance and pattern formation in the nervous system are reported to be involved in controlling the number of progenitor progenies[60-62]. Constitutive activation or attenuation of the Notch signaling pathway, which is required for cell-fate decisions during development by cell–cell interactions[63,64], in VZ progenitors results in an altered cortical size, with an increase and reduction in apoptosis of early neural progenitor cells, respectively[60]. Ephrin A/EphA signaling, which is important for regulating axon guidance and cell migration[65,66], has also been shown to affect apoptosis and in turn to regulate the size of the cortex[61]. Pax6, an evolutionarily conserved transcription factor with crucial roles in morphogenesis, including the embryonic cortex, is reported to be essential for regulating the proliferation of cortical progenitors. Ectopically activating or overexpressing Pax6 inhibits proliferation of cortical progenitors, and causes deregulation of the cell cycle, premature genesis of neurons, and

massive cell death in different progenitor pools[62].

Together, these studies imply that proliferation and apoptosis rates in the embryonic proliferative progenitors, NEs and RGCs, are leg to develop a proper size of the cerebral cortex.

1.3 Interkinetic nuclear migration

Interkinetic nuclear migration (INM), described for the first time 77 years ago, was proposed by Saure who found a tight correlation between the morphologies of the cells and the position of the nucleus relative to the ventricle in the pseudostratified neuroepithelium of pig and chick[21]. As mentioned in section 1.1, this nuclei-moving phenomenon is a hallmark of both NEs and RGCs. It should be noted though that INM is not restricted to neural tissue or limited to vertebrate organisms. In fact, INM has also been observed in the retina and small intestine of vertebrate embryos, as well as the wing disk of Drosophila and the ectodermal layers of C.elegans[67-69].

In the pseudostratified neuroepithelium, the nuclei of NEs change position along the apical-basal axis of the tissue in coordination with cell cycle; however, mitosis occurs exclusively near the ventricular surface at the apical side. Following mitosis, the nuclei of NEs that enter G1 phase move basally away from the apical side of the VZ to the pial surface, where DNA is replicated. Upon completion of S phase, the nuclei migrate back to the ventricular surface during G2 phase to divide in the vicinity of the centrosomes, located in the apical end feet of the NEs[19,70] (Figure 1.4). This movement is repeated at every cell division cycle of NEs until they differentiate to RGCs.

The nuclei of RGCs akin to NEs undergo the above described INM process, with the exception that the distance traveled along the cortical wall is different. They do not travel basally all the way to the pial surfaces, but to the basal most position within the VZ (up to 100 μm)[2,71]. By performing time-lapse imaging in the neocortex, several groups have observed this

oscillatory movement of nuclei among the cycling neuronal progenitor cells in acute slices of embryonic ferret and rodent brains[9,72,73]. Of note, because of the apical location of the nuclei of NEs and RGCs, these cells are also commonly referred to as apical progenitors.

While the functional implications of INM have not been completely elucidated, increasing evidence supports that INM can influence the balance between neurogenesis and progenitor pool maintenance by controlling the exposure time of apical progenitor nuclei to neurogenic versus proliferative signals along the basal-apical axis[20,23,68,74]. In this regard, a high apical and low basal gradient of Notch activity, known to prevent progenitors from differentiating, has been reported in the developing retina of chick and zebrafish[68,74]. These studies suggested that the apical progenitor nuclei encounter less Notch signal when residing at the basal side and thus favoring neurogenic divisions, while nuclei residing more apically are more likely to undergo proliferative divisions. Moreover, perturbing INM in the developing mouse cortex experimentally have been linked to cell fate changes[48,75-77]. For example, perturbation of basal-to-apical (bl-to-ap) INM has been associated with a reduction in apical progenitors and a concomitant increase in basal progenitors and/or neurons[48,75,76]. However, the consequences of the opposite situation, that is, accelerated bl-to-ap INM, on apical progenitor proliferation and genesis of neurons have till our studies not been addressed.

INM implicates dynamic changes in the microtubule (MT) and actin cytoskeleton as well as cytoskeletal and adhesion regulatory molecules[23,78-80]. The cellular machinery that controls INM involves actomyosin- and microtubule-dependent systems[20,23], with the former generally linked to the ap-to-bl leg of INM and the latter to the bl-to-ap leg in the developing rodent cortex[76,77,81-83] (but see ref 84[84]). Ample evidence has shown that 1) microtubule organizing center (MTOC, which is centrosome), 2) the centrosome-emanated MTs, and 3) the motors trafficking along the MTs are key molecular players for this tightly regulated process. As for centrosome, the centrosomal (Cep120) and peri-centrosomal (Hook3) proteins have been

Figure 1.4

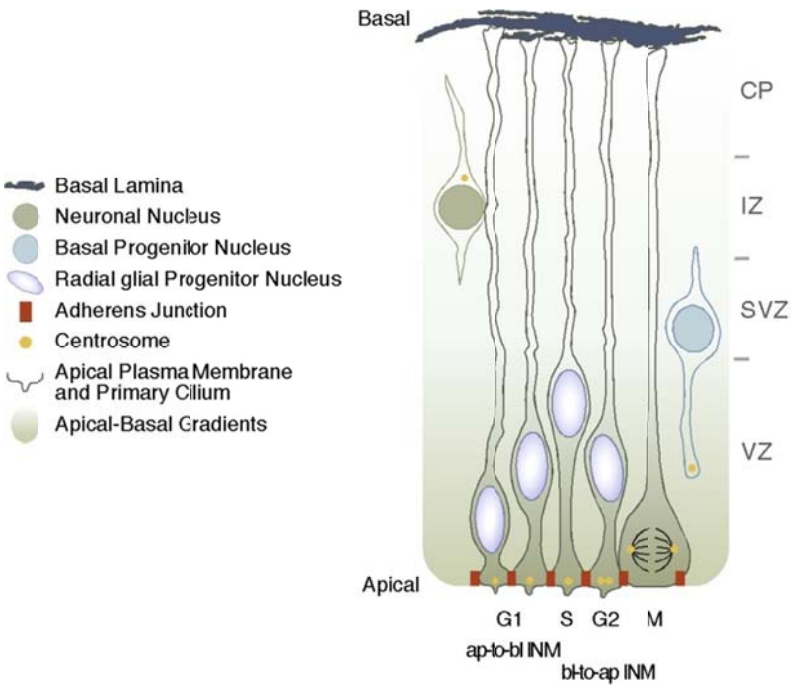

Figure 1.4. Interkinetic nuclear migration (INM) of RGCs. RGCs possess an apical-basal polarity and span the entire cortical wall from the basal lamina to the ventricular (apical) surface. They are coupled by adherens junctions at the apical side and contact the basement membrane at the basal side. The nuclei of RGCs occupy different locations along the apical-basal axis depending on their cell cycle position. After undergoing mitosis at the apical side of the neuroepithelium, the nuclei translocate basally, away from the ventricle surface, as they pass through G1, and replicate their DNA (S-phase) in the basal part of the ventricular zone (VZ). After S-phase completion, G2 phase nuclei migrate to the apical side and then undergo mitosis close to the ventricular surface.

found to be important in promoting the bl-to-ap movement. Knockdown of Cep120 and Hook3 has been shown to halt the nuclei of the apical progenitors at basal positions. This was associated with an increase in neuron production at the expense of progenitors[75,76]. In addition, the apical positioning of centrosome in apical progenitors was reported to be important for proper INM[71]. In particular, centrosomes of the apical progenitors in the *Pax6-null* mice have been shown to frequently change their positions during INM, resulted in abnormal bl-to-ap INM and ectopic division of RGCs[71]. Concerning the role of the MTs emanating from the centrosomes, the transforming acidic coiled-coil proteins (TACCs), which are necessary for the integrity of MT by promoting the growth of MTs and anchorage of MTs to the centrosome, were also shown to affect bl-to-ap INM[76]. In particular, knockdown of TACCs as describe previously results in a ectopic division of RGCs and concomitant with an increase in neuron production at the expense of progenitors[76]. Regarding motor proteins, a minus-end-oriented dynein associated protein called Lis1 has been reported to facilitate the bl-to-ap INM, by coordinating the movement of nuclei at bl-to-ap direction[81,85]. NudC, a regulator of dynein, is also required for the bl-to-ap nuclear migration in the rat neocortex[86]. Finally, more recently, a plus-end-directed kinesin called Kinesin 3 was identified to move the nucleus in an opposite direction, i.e. ap-to-bl, during INM[84]. Even though most of the above studies point to the importance of centrosomal proteins in INM and maintenance of the progenitor pool, little is known, however, about their regulation in these events.

1.4 DOCK180 family members

1.4.1 DOCK180 family

During my Ph.D. studies, I investigated the role of DOCK7, a member of the DOCK180-related superfamily of proteins (also referred to as CZH proteins), in cortical neurogenesis. The DOCK180 superfamily is evolutionary conserved and has homologues in Drosophila, C. elegans, D. discoideum, A. thaliana and S. cerevisiae[87]. In mammals, 11 of DOCK180 family members

have been identified designated as DOCK1 (also known as DOCK180) through DOCK11, which have been further classified into four classes based on the sequence similarity and domain organization. These four classes are: DOCK-A subfamily (DOCK1, DOCK2 and DOCK5); DOCK-B subfamily (DOCK3 (also known as MOCA) and DOCK4); DOCK-C subfamily (also called Zir family) (DOCK6, DOCK7 and DOCK8); and DOCK-D subfamily (also called Zizimin family) (DOCK9, DOCK10 and DOCK11)[88,89](Figure 1.5). DOCK180 was the first identified family member. It was identified as a 180-kDa c-Crk-interacting protein and subsequently shown to be involved in the reorganization of the actin cytoskeleton in a small GTPase depending manner[90-92]. A follow-up biochemical study demonstrated that DOCK180 possess Rac-specific guanine-nucleotide exchange factor (GEF) activity, despite the fact it lacks a typical tandem Dbl-homology and Pleckstrin-homology (DH-PH) catalytic domain found in canonical Rho-GEFs[87,93]. Instead, as further discussed below, DOCK180 contains a DOCK Homology Region 2 (DHR-2) domain that catalyze the exchange of GDP for GTP on Rac[87,88]. This domain is conserved among all DOCK180 family members, acting on Rac and /or Cdc42. Hence the DOCK180 family of proteins emerged as a novel class of Rho-GEFs.

1.4.2 Role of GTPases and GEFs

Rho family members, including Rac, Cdc42 and RhoA, belong to the Rho subfamily, which constitutes a branch of the Ras superfamily of small GTPases. Small GTPases are low molecular weight GTP binding proteins which function as binary switches by cycling between an active GTP-bound state and an inactive GDP-bound state. The transition between these two forms is tightly regulated by different regulators[94], including GEFs (GDP/GTP exchange factors, positive regulators), GAPs (GTPase activating proteins, negative regulators) and GDIs (GDP dissociation inhibitors) [93,95,96]. GEFs promote the generation of active GTPases by facilitating the intrinsic slow exchange reaction of the GDP-bound GTPase with free cytoplasmic GTP. It is only in their GTP-bound form that the small GTPases interact with their effector proteins, thereby

Figure 1.5

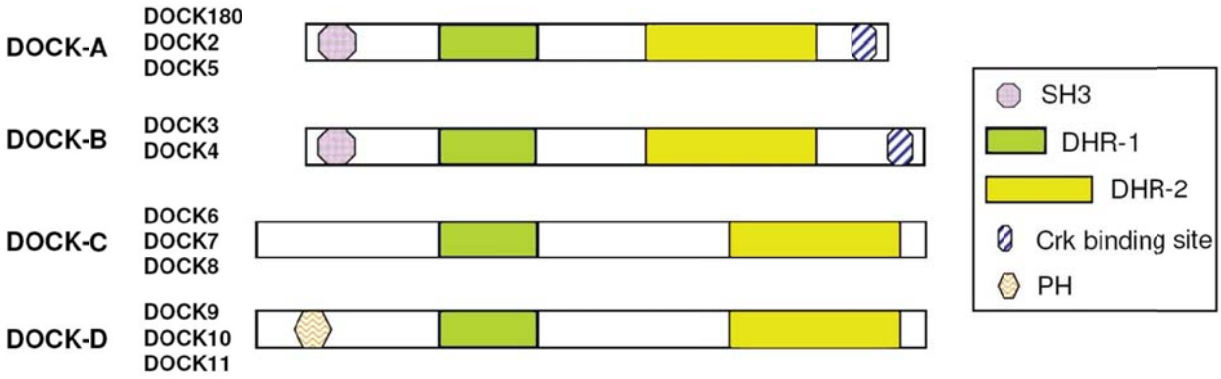

Figure 1.5. Schematic view of DOCK180 family.

controlling many different cellular processes, including cytoskeletal (microtubule and actin) rearrangements, cell mobilization, cell-cell and cell-ECM adhesions, gene transcription and cell viability[94,97]. Importantly, these various cellular processes largely depend on the spatial-temporal regulation of the GTPase activity controlled by different GEFs and GAPs. It should be noted, however, we found the GEF activity of DOCK7 does not involve cortical neurogenesis.

1.4.3 DHR1 and DHR2 motifs

All members of DOCK180 family share two evolutionarily conserved domains, named DOCK Homology Region-1 (DHR-1) and DOCK Homology Region-2 (DHR-2)[87,98](Figure 1.5). Similar to the DH-PH domain-containing GEFs, the proteins containing a DHR-2 domain interact with nucleotide-free Rho GTPases, reflecting an intermediate stage of the reaction that causes the exchange of GDP for GTP on the GTPase[98-100]. The DHR-2 domains of DOCK-A (DOCK1, 2 and 5) and DOCK-B (DOCK3 and 4) have been found to bind and activate specifically Rac[89,101]; DOCK9, 10, and 11 (DOCK-D subfamily) were reported to bind and activate exclusively Cdc42[98,102], while members of the DOCK-C class, DOCK6, 7 and 8, were reported to act on GEFs for both Rac and Cdc42 [100,103,104]. Recently, the crystal structure studies revealed the molecular basis for DOCK-GTPase specificity by comparing the DHR2 domain between DOCK2 and DOCK9[105,106]. $DOCK2^{DHR2}$ and $DOCK9^{DHR2}$ exhibit similar tertiary structures. However, the key determinants of selectivity of Cdc42 and Rac for their cognate $DOCK^{DHR2}$ are a Phe or Trp residue within β3 (residue 56) and a divergent residue with β2 at position 27 of the GTPases. DOCK proteins, therefore, select their cognate GTPases through recognition of structural differences within the β2/β3 strands[105]. Deletion of the DHR-2 domain in DOCK180 has been shown to abolish its ability to activate Rac and to promote cell migration and phagocytosis, highlighting the importance of this domain for the function of DOCK180[87,107]. Similarly, deletion of this domain in a member of DOCK180 family members has been shown to affect their function (see further section 1.4.4, below).

The DHR-1 domain is located N-terminally to the DHR-2 domain in all DOCK180 family members[87,98]. The amino acid sequence of DHR-1 for several DOCK180 family members shows a weak homology to the C2 domain, a well characterized lipid-binding domain[87]. In the case of DOCK180, DOCK2 and DOCK4, this domain has been shown to specifically interact with phosphatidylinositol-3,4,5-triphosphate (PtdIns(3,4,5)P_3) lipids at the leading edge of cultured cells in a phosphatidylinositol 3-kinase (PI3K)-dependent manner[108-110]. Importantly, these studies indicated that deletion of the DHR1 domain abolishes Rac-dependent cell elongation and migration. Thus, DOCK-Rac signaling is spatially controlled by the DHR-1 domain, while Rac activation is regulated by the DHR-2 domain, thereby causing productive Rac signaling. In the case of DOCK7, it remains to be seen whether its DHR1 domain binds to PtdIns(3,4,5)P_3 lipids; however, based on the sequence homology this is likely to be the case.

Notably, besides the DHR1 and DHR2 domain, little sequence homology is observed throughout the rest of the protein sequences. In case of DOCK-A and DOCK-B family the presence of an SRC Homology 3 (SH3) domain is observed; the latter is however absent in DOCK-C and DOCK-D family members. The N-terminally located SH3 domain was shown to have intramolecular interaction with the C-terminal DHR2 domain to mediate the autoinhibition of GEF activity within DOCK proteins[111].

1.4.4 Biological functions of DOCK180 Family members

Over the past few years, an increasing numbers of studies on DOCK180 family members have been published. These reports revealed that this superfamily regulate several important and diverse biological processes. A brief summary of a few of them is provided below.

DOCK180 is ubiquitously expressed except for lymphocytes. Studies in mammalian cells suggest that DOCK180 functions as a regulator of Rac in response to integrin activation to control actin cytoskeletal remodeling, cell spreading and migration[87,91]. Moreover, DOCK180

was more recently demonstrated to play an essential role in mouse embryogenesis. *Dock180-null* embryos display a dramatic reduction in skeletal muscle tissues due to a failure in myoblast fusion[112].

DOCK2, on the other hand, is selectively expressed in hematopoietic cells and knockout DOCK2 mice display defects in lymphocyte migration and defective Rac signaling in response to chemokine stimulation. Subsequent studies further established an important role for DOCK2 in lymphocyte development, homing, activation, and migration/recirculation processes[113-115].

DOCK3, which is highly expressed in neurons, has been shown to regulate N-cadherin-dependent cell-cell adhesion and neuronal morphology[116]. DOCK3 knockout mice have central axon dystrophy and impaired sensorimotor function, which appears to be mainly due to altered Rac activation and actin organization in cortical neurons[117]. In addition, the disruption of the *DOCK3* gene in humans has been linked to attention-deficit hyperactivity disorder (ADHD)[118].

Dock4 was initially identified from the selected homozygous genomic deletions in the mouse NF2 and TP53 tumor model and had been shown to possess tumor suppressor properties both *in vitro* and *in vivo*[119]. More recently, it was found that DOCK4 is highly expressed in hippocampal neurons of developing rat brain and shown to regulate dendritic morphogenesis likely via the activation of Rac[120].

The function of DOCK5 was initially linked to myofiber development[112]. More recent studies further indicated that DOCK5 also play a role as a regulator of osteoclast function and a potential novel target to develop antiosteoporotic treatments[121].

Thus far little is known about the function of DOCK6. A recent study implicated DOCK6 in neurite out-growth in mouse N1E-115 neuroblastoma cells in a Rac/Cdc42 dependent manner[100]. Interestingly, a *DOCK6* mutation in humans was recently linked to Adams-Oliver syndrome (AOS), which is characterized by a combination of aplasia cutis congenita (ACC) and

terminal transverse limb defects (TTLD). Cells of patients with this DOCK6 mutation displayed a defective actin cytoskeleton, suggesting that DOCK6 may exert its effects via the activation of Cdc42 and Rac1 and subsequently actin remodeling[122].

DOCK8 was initially identified as a Cdc42 interacting protein in a yeast two-hybrid screen, and suggested to play a role in the organization of filamentous actin[123]. In humans, DOCK8 has been associated with lung cancer, mental retardation and developmental defects[124,125], and more recently, DOCK8 has been shown to play an essential role in humoral immune responses. In particular, DOCK8 appears to be critical for the formation of the B cell immunological synapse and is essential for T-cell survival and $CD8^+$ T-cell memory[126-128].

DOCK9, also called Zizimin-1, was first shown to promote filopodia formation in fibroblasts cells via the interaction and activation of Cdc42 through its DHR2 domain[98]. Subsequently, DOCK9 was found to play a role in dendrite development of rat hippocampal neurons, again in Cdc42 dependent manner[129].

By screening a siRNA library targeting GEFs for Rho-family GTPases, DOCK10 was identified as a key player in amoeboid and mesenchymal movement and tumor cell invasion in a three-dimensional environment. DOCK10 promotes melanoma cell invasion through Cdc42 signaling, which is novel from the canonical Rho and/or Rac-dependent mesenchymal movement in this type of tumor[130]. In addition, DOCK10 was found to be preferentially expressed in lymphocytes and shown to be upregulated upon interleukin-4 (IL4) treatment in chronic lymphocytic leukemias (CLLs), thereby connecting IL4 signaling to small Rho GTPase function in B cells[131]. While the mRNA of DOCK11 was found to be mainly expressed in peripheral blood (PB) leukocytes[131], its biological function remains, however, uncharacterized.

1.4.5 Studies on DOCK7

DOCK7 was initially identified in the Van Aelst lab as a novel upstream regulator of Rac GTPases in a yeast two-hybrid screen using a human fetal brain cDNA library and the dominant

negative mutant form of Rac1 (Rac1N17) as bait[132]. Dr. Uchida, a former postdoctoral fellow in the Van Aelst laboratory, subsequently showed that Rac is activated by DOCK7 and that its DHR-2 domain is important for this activation. DOCK7 is highly expressed in major regions of the brain, including hippocampus and cortex, during early stages of development. Importantly, they showed that the protein is asymmetrically distributed in unpolarized hippocampal neurons and selectively expressed in the axon. DOCK7 was then shown to play a critical role in the early steps of axon formation in cultured hippocampal neurons. In particular, knockdown of DOCK7 abolishes axon formation, while ectopic expression of DOCK7 triggers the formation of multiple axons. Finally, Uchida et al provided insight into the underlying mechanism. They found that through local Rac activation, DOCK7 mediates the laminin-induced phosphorylation (at Ser16) and inactivation of the MT-destabilizing protein stathmin/Op18 and that this event is important for the development of the axon[103,133,134](Figure 1.6). Thus, these findings unveiled a novel pathway linking DOCK7, a GEF for Rac GTPases, to a microtubule regulatory protein, stathmin, and highlighted the concept that spatially controlled regulation of MT network is crucial for the formation of the axon and the polarization of the neuron.

Other than its role in axon formation, DOCK7 was more recently reported to play a role in the peripheral nervous system (PNS), namely Schwann cells[104,135]. Schwann cells are the principal glia of the PNS. During mid-embryonic to postnatal developmental stage, Schwann cells proliferate, migrate, and ultimately undergo a number of morphological changes to form a myelin sheath, which wraps around axons of motor and sensory neurons. DOCK7 was found to promote ErbB2-induced Schwann cells migration. In particular, ErbB2 was shown to trigger the phosphorylated of DOCK7 on Tyr-1118 residue, which lead to the activation of DOCK7 GEF activity towards Rac/Cdc42 and subsequent activation of c-JNK kinase.

During my Ph.D studies, I extended previous studies of the Van Aelst Lab to investigate the role of DOCK7 in cortical neurogenesis. In chapter two, I describe the evidence we obtained

Figure 1.6

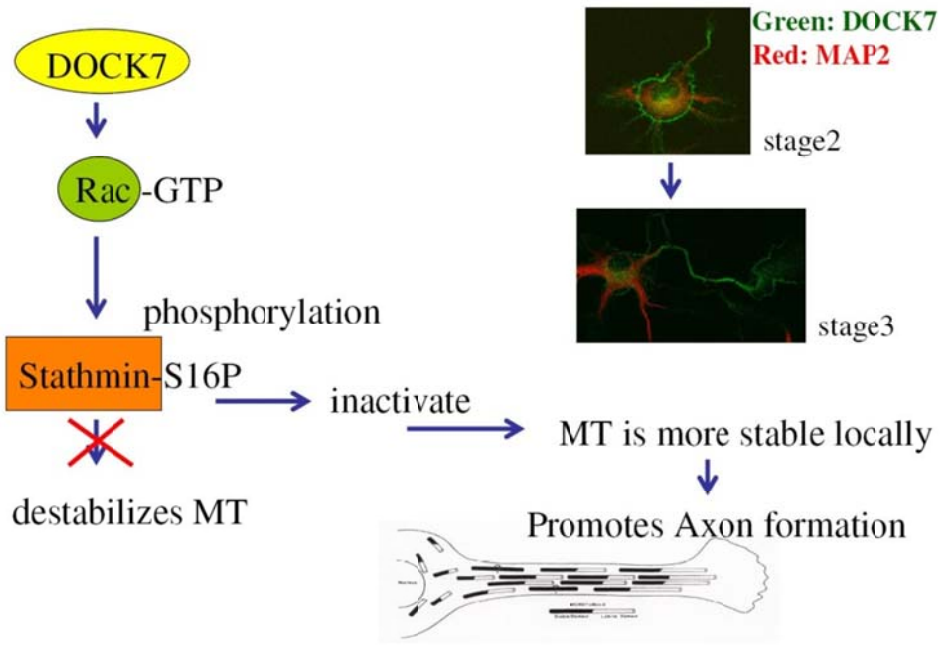

Figure 1.6 DOCK7 is important for priming one neurite to become the axon in developing hippocampal neurons[103].

for a cortical role for in controlling the genesis of neurons from cortical progenitors. The cellular mechanism as to how DOCK7 exerts its function in cortical neurogenesis, which is interkinetic nuclear migration (INM), is described in chapter three. In chapter four, I describe DOCK7's interacting partner--TACC3, a centrosome- and microtubule-associated protein, and the molecular mechanism as to how the DOCK7-TACC3 interaction controls the INM and neurogenesis. In the final chapter, I summarize all my studies and discuss them in the context of future studies. These studies have resulted in a publication in Nature Neuroscience: "DOCK7 interact with TACC3 to regulate interkinetic nuclear migration and cortical neurogenesis;
Yu-Ting Yang, Chia-Lin Wang and Linda Van Aelst; *Nature Neuroscience*. 2012; In press".

CHAPTER TWO

DOCK7 plays an important role in regulating progenitor proliferation versus neuronal differentiation during cortical development

2.1 Introduction

Previous studies in the Van Aelst laboratory demonstrated a critical role for DOCK7 in the development of the axon and establishment of axon-dendrite polarity of primary cultured hippocampal neurons and that it does so by regulating microtubule growth in the nascent axon through Rac activation and subsequent inactivation of stathmin/Op18, a microtubule-destabilizing protein[103]. These studies were performed in a two-dimensional tissue culture setting, where neurons resided in the presence of relatively few external cues, in contrast to an *in vivo* setting, where neurons are generated within a highly oriented three-dimensional neuroepithelium exposed to a rich environment of cues. Hence, the initial goal of my thesis study was to monitor neuronal polarization during the migration of newborn developing neurons within an intact brain structure and establish DOCK7's role in this process. To this end, I decided to focus on embryonic neocortex as the process of nascent neuron migration in the developing neocortex has been intensively studied and well documented[7,15]. I first examined the expression levels and distribution of DOCK7 in the developing neocortex. As detailed in section 2.2.1, we found that DOCK7 is expressed in both neurons and neuronal progenitors at the developing neocortex. In order to manipulate DOCK7 levels, I next implemented the *in utero* electroporation technique in the lab, of which a brief description is given below.

The *in utero* electroporation methodology was initially developed by Dr. Tabata and colleagues[136] (Figure 2.1). This method involves the injection of plasmids coexpressing proteins or short hairpin RNAs (shRNA) of interest with a fluorescent marker protein (e.g. EGFP or dsRed) into the lateral ventricle of embryonic mouse brain, followed by the delivery of electric pulses to achieve efficient transfection of plasmids into the brain. The advantage of this method is that it is a spatial and temporal dependent transfection. Spatially, the site of transfection can be manipulated by changing the direction of electroporation for gene targeting into specific regions of brain[137]. Temporally, transfection can be done at early or late neocortical developmental stages to label deeper or upper layer neurons, respectively. In this dissertation, constructs co-expressing shRNA or cDNA of interest together with a fluorescent marker protein were introduced into VZ cells of mouse embryonic brains at E13.5 by placing the electrodes at about 30°- 60° from the brain's horizontal plane so as to direct the current and DNA transfection towards the VZ. In brief, timed pregnant CD-1 mice at E13.5 were anesthetized and subjected to abdominal incision to expose the uterine horns. Approximately 1 μl of plasmid solution was injected into the lateral ventricle of each embryo with a pulled-glass, beveled, capillary tube. The head of each embryo was placed between custom-made tweezer electrodes, and electroporation was achieved with five 35 V pulses of 50 msec at 950-msec intervals. The uterine horns were then repositioned into the abdominal cavity and the abdominal wall and skin were sutured. The pregnant mice were recovered and embryonic brains were analyzed at indicating time points.

I then employed the above *in utero* electroporation method with as goal to assess DOCK7's role in the polarization of newborn cortical neurons. Interestingly, I observed that knockdown of DOCK7 resulted in accumulation of transfected progenitor cells in the VZ/SVZ, suggesting a potential role for DOCK7 in the genesis of neurons from progenitor cells. This finding prompted us to examine in detail the involvement of DOCK7 in cortical progenitor

Figure 2.1

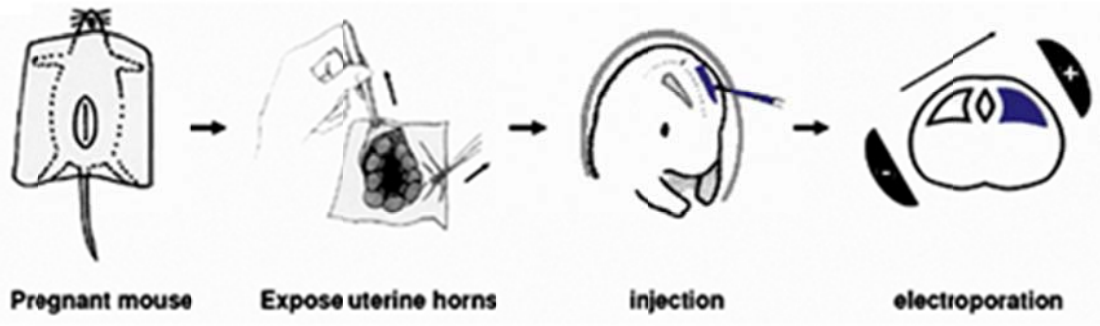

Figure 2.1. Schematic representation of *in utero* electroporation system. The DNA solution was injected into the lateral ventricle through the uterine wall with a glass micropipette. The DNA-injected embryos, with the surrounding uterus, were held by forceps-type electrodes and received electrical pulses.

proliferation, differentiation and neurogenesis in the developing neocortex; the results of which are described below.

2.2 Results

2.2.1 Expression pattern and subcellular localization of DOCK7 in the developing neocortex

To assess the role of DOCK7 during cortical development, I began by examining its expression pattern and distribution in the mouse developing cortex. Western blot analysis of cortical lysates from developing embryonic and postnatal stages showed that DOCK7 is expressed as early as embryonic day 11 (E11), and that expression persists until at least postnatal day 3 (P3), implying that DOCK7 is expressed during active neocortical neurogenesis (Figure 2.2a). To determine the spatial expression pattern(s) of DOCK7 in the developing cerebral cortex, I performed immunohistochemistry using affinity-purified DOCK7 antibody[103] on cryosections of mouse brains around the onset of neocortical neurogenesis (E9.5 and E10.5) and at E13.5. DOCK7 immunoreactivity was undetectable at E9.5 and weak at E10.5 in the nestin-positive neuroepithelial cells (Figure 2.2b). Interestingly, DOCK7 expression was relatively high at E13.5 in Tuj1-positive neurons in cortical plate and nestin-positive VZ progenitors (Figure 2.2b and 2.3a). This observation suggested that onset of DOCK7 expression correlates with the onset of neurogenesis.

Noteworthy, the immunofluorescence of DOCK7 in the VZ of E13.5 cortices was particularly strong at the ventricular (apical) surface (Figure 2.3a), where centrosomes of APs reside[19,42,76]. Of note, centrosomes play key roles in the nucleation, anchorage and organization of microtubules, as well as in the regulation of cell cycle progression, cell polarization and ciliogenesis; all these events are critical for the proper development of the neocortex[138-142]. Upon closer examination of the apical endfeet of nestin-positive progenitors, I observed an

Figure 2.2

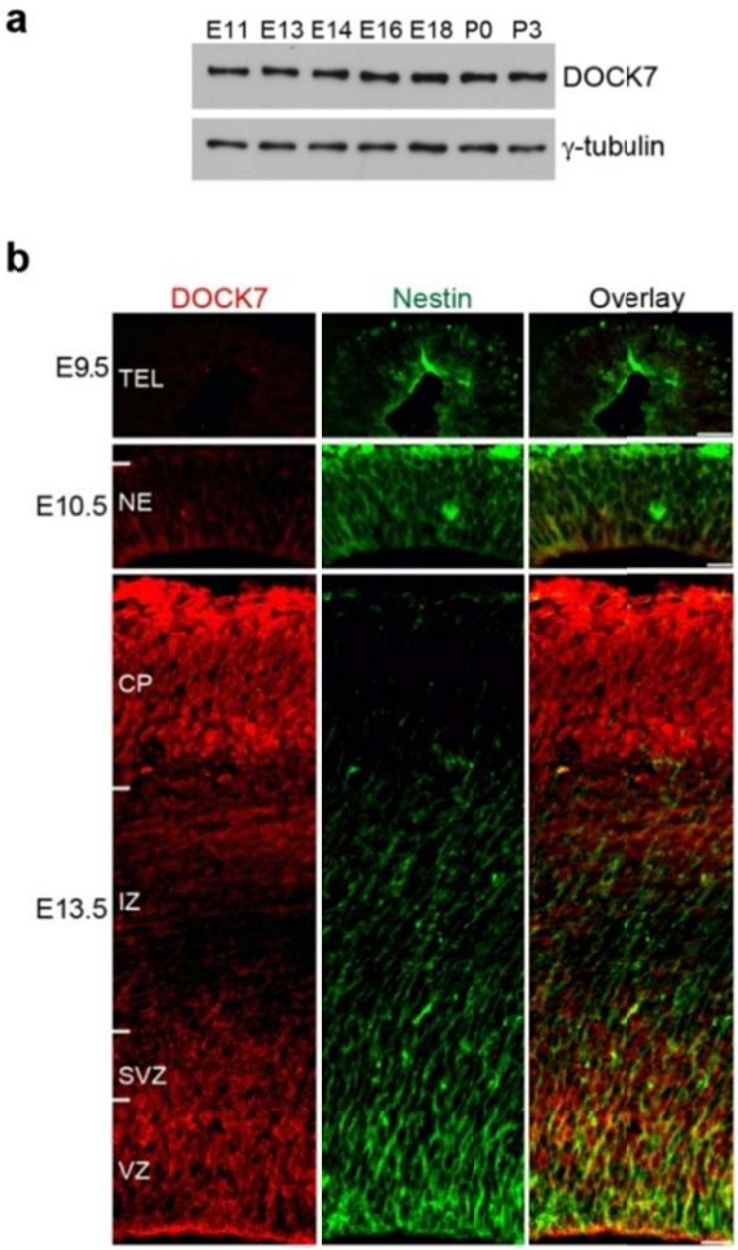

Figure 2.2. Expression and distribution of DOCK7 in the developing mouse cortex. (a) DOCK7 levels in cortical lysates at different developmental stages. γ-tubulin was used as a loading control. **(b)** DOCK7 expression in the developing neocortex at E9.5, E10.5, and E13.5. Horizontal cryosections of whole mouse embryos (E9.5 and E10.5) or coronal cryosections of mouse brains (E13.5) were immunostained for DOCK7 (red) and neural stem/progenitor marker nestin (green). Neurogenesis in the neocortex of mice starts at around E10.5. TEL, telencephalon; NE, neuroepithelium; VZ, ventricular zone; SVZ, subventricular zone; IZ, intermediate zone; CP, cortical plate. Scale bars, 20 μm.

Figure 2.3

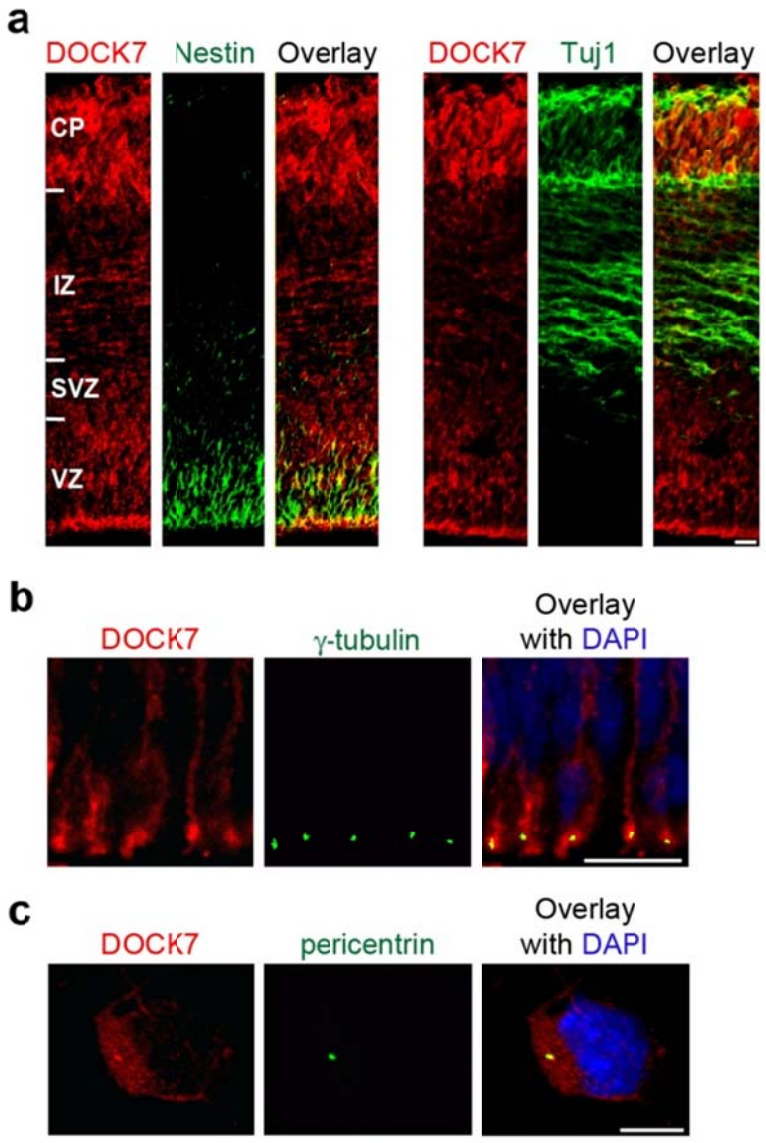

Figure 2.3. Subcellular localization of DOCK7 in the developing mouse cortex. (a) Coronal cryosections of the neocortex at E13.5 immunostained for DOCK7 (red) and neural stem/progenitor marker nestin (green, left panels) or neuronal marker class III β-tubulin Tuj1 (green, right panels). VZ, ventricular zone; SVZ, subventricular zone; IZ, intermediate zone; CP, cortical plate. **(b)** Coronal brain slices of the neocortex at E13.5 immunostained for DOCK7 (red) and centrosomal marker γ-tubulin (green), and counterstained with DAPI (blue). An enlarged view of the apical endfeet of VZ progenitors is shown. **(c)** Cultured cortical progenitors isolated from E13.5 neocortices immunostained for DOCK7 (red) and centrosomal marker pericentrin (green), and counterstained with DAPI (blue). Scale bars: 15 μm in a; 10 μm in b; 5 μm in c.

overlapping staining of DOCK7 with the centrosomal marker γ-tubulin, suggesting the presence of DOCK7 at the centrosome (Figure 2.3b). To further verify this, I examined the subcellular localization of DOCK7 in cultured cortical progenitors prepared from E13.5 mouse cortices. While DOCK7 fluorescence was detectable throughout the cytoplasm, an intense signal was distinctive at the centrosome, where DOCK7 colocalized with the centrosomal marker pericentrin (Figure 2.3c). Thus, these data confirm the presence of DOCK7 at the centrosome in cortical progenitors.

2.2.2 Altered DOCK7 levels affect VZ progenitor proliferation *in utero*

Next, I asked whether DOCK7 affects progenitor proliferation in the embryonic mouse neocortex. To approach this, a vector that expresses a shRNA targeting the 3'-untranslated region (UTR, Dock7#2) of mouse *DOCK7* mRNA[103] was used to reduce DOCK7 expression levels in the mouse neocortex via *in utero* electroporation. Knockdown efficiency in cortical progenitors was verified before the initiation of the functional studies. Western blot analysis showed that Dock7#2 shRNA significantly reduced DOCK7 levels in cortical progenitor cells, whereas a control shRNA (scr#1) did not have such an effect (Figure 2.4). Notably, DOCK6 levels were not affected upon DOCK7 knockdown and DOCK8 expression was not detectable in cortical progenitors; these proteins are most closely related to DOCK7 (Figure 2.5).

The Dock7#2 or scr#1 shRNA construct, together with an EGFP-NLS (nuclear localization signal) expressing plasmid, was then introduced into E13.5 embryonic mouse brains by *in utero* electroporation, and BrdU was administered by intravenous injection at E15.5. BrdU, an analogue of thymidine, can be incorporated into the newly synthesize DNA in substitution for thymidine during the S phase of cell cycle. Embryonic brains were fixed 2 hours following BrdU injection, immunostained, and analyzed by confocal microscopy. I found that the percentage of BrdU-positive progenitors in the VZ was significantly higher in the Dock7#2 shRNA group than in the scr#1 shRNA group (Figure 2.6a,c). Rescue experiments using DOCK7 cDNA that lacks

Figure 2.4

Figure 2.4. Knockdown of DOCK7 levels in cortical progenitors using RNA interference (RNAi). Western blot of total lysates from cultured cortical progenitors isolated from E13.5 mouse cortices transfected with indicated plasmids shows effective knockdown of endogenous DOCK7 levels by Dock7#2 shRNA (Dock7#2), but not control scr#1 shRNA (src#1), and successful replacement with RNAi-resistant FLAG-DOCK7-WT [blotted with anti-DOCK7 antibody (top panel), anti-FLAG antibody (middle panel) and anti-γ-tubulin antibody as a loading control (lower panel)]. Asterisk indicates non-specific band.

Figure 2.5

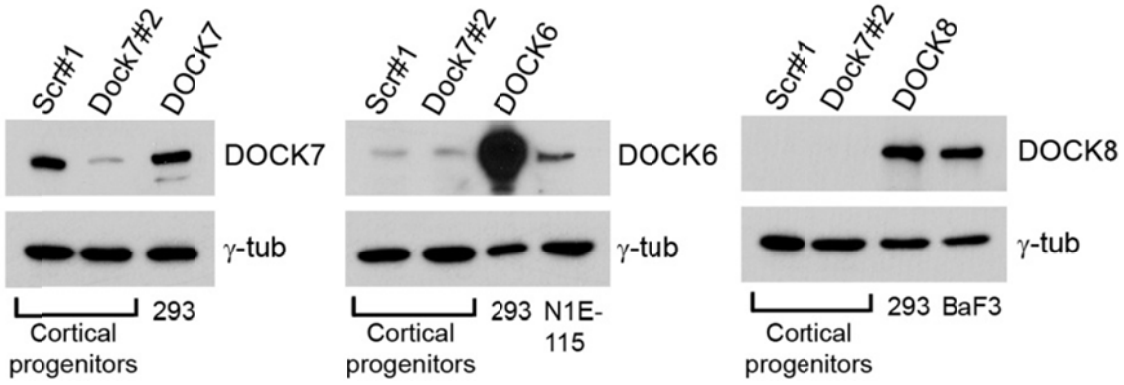

Figure 2.5. Knockdown of DOCK7 does not affect levels of DOCK6 expression, and DOCK8 is not expressed in cortical progenitors. Western blot of total lysates from cultured cortical progenitors isolated from E13.5 mouse cortices transfected with plasmids expressing control scrambled shRNA (scr#1) or Dock7#2 targeting shRNA (Dock7#2), HEK-293 cells (293) ectopically expressing FLAG-DOCK7 (DOCK7), FLAG-DOCK6 (DOCK6) or FLAG-DOCK8 (DOCK8), mouse N1E-115 neuroblastoma cells (N1E-115), or mouse BaF3 pro-B cells (BaF3) were blotted with anti-DOCK7 (left panel), anti-DOCK6 (middle panel) or anti-DOCK8 (right panel) antibody, respectively. Anti-γ-tubulin (γ-tub) blot was included to provide a loading control (lower panels).

the 3'UTR and is therefore resistant to Dock7#2 shRNA-mediated RNAi (Fig 2.4 lane 3) demonstrated that the observed effect of DOCK7 RNAi is specific (Fig. 2.6a,c). I further performed immunostainings for phospho-histone H3 (PH3), a mitotic marker, and determined the mitotic index (i.e. the percentage of transfected cells that are PH3-positive in the VZ). This index was considerably higher in the Dock7#2 shRNA group compared to the control and rescue groups (Fig. 2.6b,d). Thus, DOCK7 knockdown increases the percentage of proliferating VZ progenitors in the embryonic neocortex.

The impact of ectopic DOCK7 expression in cortical progenitors was also examined by introducing FLAG-tagged DOCK7 cDNA or empty control vector together with an EGFP-NLS plasmid into E13.5 embryonic mouse brains. BrdU labeling and embryonic brain analysis was performed as described above. In this experiment, I observed the opposite effects. The percentage of BrdU-positive transfected cells, as well as the mitotic index, was significantly reduced in the FLAG-DOCK7 expressing group compared to the control vector group (Fig. 2.7 a-d). To exclude the possibility that the reduction in the number of proliferating progenitors is due to programmed cell death, I examined brain slice for the apoptosis marker, cleaved Caspase-3[143]. Immunohistochemistry for cleaved Caspase-3 2 days post-electroporation of FLAG-DOCK7 expressing vector showed that cell survival was unaffected (Fig 2.8). Thus, DOCK7 overexpression decreases the percentage of proliferating VZ progenitors in the embryonic neocortex without triggering apoptosis of these progenitors.

To gain further insight into how altered DOCK7 expression could affect the progenitor pool size, I analyzed in more detail the proliferative status of VZ progenitors, by performing BrdU pulse-labeling, to visualize S-phase cells, combined with Ki67 staining, a cell proliferation maker which is present during all active phases of the cell cycle (G_1, S, G_2, and mitosis) but absent from resting cells (G_0), to reveal cells that entered the cell cycle[144].

In a first set of experiments, embryos were electroporated at E13.5, a 24 hours pulse of

Figure 2.6

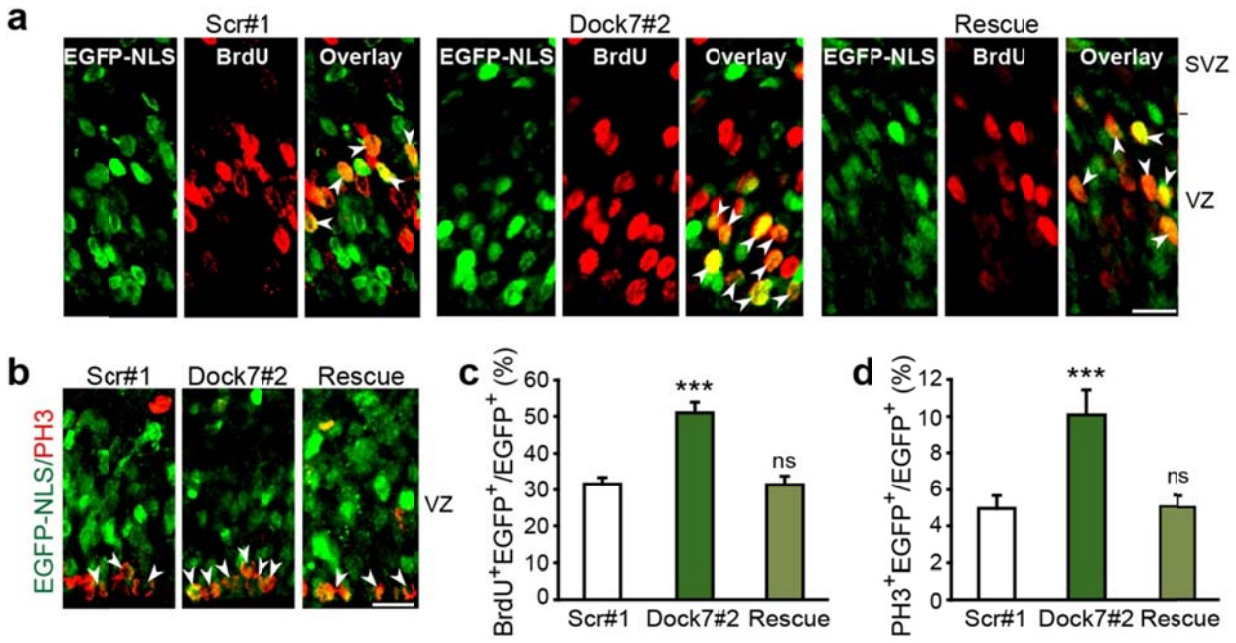

Figure 2.6. DOCK7 depletion enhances VZ progenitor proliferation. (a-d) Analysis of proliferating S-phase ($BrdU^+$) and mitotic ($PH3^+$) cells. Mouse embryos were co-electroporated at E13.5 with plasmids expressing EGFP-NLS marker protein and non-targeting shRNA (scr#1), Dock7 targeting shRNA (Dock7#2) or Dock7 shRNA and FLAG-DOCK7 (rescue), pulse labeled with BrdU for 2 h at E15.5 (a,c), or unlabeled (b,d), and sacrificed. Coronal brain slices were co-immunostained with anti-EGFP (green) and anti-BrdU (red)(a,c) or anti-PH3 (red)(b,d) antibodies. **(a,b)** Confocal images of the VZ (including SVZ in a) of neocortices. Arrowheads indicate transfected cells that are $BrdU^+$ (a) or $PH3^+$ (b). **(c,d)** Quantification of the transfected cells that are $BrdU^+$ (c) or $PH3^+$ (d) in VZ. Data are mean ± s.e.m.; *n* = 921-1897 cells from at least 3 animals for each condition. ****P* < 0.001; ns, not significant; one-way ANOVA (c,d). Scale bars, 20 μm.

Figure 2.7

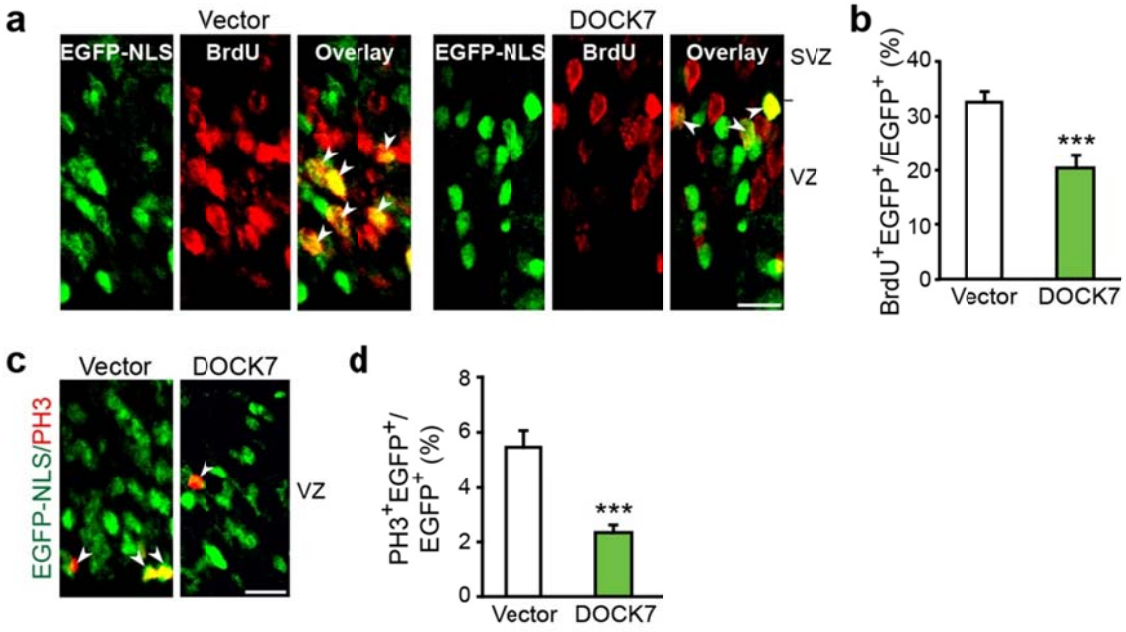

Figure 2.7. Ectopic DOCK7 expression reduces the VZ progenitor proliferation. (a-d) Analysis of proliferating S-phase ($BrdU^+$) and mitotic ($PH3^+$) cells. Mouse embryos were co-electroporated at E13.5 with plasmids expressing EGFP-NLS marker protein and empty control vector (vector) or FLAG-DOCK7 (DOCK7), pulse labeled with BrdU for 2 h at E15.5 (a,b), or unlabeled (c,d), and sacrificed. Coronal brain slices were co-immunostained with anti-EGFP (green) and anti-BrdU (red)(a,b) or anti-PH3 (red)(c,d) antibodies. **(a,c)** Confocal images of the VZ (including SVZ in a) of neocortices. Arrowheads indicate transfected cells that are $BrdU^+$ (a) or $PH3^+$ (c). **(b,d)** Quantification of the transfected cells that are $BrdU^+$ (b) or $PH3^+$ (d) in VZ. Data are mean ± s.e.m.; *n* = 1096 -1738 cells from at least 3 animals for each condition. ***P < 0.001; Student's *t*-test (b,d). Scale bars, 20 μm.

Figure 2.8

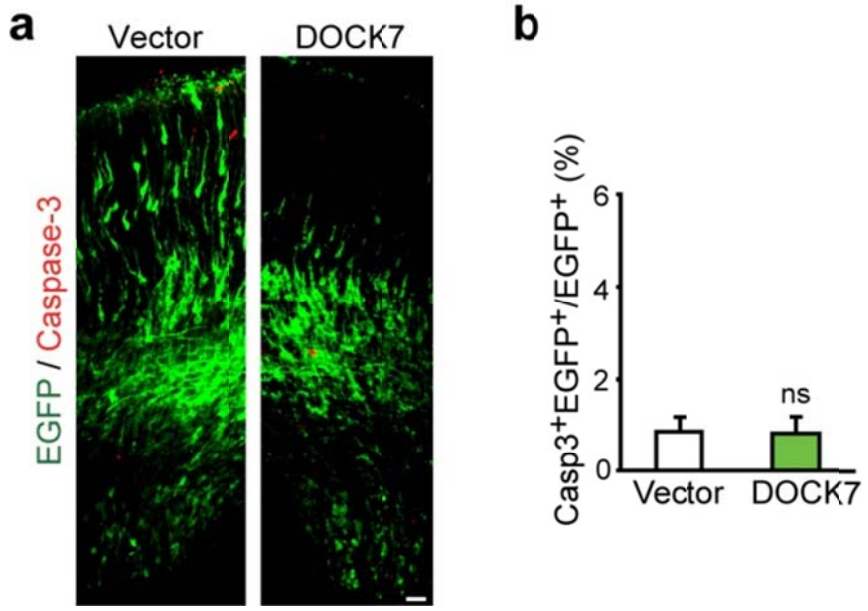

Figure 2.8. Ectopic DOCK7 expression does not affect cortical progenitor cell survival. Mouse embryos were co-electroporated at E13.5 with plasmids expressing EGFP marker protein and FLAG-DOCK7 (DOCK7) or empty control vector (vector), and sacrificed at E15.5. Coronal brain slices were co-immunostained for Caspase-3 (red) and EGFP (green). **(a)** Confocal images of neocortices. Scale bar, 25 μm. **(b)** Quantification of the transfected cells that are Caspase-3 positive ($Casp3^+$) (vector, *n* = 3031 cells; DOCK7, *n* = 2961 cells; from 3 animals for each condition). Data are shown as mean ± s.e.m. *P* = 0.605; ns, not significant; Student's *t*-test.

BrdU was administered 2 days later, and the fractions of transfected cells that entered the cell cycle ($BrdU^+$, $Ki67^+$) or withdrew from the cell cycle ($BrdU^+$, $Ki67^-$) were quantified. I observed that the percentage of BrdU and Ki67 double-positive cells was increased in the Dock7#2 shRNA group (Figure 2.9a,b), and decreased in the FLAG-DOCK7 group (Figure 2.9d,e). Conversely, I found that the percentage of BrdU-positive and Ki67-negative cells was decreased in the Dock7#2 shRNA group (Figure 2.9a,c), and increased in the FLAG-DOCK7 group (Figure 2.9d,f). These data indicate that DOCK7 knockdown favors the maintenance of cells as cycling progenitors, whereas ectopic DOCK7 expression promotes cell cycle exit. In the second set of experiments, embryos were electroporated at E13.5, a short BrdU pulse (30 min) was delivered 2 days later, and the ratio of cycling Ki67-positive progenitors in S phase ($BrdU^+$) over Ki67-positive progenitors in the VZ was measured (Ratio = $Ki67^+BrdU^+EGFP^+$ / $Ki67^+EGFP^+$). This ratio had was not significantly different between the Dock7#2 shRNA, FLAG-DOCK7, and control transfected groups (Figure 2.10a,b), implying that altering DOCK7 levels does not appreciably affect cell cycle duration. Moreover, by flow cytometric analysis, I found that knockdown of DOCK7 in mouse neuroblastoma Neuro-2A cells did not alter the distribution of cells along the cell cycle (Figure 2.10c). Thus, DOCK7 levels likely affect the progenitor pool size by influencing cell cycle exit/re-entry, but not cell cycle duration of progenitors in the VZ.

2.2.3 DOCK7 is required for the genesis of neurons

Between stages E13.5 and E16.5, as mentioned in chapter 1.2, VZ located radial glial progenitor cells (RGCs) largely switch from proliferative divisions that produce two RGCs to neurogenic divisions that generate at least one neuron, either directly from the RGC or indirectly via a basal progenitor (BP); the latter of which typically undergoes one subsequent division to produce two neurons[9-11,27-29]. Hence, based on my findings that DOCK7 knockdown increases the size of the VZ progenitor pool and ectopic DOCK7 expression causes a reduction, we postulated that DOCK7 could play a role in controlling the switch of RGCs from proliferation to

Figure 2.9

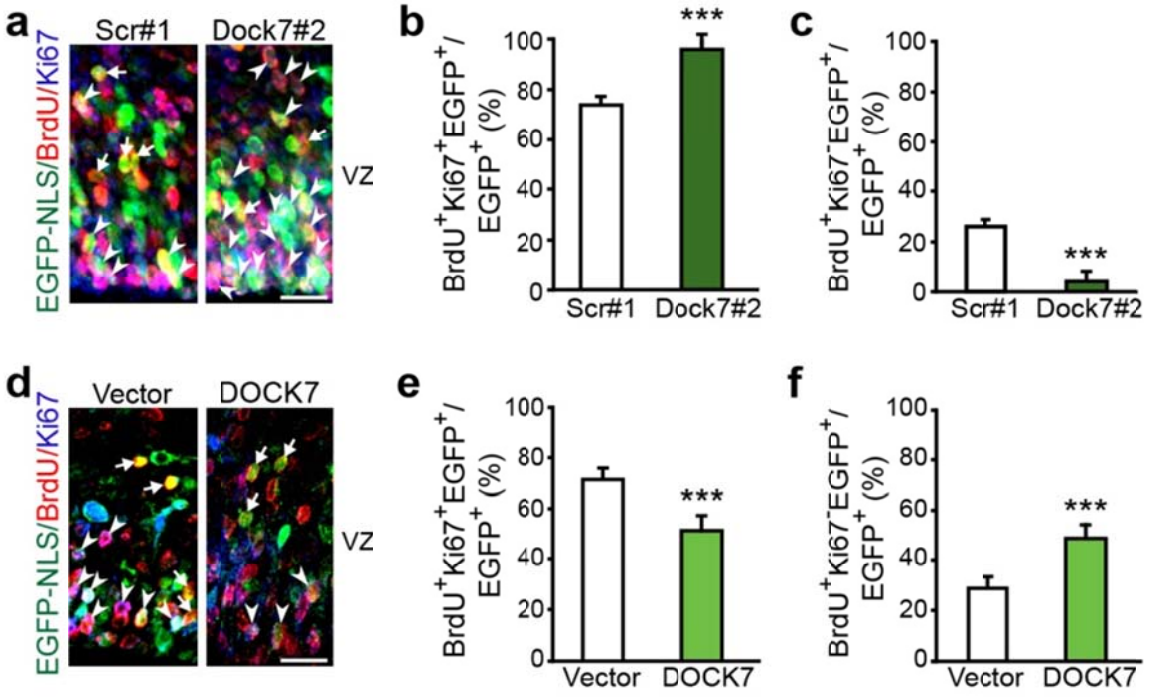

Figure 2.9. DOCK7 modulates the cell cycle kinetic of VZ progenitors. (a-f) Analysis of cell cycle re-entry and exit. Mouse embryos were electroporated at E13.5 with plasmids expressing EGFP-NLS marker protein and non-targeting shRNA (scr#1) or Dock7 targeting shRNA (Dock7#2) (a,b,c) and with plasmids expressing EGFP-NLS marker protein and empty control vector (vector) or FLAG-DOCK7 (DOCK7) (d,e,f) and pulse labeled with BrdU at E15.5 for 24 h. Coronal brain slices were co-immunostained for EGFP (green), BrdU (red) and Ki67 (blue). **(a,d)** Confocal images of the VZ of neocortices. Cycling $Ki67^+$ $BrdU^+$ $EGFP\text{-}NLS^+$ cells and $Ki67^-$ $BrdU^+$ $EGFP\text{-}NLS^+$ cells withdrawn from the cell cycle are indicated with arrowheads and arrows, respectively (a,d). **(b,c,e,f)** Quantification of the transfected cells in VZ that remained in the cell cycle ($BrdU^+$ $Ki67^+$; b,e) and those that exited the cell cycle ($BrdU^+$ $Ki67^-$; c,f**)**. Data are mean ± s.e.m.; *n* = 867-1292 cells from at least 3 animals for each condition. ***$P < 0.001$; Student's *t*-test. Scale bars, 20 μm.

Figure 2.10

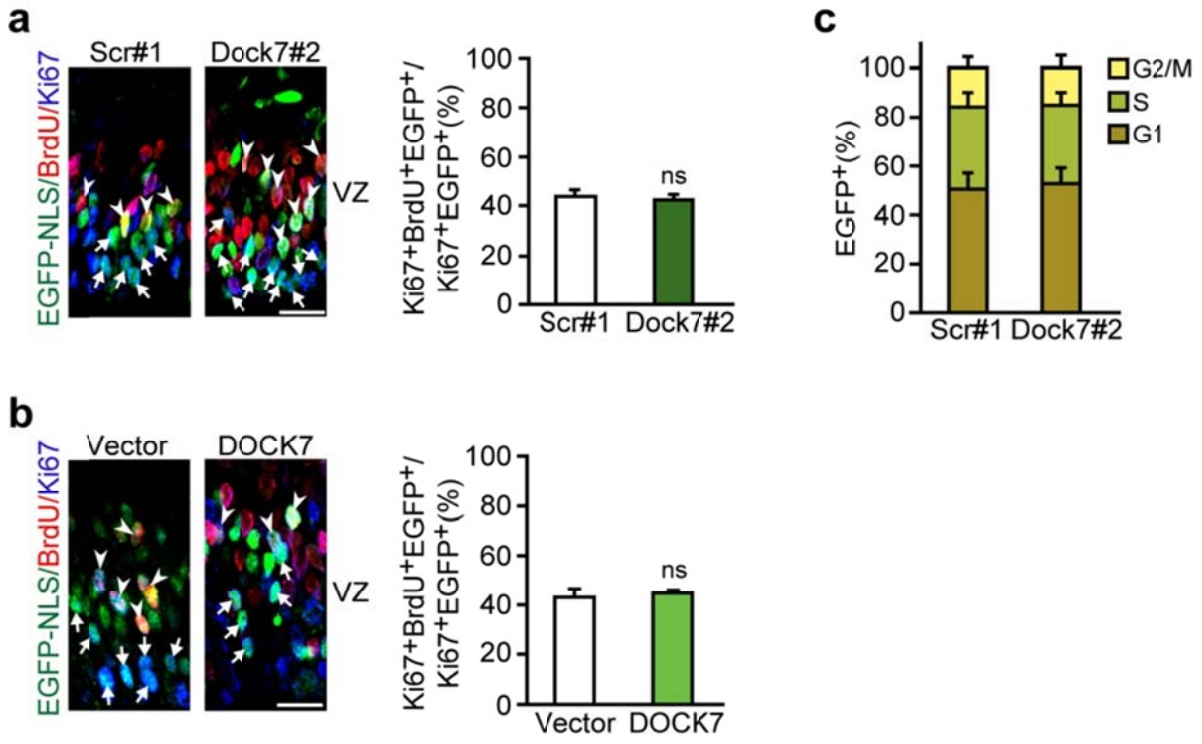

Figure 2.10. DOCK7 does not affect cell cycle duration. (a,b) Mouse embryos were co-electroporated at E13.5 with plasmids expressing EGFP-NLS marker protein and non-targeting shRNA (scr#1) or Dock7 targeting shRNA (Dock7#2) (a), or empty control vector (vector) or FLAG-DOCK7 (DOCK7) (b). BrdU was administrated at E15.5, and embryos were sacrificed 30 min after BrdU injection. Coronal brain slices were co-immunostained for BrdU (red), Ki67 (blue), and EGFP (green). Left panels: Confocal images of the VZ of neocortices. Arrows indicate transfected cells that are $Ki67^+$ and $BrdU^-$. Arrowheads indicate transfected cells that are $BrdU^+$ and $Ki67^+$. Scale bars, 20 μm. Data are shown as mean ± s.e.m.; *n* = 391-629 cells from 3 animals for each condition. *P* = 0.23 for Dock7#2 (a), and *P* = 0.45 for DOCK7 (b); ns, not significant; Student's *t*-test. **(c)** Neuro-2A cells were infected with lentiviral vectors co-expressing EGFP and Dock7#2 shRNA (Dock7#2) or scr#1 shRNA (scr#1). Cells were harvested 3-4 days post-infection, fixed with 0.5% PFA and 75 % cold ethanol, stained with propidium iodide (50 μg/ml), and DNA content profiles were determined by flow cytometry. The number of infected cells in each phase of the cell cycle was quantified. Data are shown as mean ± s.e.m.; *n* = 3 independent experiments. *P* > 0.288 for each phase of the cell cycle; Student's *t*-test.

differentiation/neurogenesis.

To assess this, I first examined whether DOCK7 affects the population of RGCs and/or BPs. I electroporated embryos at E13.5 with the Dock7#2 shRNA or FLAG-DOCK7 expressing vector, together with an EGFP-NLS expression plasmid, and determined the number of transfected RGCs and BPs 2 days later. To identify RGCs and BPs, brain slices were immunostained for Pax6 and Tbr2, markers of RGCs and BPs, respectively[145,146]. Knockdown of DOCK7 resulted in considerably more Pax6-positive cells, but fewer Tbr2-positive cells, compared to control scr#1 shRNA electroporated cortices (Figure 2.11a-d). On the contrary, ectopic DOCK7 expression caused a significant decrease in Pax6-positive cells, but an increase in Tbr2-positive cells, compared to the control vector condition (Figure 2.11e-h). Thus, DOCK7 depletion promotes the amplification of the RGC pool, while DOCK7 overexpression diminishes this pool and promotes the transition from RGCs to BPs.

Next, I examined whether DOCK7 affects the production of neurons. To this end, embryos were electroporated at E13.5 with the Dock7#2 shRNA or FLAG-DOCK7 expressing vector together with an EGFP expression plasmid, and I started by examining the distribution of EGFP expressing cells across the neocortical layers. Newly generated neurons at E15.5 typically migrate towards the CP through the intermediate zone (IZ), while self-renewing RGCs remain in the VZ. Compared to the control group, Dock7#2 shRNA transfected were more abundant in the VZ and less abundant in the CP and IZ (Fig 2.12a,b). In addition, I observed a decrease in the percentage of transfected cells in the SVZ, where BPs reside. Furthermore, immunostaining of the cortices with the neuronal marker Tuj1 demonstrated that the percentage of Tuj1-positive transfected cells was significantly decreased in the Dock7#2 shRNA group (Fig. 2.12c). To further confirm that silencing DOCK7 in cortical progenitors indeed perturbs the genesis of neurons, I examined neuron production at extended time periods. In particular,

Figure 2.11

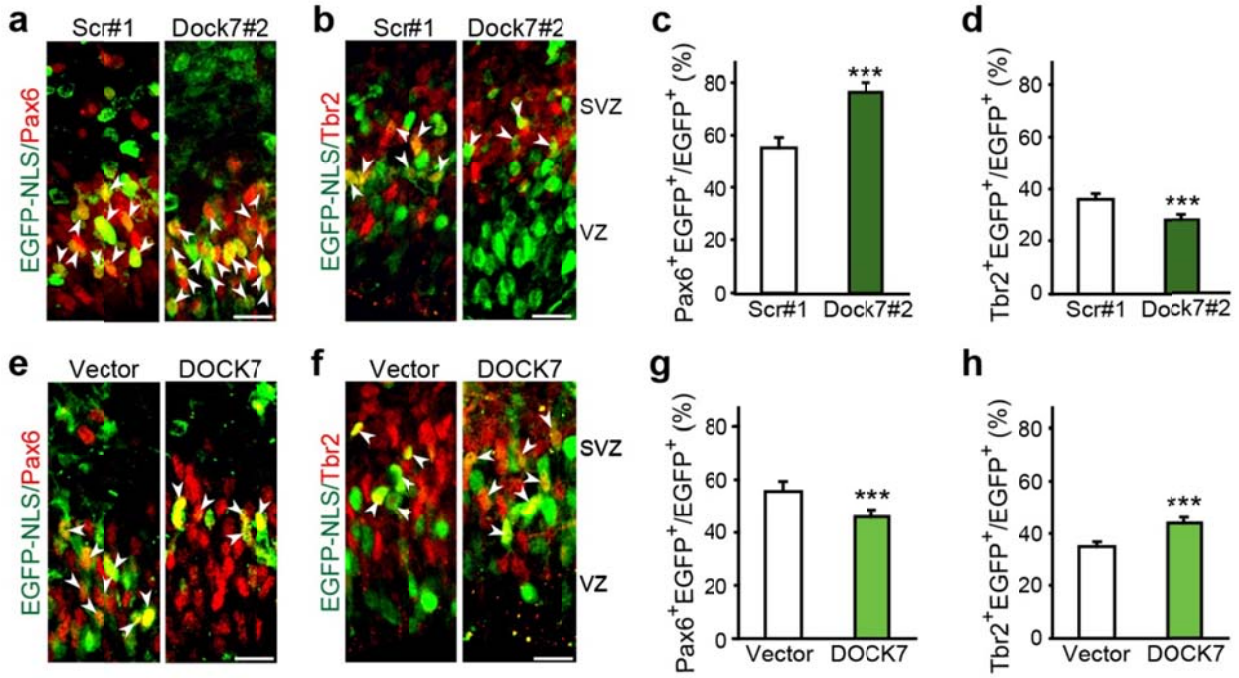

Figure 2.11. DOCK7 is required for the transition of RGCs to BPs. (a-h) Analysis of RGCs and BPs. Mouse embryos were co-electroporated at E13.5 with plasmids expressing EGFP-NLS marker protein and non-targeting shRNA (scr#1) or Dock7 targeting shRNA (Dock7#2) (a-d), or empty control vector (vector) or FLAG-DOCK7 (DOCK7) (e-h), and sacrificed at E15.5. Coronal brain slices were co-immunostained for EGFP (green) and Pax6 (red)(a,e,c,g) or Tbr2 (red)(b,f,d,h), markers for RGCs and BPs, respectively. **(a,b,e,f)** Confocal images of the VZ/SVZ of neocortices. Arrowheads indicate transfected cells that are $Pax6^+$ (a,e) or $Tbr2^+$ (b,f). Scale bars, 20 μm. **(c,d,g,h)** Quantification of the transfected cells that are $Pax6^+$ (c,g) or $Tbr2^+$ (d,h) in the VZ/SVZ. Data are mean ± s.e.m.; *n* = 853-1268 cells from at least 3 animals for each condition. ***$P < 0.001$; Student's *t*-test.

Figure 2.12

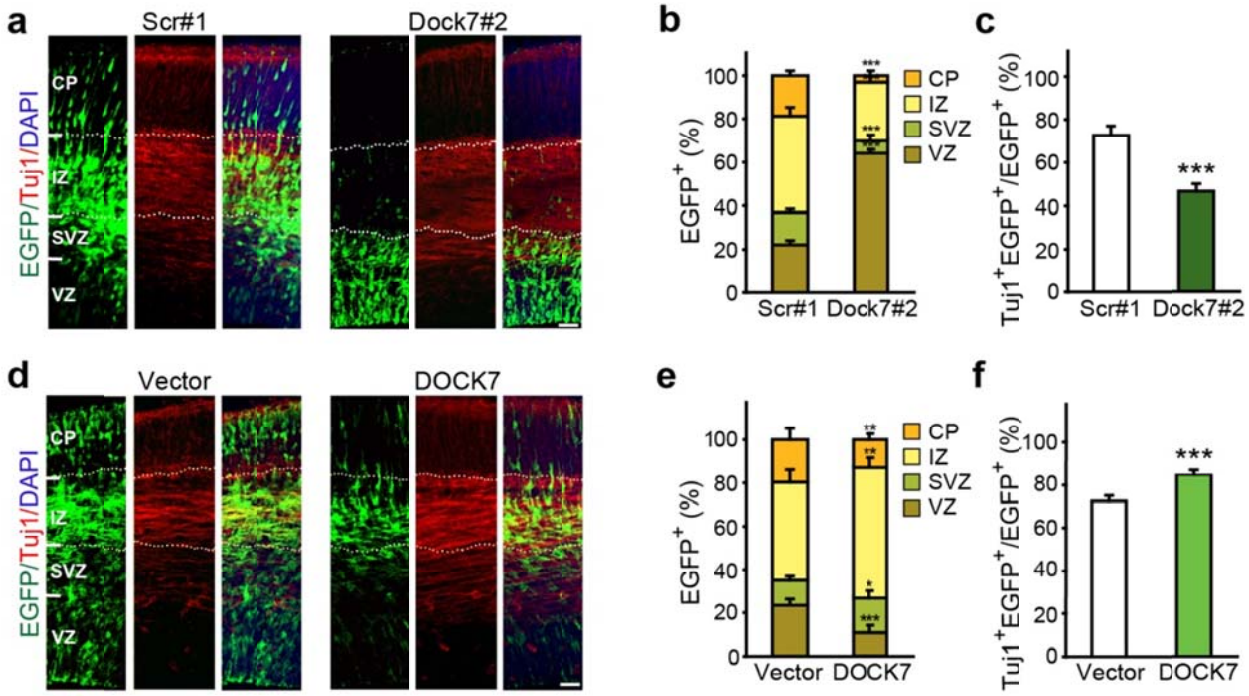

Figure 2.12. DOCK7 is required for the genesis of neuron. (a-f) Analysis of neurons. Mouse embryos were electroporated at E13.5 with plasmids expressing EGFP-NLS marker protein and non-targeting shRNA (scr#1) or Dock7 targeting shRNA (Dock7#2) (a-c), or empty control vector (vector) or FLAG-DOCK7 (DOCK7) (d-f), and sacrificed 2 d later. Coronal brain slices were co-immunostained for EGFP (green) and Tuj1 (red), and counterstained with DAPI (blue). **(a,d)** Confocal images of neocortices showing distribution of $EGFP^+$ transfected cells across neocortical layers. Scale bars, 40 μm. **(b,e)** Quantification of the distribution of $EGFP^+$ transfected cells in entire neocortex. Data are shown as mean ± s.e.m.; *n* = 1983-2453 cells from at least 3 animals for each condition (see supplemental data for details). **P* < 0.05; ***P* < 0.01; ****P* < 0.001; Student's *t*-test. **(c,f)** Quantification of the transfected cells that are $Tuj1^+$. Data are mean ± s.e.m.; *n* = 1318-2331 cells from at least 3 animals for each condition (see supplemental data for details). ****P* < 0.001, Student's *t*-test.

cortexes were electroporated at E13.5 or E15.5 and analyzed 8 or 9 days later at P1.5 and P4.5, respectively. Importantly, I found that these perturbations persisted. While in the control groups (at P1.5 and P4.5) the majority of the transfected cells were located in the cortical mantle, with only a small fraction (< 10%) residing in the proliferative VZ/SVZ, in the Dock7#2 shRNA groups ≥ 40% of the transfected cells still resided in the VZ/SVZ and the percentage of transfected cells in the cortical mantle was correspondingly reduced (Fig 2.13a,d,g,j). Consistently, the percentage of Tuj1-positive transfected cells was significantly decreased in the Dock7#2 shRNA groups (Fig 2.13b,e,h,k). Of note, I did not detect a significant difference in the percentage of GFAP-positive transfected cells between the Dock7#2 shRNA and the scr#1 shRNA groups (Fig. 2.13c,f,i,l), implying that DOCK7 knockdown does not induce premature astrocyte differentiation. Thus, these data indicate that silencing of DOCK7 impairs the genesis of neurons.

When examining the effects of DOCK7 overexpression, I observed a decrease in the percentage of transfected cells in the VZ, an increase in the SVZ and IZ, but, interestingly, a decrease in the CP (Fig. 2.12d,e). The number of Tuj1-positive transfected cells was significantly increased upon DOCK7 expression (Fig. 2.12f); however, the majority of these cells resided in the IZ, and relatively few were detectable in the CP (Fig. 2.12d,e). Notably, most of the cells located in the IZ displayed a multipolar phenotype. These data suggest that ectopic DOCK7 expression promotes the genesis of neurons, but that these neurons, although able to reach the IZ, are defective or delayed in migrating toward the CP, possibly due to a defect in the transition from multipolar to bipolar phase. Thus, in addition to controlling the genesis of neurons, DOCK7 may also play a role in the polarization and/or migration of IZ neurons.

Figure 2.13

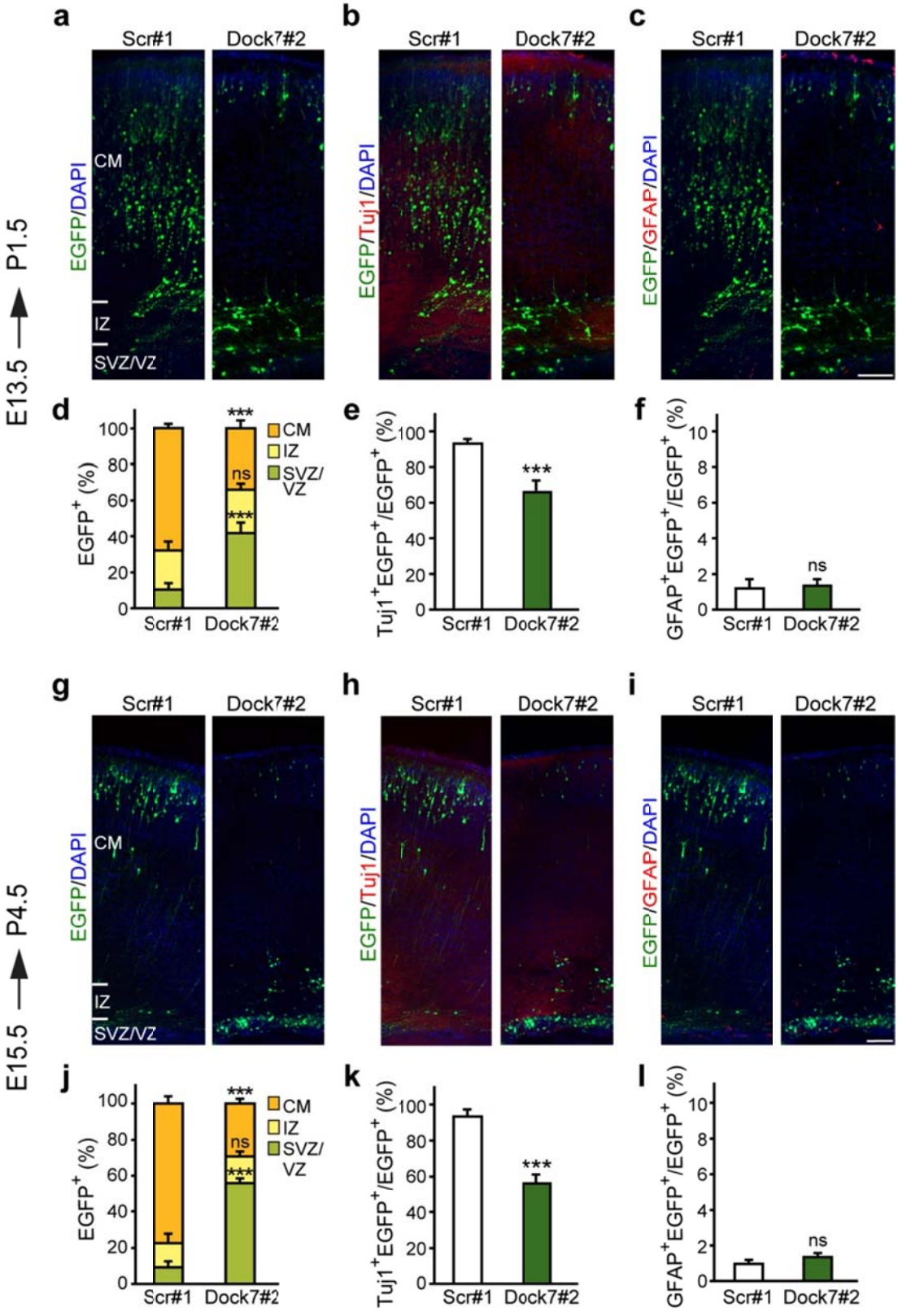
a
Scr#1
Dock7#2
EGFP/DAPI
CM
IZ
SVZ/VZ
E13.5 → P1.5
b
EGFP/Tuj1/DAPI
c
EGFP/GFAP/DAPI
d
EGFP+ (%)
CM
IZ
SVZ/VZ
ns
***
e
Tuj1+EGFP+/EGFP+ (%)
f
GFAP+EGFP+/EGFP+ (%)
g
E15.5 → P4.5
h
i
j
k
l

Figure 2.13. DOCK7 knockdown causes persistent perturbations in neurogenesis. Mouse embryos were co-electroporated at E13.5 or E15.5 with plasmids expressing EGFP marker protein and non-targeting shRNA (scr#1) or Dock7 targeting shRNA (Dock7#2), and sacrificed at P1.5 (E13.5→P1.5, a-f) and P4.5 (E15.5→P4.5, g-l), respectively. Coronal brain slices were co-immunostained for EGFP (green) and Tuj1 or GFAP (red), and counterstained with DAPI (blue). (**a,g**) Confocal images of neocortices showing distribution of $EGFP^+$ transfected cells across neocortical layers. (**d,j**) Quantification of the distribution of $EGFP^+$ transfected cells in entire neocortex. Data are shown as mean ± s.e.m.; *n* = 2051-2546 cells from 3 animals for each condition. ***$P < 0.001$; $P = 0.232$ (d) and 0.106 (j) for Dock7#2 in IZ; ns, not significant; Student's *t*-test. (**b,h**) Confocal images of neocortices showing $EGFP^+$ and $Tuj1^+$ cells. (**e,k**) Quantification of the transfected cells that are $Tuj1^+$. Data are mean ± s.e.m.; *n* = 1879-2108 cells from 3 animals for each condition. ***$P < 0.001$, Student's *t*-test. (**c,i**) Confocal images of neocortices showing $EGFP^+$ and $GFAP^+$ cells. (**f,l**) Quantification of the transfected cells that are $GFAP^+$. Data are mean ± s.e.m.; *n* = 1963-2275 cells from 3 animals for each condition. $P = 0.588$ (f) and 0.107 (l) for Dock7#2; ns, not significant; Student's *t*-test. CM, cortical mantle; IZ, intermediate zone; SVZ/VZ, subventricular zone/ventricular zone. Scale bars, 100 μm.

CHAPTER THREE

DOCK7 regulates RGCs behavior and neurogenesis through interkinetic nuclear migration (INM)

3.1 Introduction

In previous chapter, I described a critical role for DOCK7 in cortical neurogenesis, and in particular, in controlling the switch of RGCs from proliferation to differentiation. I found that DOCK7 knockdown maintains RGCs as cycling progenitors, while ectopic DOCK7 expression causes premature neuronal differentiation. We next asked the question by which cellular mechanism(s) DOCK7 affects neurogenesis and controls RGC proliferation versus differentiation.

As described in section 1.2 and 1.3 of the first chapter, several cellular parameters have been reported to influence the output of RGC progenitors. These include cell cycle duration, cell polarity, apoptosis, and more recently, INM. Perturbations in any of these processes have been linked to the abnormal development of the neocortex.

In this chapter, I describe the various experiments performed to asses which of these cellular processes of DOCK7 impinge on to control proliferation versus differentiation of RGCs and subsequently as detailed below, I found that DOCK7 does not affect RGC apoptosis, adhesion or cell cycle duration, but exerts its effect by influencing the basal-to-apical (bl-to-ap) INM process.

3.2 Results

3.2.1 DOCK7 does not affect programmed cell death (apoptosis), cell cycle duration nor the polarity and adhesion of radial glial cells

As already alluded to before in chapter 2, our data indicate that DOCK7 does not induce apoptosis of RGCs. First, silencing of DOCK7 results in an increase of VZ cortical progenitors (Figure 2.6). Second, while ectopic expression of DOCK7 causes a decrease in the number of VZ progenitors, immunohistochemistry for cleaved Caspase-3 at 2 days post electroporation of FLAG-DOCK7 expressing vector showed that all survival was unaffected (Figure 2.8). Thus, these data indicated that apoptosis is not responsible for the decrease in the number of proliferating progenitors. Taken together, DOCK7 does not affect apoptosis of VZ progenitor cells.

Our data also indicated that DOCK7 does not affect cell cycle duration. As discussed in chapter two, when measuring the ratio of cycling Ki67-positive progenitors in S phase ($BrdU^+$) over Ki67-positive progenitors in the VZ, we found that this ratio was not significantly different between Dock7#2 shRNA, FLAG-DOCK7 and control groups (Figure 2.10a,b). These data imply that altering DOCK7 levels does not affect cell cycle duration. These findings were further corroborated in Neuro-2A cells, by performing flow cytometric analysis (Figure 2.10c). Thus, DOCK7 does not exert its effects on neurogenesis by influencing the cell cycle duration.

Furthermore, we found that DOCK7 does not appear to affect RGC polarity and adhesion. I performed immunostaining for adherens junction molecules, β-catenin and zo-1, on brain slices from embryos co-electroporated with plasmids expressing EGFP and DOCK7 shRNA, FLAG-DOCK7 or control vectors. As shown in Figure 3.1, β-catenin and zo-1 in immunostainings were intact in EGFP positive transfected RGCs of all groups. Thus, DOCK7 is unlikely to exert its effects by influencing RGC adhesion/polarity. I then examined whether

Figure 3.1

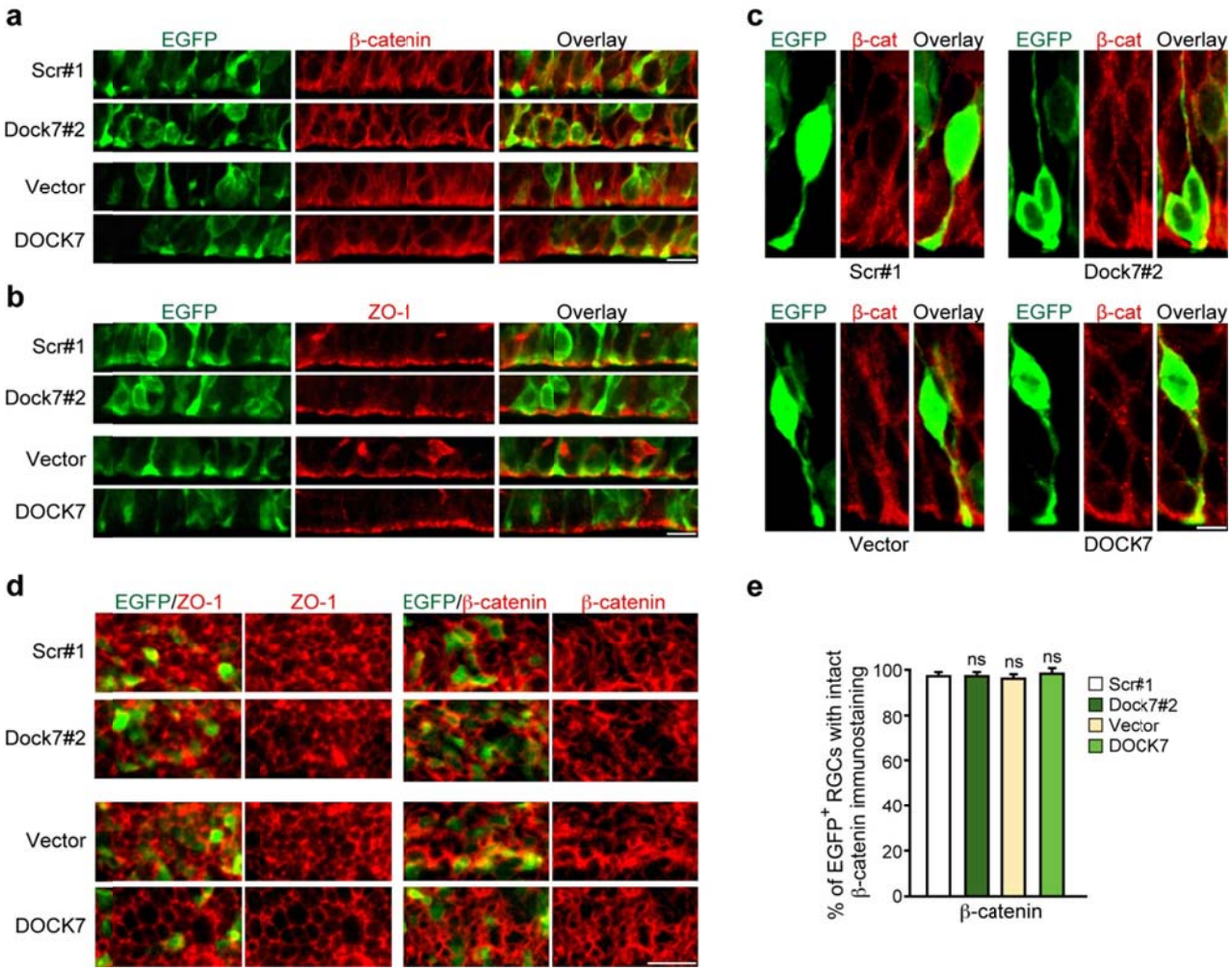

Figure 3.1. DOCK7 does not affect radial glial cell (RGC) adhesion and polarity. Mouse embryos were co-electroporated at E13.5 with plasmids expressing EGFP marker protein and non-targeting shRNA (scr#1), Dock7 targeting shRNA (Dock7#2), empty control vector (vector) or FLAG-DOCK7 (DOCK7), and sacrificed at E15.5. Coronal brain slices were co-immunostained for EGFP (green) and β-catenin (a,c,d; red) or ZO-1 (b,d; red), markers for adherens junctions (AJs). **(a,b)** Confocal images of apical endfeet of RGCs in electroporated regions. AJs, visible as a straight line in the X-Y axis by β-catenin (a) or ZO-1 (b) immunostainings, are intact in EGFP$^+$ transfected RGCs of all groups. Scale bars, 10 μm. **(c)** Enlarged views of the cell body and apical process of RGCs are shown. Scale bar, 5 μm. β-cat, β-catenin. **(d)** *En face* view of the ventricular surface (X-Z axis) showing that AJs, visible as honeycomb structures by ZO-1 (left panels) or β-catenin (right panels) immunostainings, are intact in EGFP$^+$ transfected RGCs of all groups. Scale bar, 10 μm. **(e)** Quantification of EGFP$^+$ transfected RGCs displaying intact β-catenin immunostaining. Data are shown as mean ± s.e.m.; *n* = 312-612 cells; from 3 animals for each condition. *P* = 0.883 for Dock7#2, 0.571 for vector and 0.649 for DOCK7; ns, not significant; one-way ANOVA.

altered DOCK7 expression influences RGC proliferation and/or differentiation by controlling the INM process.

3.2.2 DOCK7 is important for INM

The cell-cycle-dependent nuclear position change is known as interkinetic nuclear migration (INM) (see section 1.3 in chapter 1). The first hint for a role of DOCK7 in INM came from my BrdU labeling experiments, where I noticed a difference in the location of BrdU-labeled nuclei of control, Dock7#2 shRNA, and FLAG-DOCK7 expressing cells (Figure 2.6a and 2.7a, arrowheads). Compared to the control group, the distribution of the BrdU-positive nuclei was shifted toward the apical surface in the Dock7#2 shRNA group, whereas in the FLAG-DOCK7 group the nuclei were positioned more basally in the upper VZ. To further establish whether and how altered DOCK7 expression affects INM, I set up time course experiments to examine in more detail the migration of RGC nuclei compared with cell cycle progression from S to M phase (Figure 1.4). To this end, embryos were co-electroporated at E13.5 with plasmids expressing EGFP-NLS marker protein and non-targeting shRNA (scr#1), Dock7 targeting shRNA (Dock7#2), empty control vector (vector) or FLAG-DOCK7 (DOCK7). BrdU was administrated 2 days later, and the positions of BrdU-labeled nuclei of transfected cells were detected 15 min, 2 hours, 4 hours, and 6 hours after BrdU injection (Figure 3.2).

At the 15 min time point, the majority of the BrdU-labeled nuclei of control, Dock7#2 shRNA, and FLAG-DOCK7 expressing VZ cells were located in the upper half of the VZ, consistent with the known location of RGC nuclei in S phase[147] (Figure 3.2a,b). BrdU-labeled control nuclei begun to migrate toward the ventricle surface (VS) within 2 hours, and continued to do so for about another 4 hours (Figure 3.2a,b; scr#1, vector), in concurrence with an S phase duration about 4 hours and G2 phase duration about 2 hours at this developmental stage[77,147]. After reaching the VS, they entered apical mitosis (< 20 μm from VS), as determined by their PH3 immunoreactivity (Figure 3.2c,d). Interestingly, DOCK7 knockdown accelerated the

Figure 3.2

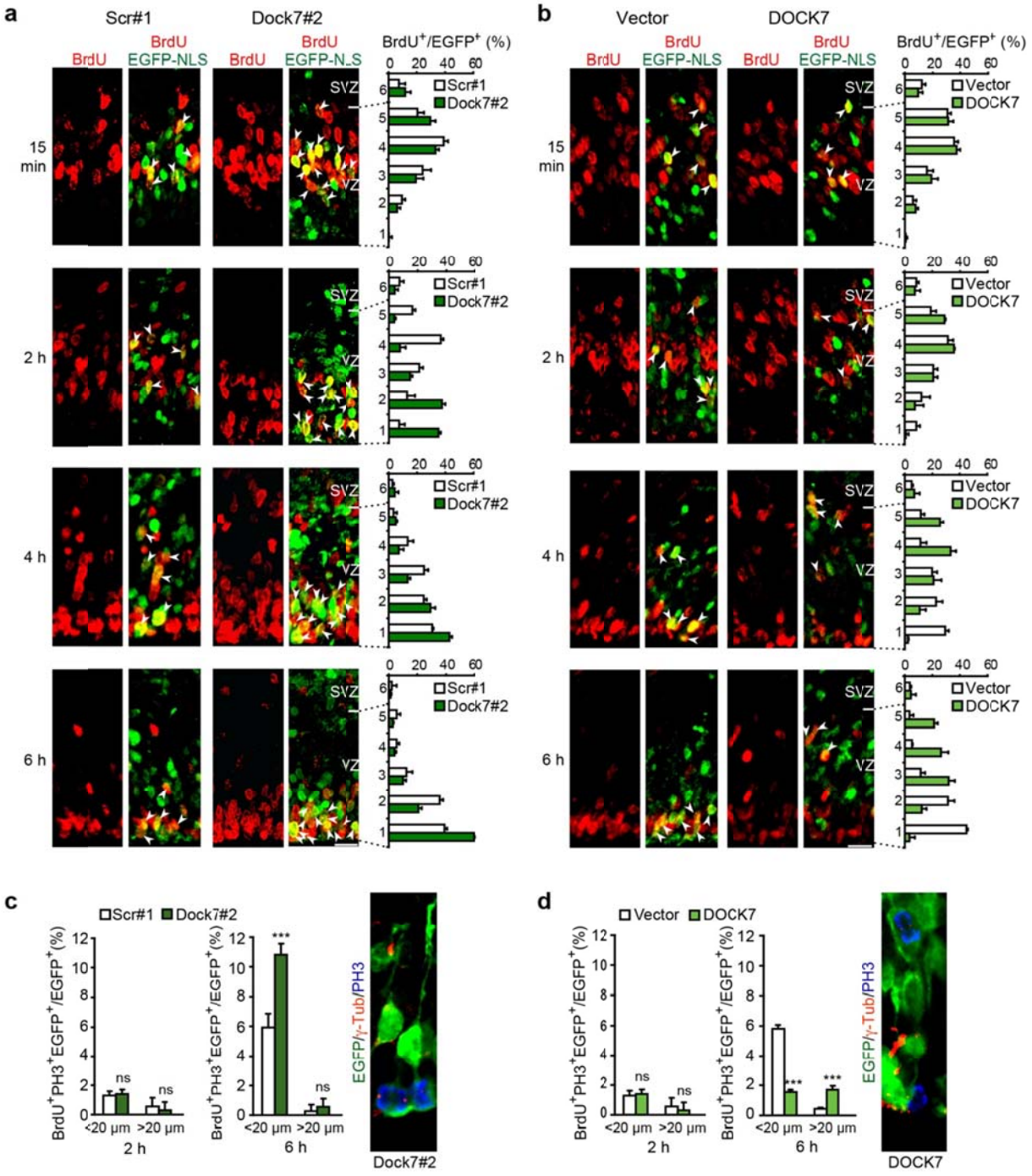
a
Scr#1
Dock7#2
BrdU
BrdU EGFP-NLS
BrdU EGFP-N_S
BrdU+/EGFP+ (%)
Scr#1
Dock7#2
15 min
2 h
4 h
6 h
SVZ
VZ
b
Vector
DOCK7
c
Scr#1 Dock7#2
BrdU+PH3+EGFP+/EGFP+ (%)
ns
***
<20 μm >20 μm
2 h
6 h
EGFP/γ-Tub/PH3
Dock7#2
d
Vector DOCK7
DOCK7

Figure 3.2. DOCK7 controls basal-to-apical INM of RGCs. (**a-d**) Mouse embryos were electroporated at E13.5 with a plasmid expressing EGFP-NLS marker protein together with one of the indicated plasmids, pulse labeled with BrdU at E15.5, and sacrificed 15 min, 2 h, 4 h or 6 h after BrdU injection. Coronal brain slices were co-immunostained for EGFP (green) and BrdU (red) (a,b) and for EGFP (green), BrdU (cy5) and PH3 (red) (c,d, left). (**a**,**b**) Left panels: Confocal images showing the position of $BrdU^+$ and $EGFP\text{-}NLS^+$ labeled nuclei in neocortices of embryos electroporated with plasmids expressing scr#1 shRNA (scr#1) or Dock7#2 shRNA (Dock7#2) (a) or empty control vector (vector) or FLAG-DOCK7 (DOCK7) (b), at indicated times after BrdU injection. Scale bars, 20 μm. Arrowheads indicate $BrdU^+$ nuclei of transfected cells. Right panels: Distribution of $BrdU^+$ transfected cells quantified as percentage of all transfected cells per bin (one bin: 20 μm high) across the VZ and part of SVZ, which was divided into 6 bins. Data are mean ± s.e.m.; n = 383-601 cells from at least 3 animals for each condition (see supplemental data for details). (**c,d**) Quantification of the transfected cells that are $BrdU^+$ and $PH3^+$ at apical (< 20 μm) or more basal (> 20 μm) locations relative to the ventricular surface in VZ at 2 h and 6 h after BrdU injection. Data are mean ± s.e.m.; n = 754-1009 cells from at least 3 animals for each condition. ***P < 0.001; ns, not significant; Student's t-test. Right panels: Representative images of RGCs expressing EGFP and Dock7#2 shRNA (c) or FLAG-DOCK7 (d) immunostained for EGFP (green), PH3 (blue) and centrosomal marker γ-tubulin (red).

bl-to-ap movement (Figure 3.2a, Dock7#2). Whereas, for instance, after 2 hours only a few of the control BrdU-labeled nuclei had reached the apical region of the VZ, a much larger fraction of BrdU-labeled nuclei of the Dock7#2 shRNA transfected cells had already arrived this location (Figure 3.2a), where most of them seemed to stay for approximately another 4 hours to only then enter mitosis at the apical surface (Figure 3.2c). Indeed, an increase in the number of $BrdU^+$, $PH3^+$ VZ cells in the Dock7#2 shRNA group compared to the control group was observed at 6 hours, but not at 2 hours, following BrdU injection (Figure 3.2c). Conversely, when examining the nuclei position of FLAG-DOCK7 expressing VZ cells, I noticed that the bl-to-ap migration of BrdU-labeled nuclei was delayed, with many of the nuclei remaining in the upper half of the VZ at 6 hours following BrdU injection (Figure 3.2b). Interestingly, this extended stay at basal locations was associated with an increased number of mitoses away from the apical surface, as judged by the higher percentage of $BrdU^+$, $PH3^+$ cells at basal positions (> 20 μm from VS) in the DOCK7 group compared to the control vector group (Figure 3.2d).

To substantiate and extend the above findings, in collaboration with Chia-Lin Wang, a postdoctoral fellow in the Van Aelst Lab, I carried out time-lapse imaging on acute cortical slices 2 days after *in utero* electroporation of plasmids expressing empty control vector, FLAG-DOCK7, scr#1 shRNA, or Dock7#2. EGFP (green) and a mKO2-F (orange) expressing plasmids were co-electroporated to fluorescently label both the cytoplasm (EGFP) and the plasma membrane (mKO2-F, which contains a Cys-Ala-Ala-Xaa farnesylation motif) of the RGCs. Acute brain slices were prepared and imaged over 8 to 10 hour time period. We found that cell bodies of most control vector expressing RGCs migrated toward the ventricle in a steady velocity (10.82±1.34 μm/h) and then divided at the apical surface (Figure 3.3a,e; Video 1). In contrast, cell bodies of

a significant fraction of DOCK7 overexpressing cells remained at basal locations and the cells divided away from the ventricular surface (Figure 3.3b,e; Video 2). Some cell bodies of the DOCK7 overexpressing cells were observed to move slowly toward the ventricle (3.89±1.23 μm/h). However, the traveling distance was quite short, and those cells still divided away from the ventricular surface (Video 3). These findings support that DOCK7 overexpression hampers bl-to-ap INM, leading to extended time of residence of RGC nuclei at basal locations and the occurrence of ectopic mitoses. On the other hand, we found that cell bodies of most Dock7#2 shRNA expressing cells migrated faster toward the ventricular surface (17.32±2.07 μm/h), than those of control scr#1 shRNA expressing cells (10.35±1.43 μm/h), where, importantly, they then resided for several hours before undergoing apical mitoses (Figure 3.3c-e; Videos 4-6). These observations corroborate that DOCK7 knockdown accelerates bl-to-ap INM, leading to an extended residence of RGC nuclei at apical locations and occurrence of apical mitoses. Taken together, our data unveil that DOCK7 plays a critical role in the regulation of the bl-to-ap INM process.

Figure 3.3

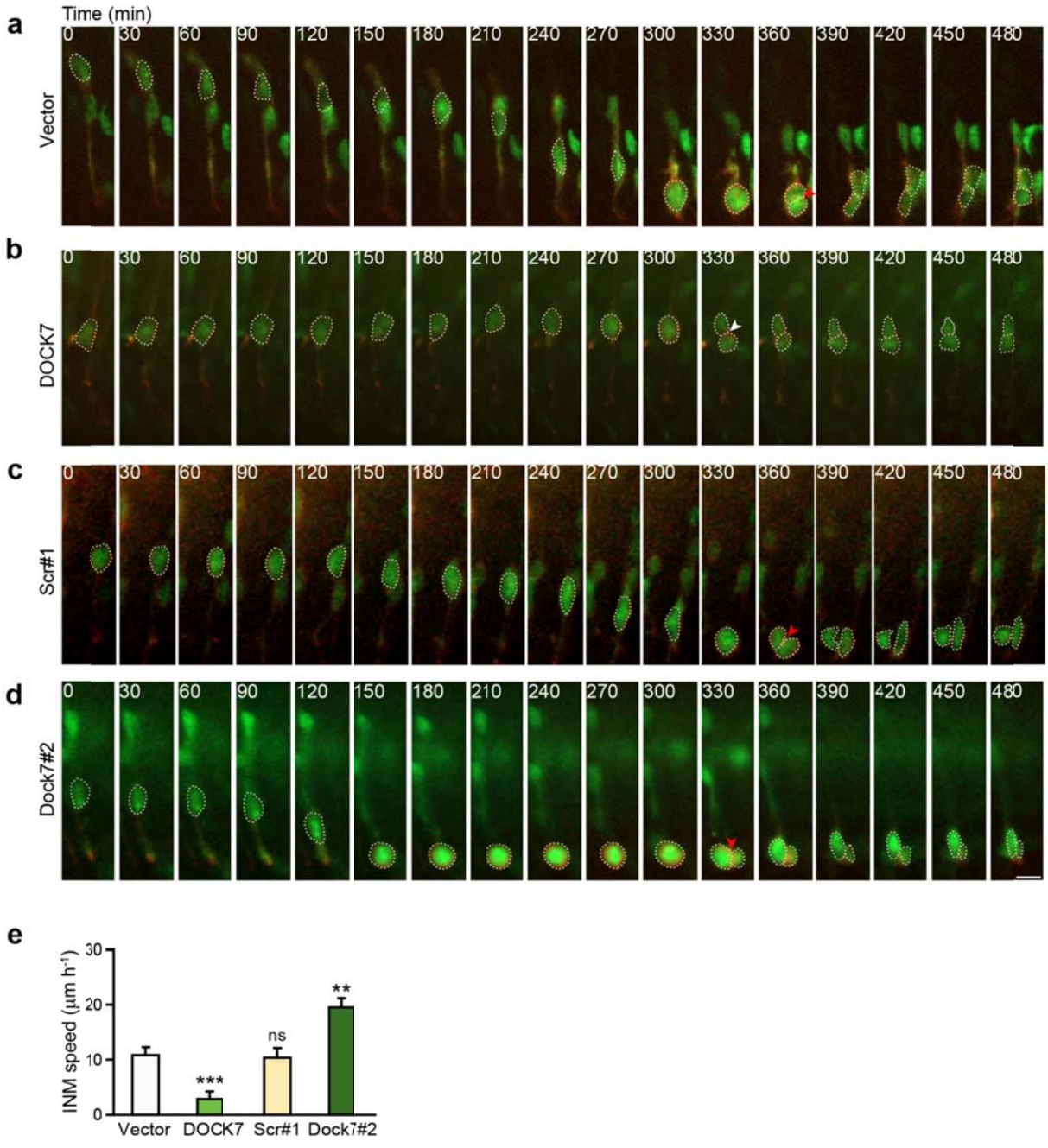
a
Time (min)
0 30 60 90 120 150 180 210 240 270 300 330 360 390 420 450 480
Vector
b
DOCK7
c
Scr#1
d
Dock7#2
e
INM speed (μm h-1)
30
20
10
0
***
ns
**
Vector DOCK7 Scr#1 Dock7#2

Figure 3.3. Altered DOCK7 expression affects apically directed INM of RGCs in acute cortical slices. (**a-e**) Mouse embryos were co-electroporated with plasmids expressing EGFP and mKO2-F marker proteins, and empty control vector (vector) (a), FLAG-DOCK7 (DOCK7) (b), non-targeting shRNA (scr#1) (c) or Dock7 targeting shRNA (Dock7#2) (d) at E13.5, and time-lapse imaging was performed 2 days later. (**a-d**) Time-lapse video sequences of EGFP and mKO2-F positive transfected cells undergoing INM. Ventricular surface is located at the bottom of the images. Time is denoted in the upper left corner. Cell bodies are delineated by dashed lines. Red arrowheads indicate mitosis at apical surface; white arrowhead indicates ectopic mitosis. Scale bar, 10 μm. (**e**) Quantification of bl-to-ap INM velocity. Data are mean ± s.e.m.; *n* = 19-43 cells from at least 3 experiments for each condition. ***P* < 0.01; ****P* < 0.001; ns, not significant; one-way ANOVA.

CHAPTER FOUR

DOCK7 controls INM and neurogenesis by antagonizing TACC3's microtubule growth promoting function

4.1 Introduction

In chapters two and three, I described the evidence we obtained demonstrating that DOCK7 influences RGC proliferation versus differentiation and neurogenesis by controlling the basal-to-apical step of INM. We next wanted to gain insight into the molecular mechanism(s) by which DOCK7 controls INM and neurogenesis. To this end I first explored whether DOCK7's GEF activity toward Rac GTPases is involved. As described below in results section 4.2.1, I focused that the GEF activity of DOCK7 is not required for its role in INM and neurogenesis.

These findings indicated that other interactions are important for the latter functions of DOCK7. To identify potentially relevant interactions, we decided to revisit the results of yeast two hybrid screens performed by a previous student in the lab, Keisha John, who used 3 different DOCK7 fragments as baits to screen an embryonic mouse brain cDNA library. Among the DOCK7-interacting candidates, three coded for the transforming acidic coiled-coil 3 protein, TACC3, which was of particular interest to us for the following reasons.

TACC3, a centrosome- and microtubule-associated protein, belongs to the TACC family harboring a highly conserved C-terminal coiled-coil domain[148]. The TACC3 protein is localized to the centrosome and mitotic spindles and is expressed in a variety of tissues during embryonic development, including the cerebral cortex[149,150](and see Figure 4.1). TACC3 was found to be important for centrosome integrity, spindle stability[151], MT growth and nuclear migration[152]. Of

particular interest, a more recent study implicated the TACC proteins together with the centrosomal protein Cep120 in the regulation of INM and maintenance of the neural progenitor pool during mouse neocortical development[76]. In particular, Tsai and colleagues showed that INM is dependent on Cep120 and TACC mediated the regulation of centrosomal-associated MTs, which maintain the coupling between the centrosome and the nucleus. In this process, Cep120 regulates the centrosomal localization of TACCs, which in turn promote the growth of centrosome-associated MTs. Knockdown of either Cep120 or TACCs impaired INM and disrupted the ability of progenitors to undergo mitosis apically, and these cells instead divided at a more basal position, away from the ventricular surface[76]. Significantly, the INM defects resulting from loss of Cep120 or TACCs were accompanied by accelerated cell cycle exit and premature differentiation of neocortical progenitors into neurons, resulting in a depletion of the proliferating progenitor pool[76]. Notably, no effect on cell cycle length and mitotic spindle orientation was observed[76]. Together, their data suggest that the function of Cep120 and TACC proteins is to regulate centrosome-mediated INM and thereby to regulate the mode of division of the cortical progenitor cells.

This chapter describes the experiments we performed to address the physiological importance of the DOCK7/TACC3 interaction in controlling INM and neurogenesis. These experiments were performed in collaboration with Chia-Lin Wang, a postdoctoral fellow in the Van Aelst laboratory. Our studies revealed that DOCK7 interaction with TACC3 is important for its effects on INM and neurogenesis. Specifically, we showed that DOCK7 exerts its effects by antagonizing the MT growth and stabilizing function of TACC3. These results reveal the molecular mechanism by which DOCK7 controls INM thereby influences RGC proliferation versus differentiation and consequently neurogenesis in the developing neocortex.

4.2 Results

4.2.1 DOCK7 controls INM and neurogenesis independently of its GEF activity towards Rac

In order to gain further insight into the molecular mechanism(s) by which DOCK7 controls INM and neurogenesis, we started by exploring whether the GEF activity of DOCK7 is involved. DOCK7, similar to other DOCK180 family members, contains a conserved DHR2 domain that catalyzes the exchange of GDP for GTP on Rac and/or Cdc42 GTPases[87,103,104]. This domain, as described in chapter one, was shown to be important for DOCK7's role in axon formation[103]. To determine whether it is also important for DOCK7's role in INM and genesis of neurons, we expressed the DOCK7ΔDHR2 mutant[103] together with DOCK7#2 shRNA in cortical progenitors and tested whether this mutant is able to rescue the DOCK7 RNAi-evoked effects on INM, RGC expansion and neuron production. To our surprise, DOCK7ΔDHR2 was able to rescue all phenotypes to a similar degree as seen with DOCK7 WT (Figure 4.6). This finding indicated that the DHR2 domain of DOCK7 and its GEF activity toward Rac/Cdc42 are dispensable for DOCK7's role in INM and cortical neurogenesis.

4.2.2 DOCK7 interacts with TACC3 *in vitro* and *in vivo*

We next test whether DHR1 domain is required. We expressed the DOCK7ΔDHR1 mutant together with DOCK7#2 shRNA in cortical progenitors and tested whether this mutant is able to rescue the DOCK7 RNAi-evoked effects on RGC expansion and neuron production. As shown in Figure 4.2, DHR1 domain of DOCK7 is not required for its role in INM and neurogenesis. Since both DHR2 and DHR1 domains of DOCK7 are not required for INM and corticogenesis, we decided to search for DOCK7-interacting proteins other than small GTPases. To this end, we started by scrutinizing the results of YTH screens performed by K. John using an embryonic mouse brain cDNA library and 3 fragments of DOCK7 as bait (Figure 4.3a).

Figure 4.1

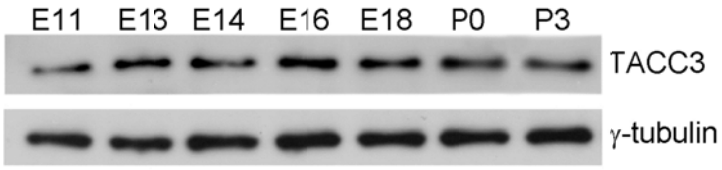

Figure 4.1. Expression of TACC3 in embryonic mouse cortex. Lysates from embryonic day 11 (E11), E13, E14, E16, and E18, and postnatal day 0 (P0), and P3 mouse cortices were subjected to Western Blot analysis using anti-TACC3 antibody. γ-tubulin was used as a loading control.

Figure 4.2

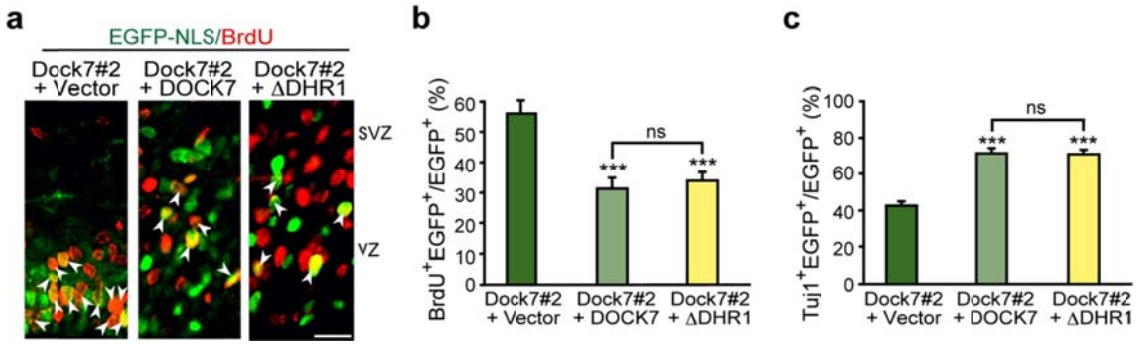

Figure 4.2. The DHR1 domain of DOCK7 is not required for its role in INM and neurogenesis. Mouse embryos were co-electroporated at E13.5 with plasmids expressing EGFP-NLS (a,b) or EGFP (c) marker protein and plasmids expressing Dock7 targeting shRNA (Dock7#2) and empty control vector (vector), FLAG-DOCK7 WT (DOCK7) or FLAG-DOCK7ΔDHR1 (ΔDHR1), pulse labeled with BrdU for 2 h (a,b) at E15.5, or not labeled (c), and sacrificed. Coronal brain slices were co-immunostained for EGFP and BrdU (a,b) or Tuj1 (c). (**a**) Confocal images of the VZ/SVZ of electroporated neocortices co-immunostained for EGFP (green) and BrdU (red). Arrowheads indicate transfected cells that are $BrdU^+$. Scale bar, 20 μm. (**b**) Quantification of the percentage of transfected cells that are $BrdU^+$ in VZ. Data are mean ± s.e.m.; *n* = 1137-1189 cells; from 3 animals for each condition. ***$P < 0.001$; $P = 0.205$ between Dock7#2+DOCK7 and Dock7#2+DOCK7ΔDHR1; ns, not significant; one-way ANOVA. (**c**) Quantification of the percentage of transfected cells that are $Tuj1^+$ in entire neocortex. Data are mean ± s.e.m.; *n* = 2098-2211 cells; from 3 animals for each condition. ***$P < 0.001$; $P = 0.576$ between Dock7#2+DOCK7 and Dock7#2+DOCK7ΔDHR1; ns, not significant; one-way ANOVA.

Figure 4.3

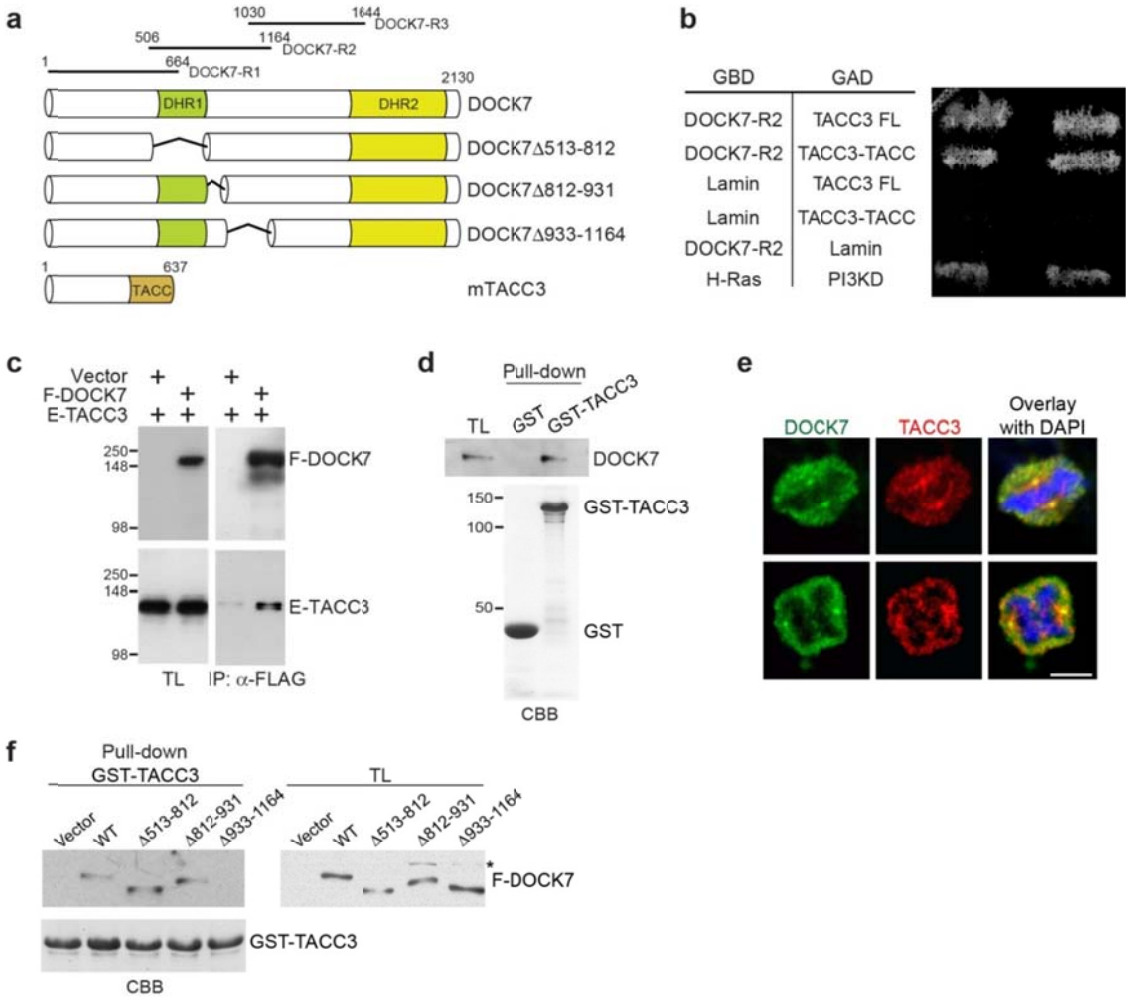
a
1030
1644
DOCK7-R3
506
1164
DOCK7-R2
1
664
DOCK7-R1
2130
DHR1
DHR2
DOCK7
DOCK7Δ513-812
DOCK7Δ812-931
DOCK7Δ933-1164
1
637
TACC
mTACC3
b
GBD
GAD
DOCK7-R2
TACC3 FL
DOCK7-R2
TACC3-TACC
Lamin
TACC3 FL
Lamin
TACC3-TACC
DOCK7-R2
Lamin
H-Ras
PI3KD
c
Vector
F-DOCK7
E-TACC3
250
148
98
F-DOCK7
E-TACC3
TL
IP: α-FLAG
d
Pull-down
TL
GST
GST-TACC3
DOCK7
GST-TACC3
GST
150
100
50
CBB
e
DOCK7
TACC3
Overlay with DAPI
f
Pull-down
GST-TACC3
TL
Vector
WT
Δ513-812
Δ812-931
Δ933-1164
F-DOCK7
GST-TACC3
CBB

Figure 4.3. DOCK7 interacts with TACC3. (a) DOCK7 and TACC3 domain structure and deletion constructs. The DOCK7-R1, R2 and R3 fragments used as baits in yeast two hybrid (YTH) screens are indicated at the top. **(b)** YTH interaction between DOCK7-R2 and TACC3. The PJ69a yeast strain was transformed with plasmids expressing DOCK7-R2 fused to the GAL4 DNA-binding domain (GBD), and full-length (TACC3 FL) or TACC-motif of TACC3 (TACC3-TACC) fused to the GAL4 activation domain (GAD), and transformed colonies were tested for growth on medium lacking histidine. Lamin was included as a negative control, and H-Ras and PI3-kinase delta (PI3KD) as positive control for YTH interaction. **(c)** DOCK7 associates with TACC3 in mammalian cells. Cell lysates from HEK293 cells transiently expressing FLAG-DOCK7 (F-DOCK7) and/or EGFP-TACC3 (E-TACC3) were incubated with anti-FLAG antibody and immunoprecipitates (IP) were analyzed by Western blotting with anti-FLAG and anti-EGFP antibodies. TL, total cell lysate. **(d)** GST-TACC3 fusion protein, or GST alone, immobilized on glutathione beads was incubated with extracts from E13.5 mouse cortices. Bound DOCK7 was detected by immunoblotting with anti-DOCK7 antibody. TL, total cell lysate. GST-TACC3 fusion protein, or GST alone, was visualized by Coomassie Brilliant Blue (CBB) staining (lower panel). **(e)** DOCK7 colocalizes with TACC3 at the centrosome of mitotic human neuroblastoma SK-N-BE cells. SK-N-BE cells were co-immunostained for DOCK7 (green) and TACC3 (red), and counterstained with DAPI (blue). Confocal images of cells in metaphase (top) and in anaphase (bottom) are shown. Scale bar, 2 μm. (**f**) Mapping the TACC3-binding region in DOCK7. GST-TACC3 fusion protein (lower panel, CBB staining) immobilized on beads was incubated with extracts from HEK293 cells expressing empty control vector (vector), FLAG-DOCK7 wild type (WT) or one of the indicated FLAG-DOCK7 deletion constructs. The bound proteins were detected by immunoblotting with anti-FLAG antibody. TL, total cell lysate. Asterisk indicates non-specific band.

Among the DOCK7-interacting candidates, two of the positive clones contained identical cDNAs matching the TACC domain encoding sequence of TACC3, and another contained full-length TACC3. All these clones were obtained using DOCK7-R2 (aa 506-1164) as bait (Figure 4.3a). As mentioned above, TACC3 is a member of the TACC family, centrosome- and microtubule-associated proteins, which have been implicated in centrosome-directed microtubule growth, nuclear migration, and, significantly, in maintaining the neural progenitor pool during mouse neocortical development[76,149,152]. Notably, TACC3 is expressed throughout neurogenesis in the developing neocortex (Figure 4.1).

The interaction between DOCK7 and TACC3 was subsequently validated by several approaches. First, the YTH interaction (Figure 4.3b) was confirmed by coimmunoprecipitation experiments, using lysates prepared from HEK293 cells co-expressing FLAG-DOCK7 and EGFP-TACC3 (Figure 4.3). Second, the association between DOCK7 and TACC3 was demonstrated by a GST-fusion protein pull-down assay. As shown in Figure 4.3d, Beads loaded with GST-TACC3 efficiently pulled-down endogenous DOCK7 from lysates of E13.5 mouse cortices. Finally, colocalization studies in the human SK-N-BE neuroblastoma cell line using anti-DOCK7 and anti-TACC3 antibodies revealed that DOCK7 and TACC3 display overlapping staining patterns, particularly, at the centrosome (Figure 4.3e). Thus, these data verify the yeast two-hybrid results and demonstrate that these two proteins interact with the R2 fragment of DOCK7 sufficient for binding. To further determine the TACC3-binding domain in DOCK7, we generated several mutants containing deletions within the R2 fragment (Figure 4.3a) and tested them for their ability to interact with TACC3 in GST pull-down assays. Among these deletion mutants, we found that DOCK7Δ933-1164, henceforth called DOCK7ΔTACC3, failed to bind TACC3 (Figure 4.3f).

4.2.3 DOCK7 controls INM and neurogenesis by antagonizing TACC3 function

We next investigated the relevance of the DOCK7-TACC3 interaction in INM and

neurogenesis. A previous study showed that knockdown of TACCs halted bl-to-ap INM, decreased the number of proliferating progenitors, and increased neuron production[76], all opposite to the effects of DOCK7 knockdown. Since in the latter study a mixture of siRNAs targeting all three TACC family members was used, we first investigated whether silencing of TACC3 alone is sufficient to produce the above phenotypes. We found that this is indeed the case; knockdown of TACC3 impaired bl-to-ap INM, decreased the BrdU labeling and mitotic index, and increased the percentage of $Tuj1^+$ cells (Figure 4.4a-e). Thus, these data indicated that DOCK7 and TACC3 have opposing functions during cortical neurogenesis. Based on this finding, and the fact that centrosome-associated TACC3 promotes microtubule growth, we then asked whether DOCK7 exerts its effect on INM and neurogenesis by antagonizing TACC3 function.

If this is the case, we reasoned that simultaneous knockdown of TACC3 and DOCK7 should counteract the phenotypes resulting from DOCK7 deficiency, while a DOCK7 mutant that failed to bind TACC3 should not be able to rescue them. To test the first postulation, E13.5 embryonic cortices were electroporated with plasmids co-expressing Dock7#2 or scr#1 shRNA and EGFP-NLS (or EGFP) together with plasmids co-expressing Tacc3#1 or scr#2 shRNA and RFP-NLS (or RFP), and brains were examined 2 days later. As expected, co-electroporation of the Dock7#2 and scr#2 shRNA expressing vectors resulted in the same phenotypes as expressing Dock7#2 shRNA alone; i.e. a higher percentage of cells dividing at apical positions, an increased number of proliferating VZ progenitors, and a decrease in neuron production. Importantly, simultaneous TACC3 knockdown completely rescued these phenotypes (Figure 4.5 a-e).

To test whether a DOCK7 mutant defective in TACC3 binding is able to rescue the DOCK7 RNAi-evoked phenotypes, we co-electroporated plasmids expressing Dock7#2 shRNA and DOCK7ΔTACC3. As shown in Figure 2.6 and 4.6, both DOCK7 WT and DOCK7ΔDHR2

Figure 4.4

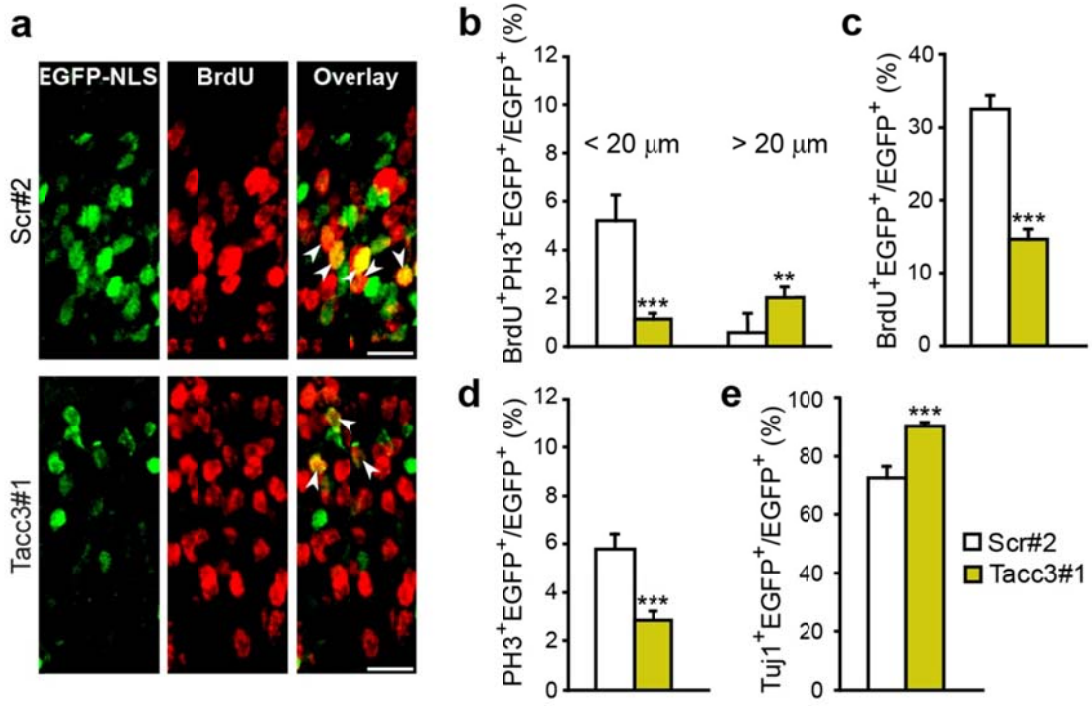

Figure 4.4. DOCK7 and TACC3 have opposing functions. Mouse embryos were electroporated at E13.5 with EGFP-NLS- (a-d) or EGFP- (e) expressing construct together with plasmids expressing non-targeting shRNA (scr#2) or Tacc3 targeting shRNA (Tacc3#1), pulse labeled with BrdU for 2 h (a,c) or 6 h (b) at E15.5, or not labeled (d,e), and sacrificed. Coronal brain slices were co-immunostained for EGFP and BrdU (a,c), BrdU and PH3 (b), PH3 (d), or Tuj1 (e). **(a)** Confocal images of the VZ/SVZ of neocortices co-immunostained for EGFP (green) and BrdU (red). Arrowheads indicate transfected cells that are $BrdU^+$. **(b-e)** Quantification of the percentage of transfected cells that are $BrdU^+$ and $PH3^+$ < 20 μm or > 20 μm away from ventricular surface in VZ (b); $BrdU^+$ in VZ (c); $PH3^+$ in VZ (d); or $Tuj1^+$ in entire neocortex (e). Data are mean ± s.e.m.; *n* = 793-2498 cells from at least 3 animals for each condition. ***P* < 0.01, ****P* < 0.001; ns, not significant; Student's *t*-test; Scale bars, 20 μm.

Figure 4.5

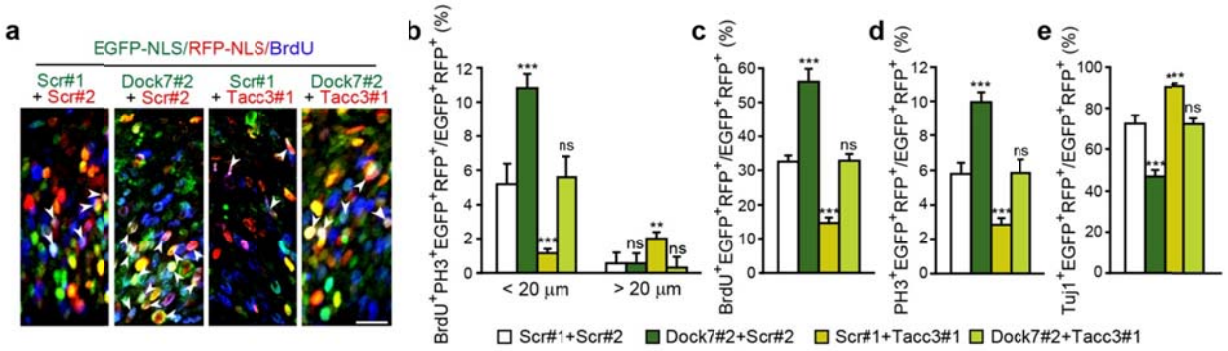

Figure 4.5. DOCK7 antagonizes TACC3 function during cortical neurogenesis (I). Simultaneous knockdown of TACC3 rescues DOCK7 knockdown phenotypes. Mouse embryos were co-electroporated at E13.5 with plasmids co-expressing EGFP-NLS (or EGFP in **e**) and scr#1 or Dock7#2 shRNA and/or plasmids co-expressing RFP-NLS (or RFP in **e**) and scr#2 or Tacc3#1 shRNA, pulse labeled with BrdU for 2 h (a,c) or 6 h (b) at E15.5, or not labeled (d,e), and sacrificed. Coronal brain slices were co-immunostained for EGFP and BrdU (a,c), BrdU and PH3 (b), PH3 (d), or Tuj1 (e). **(a)** Confocal images of the VZ/SVZ of electroporated neocortices co-immunostained for EGFP (green), RFP (red) and BrdU (blue). Arrowheads indicate double-transfected (EGFP-NLS$^+$ and RFP-NLS$^+$) cells that are BrdU$^+$. **(b-e)** Quantification of the double-transfected cells that are BrdU$^+$ and PH3$^+$ < 20 μm or > 20 μm away from ventricular surface in VZ (b); BrdU$^+$ in VZ (c); PH3$^+$ in VZ (d); or Tuj1$^+$ in entire neocortex (e). Data are mean ± s.e.m.; n = 790-2031 cells from at least 3 animals for each condition. $^{**}P < 0.01$, $^{***}P < 0.001$; ns, not significant; one-way ANOVA; Scale bars, 20 μm.

Figure 4.6

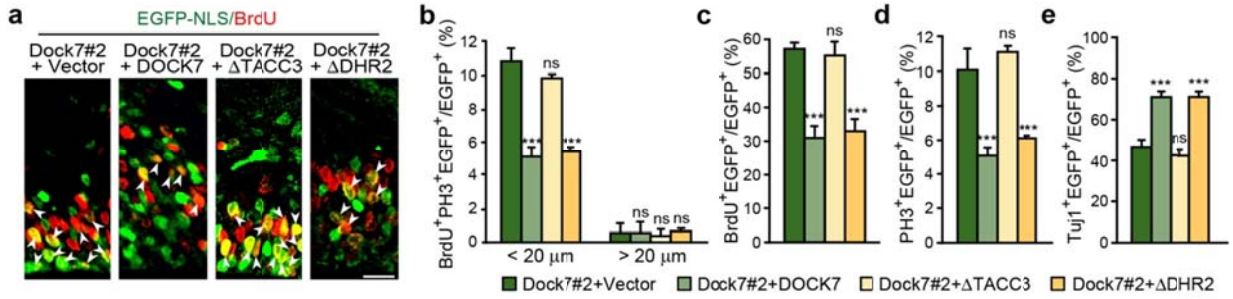

Figure 4.6. DOCK7 antagonizes TACC3 function during cortical neurogenesis (II). (a-e) DOCK7ΔTACC3 (ΔTACC3), but not DOCK7ΔDHR2 (ΔDHR2), fails to rescue DOCK7 knockdown phenotypes. Mouse embryos were electroporated at E13.5 with EGFP-NLS-expressing plasmid together with the indicated constructs, and pulse labeled with BrdU for 2 h (a,c) or 6 h (b) at E15.5, or not labeled (d,e), and sacrificed. Coronal brain slices were co-immunostained for EGFP and BrdU (a,c), BrdU and PH3 (b), PH3 (d), or Tuj1 (e). **(a)** Confocal images of the VZ/SVZ of electroporated neocortices co-immunostained for EGFP and BrdU. Arrowheads indicate transfected cells that are $BrdU^+$. **(b-e)** Quantification of the transfected cells as in b-e. Data are mean ± s.e.m.; *n* = 792-2329 cells from at least 3 animals for each condition. $^{**}P < 0.01$, $^{***}P < 0.001$; ns, not significant; one-way ANOVA; Scale bars, 20 μm.

can rescue the INM defect, the increase in dividing VZ progenitors and decrease in neuron production caused by DOCK7 RNAi. In contrast to DOCK7 WT and DOCK7ΔDHR2, DOCK7ΔTACC3 failed to rescue these phenotypes (Figure 4.6 a-e). Together, these data indicate that DOCK7 controls INM and cortical neurogenesis by antagonizing TACC3 function.

4.2.4 DOCK7 antagonizes the microtubule growth promoting and stabilizing function of TACC3

As discussed before, TACC proteins were reported to control INM of cortical neural progenitors by regulating the growth and integrity of centrosome-associated microtubules (MTs) coupling the centrosome and the nucleus[76]. Therefore, we directly assessed whether DOCK7 antagonizes the MT growth-promoting function of TACC3. We first examined this by ectopically expressing FLAG-DOCK7 and/or EGFP-TACC3 in COS7 cells, as expression of TACC3 in these cells was shown to increase the size of the MT aster emanating from the centrosome[76]. In contrast to TACC3, expression of DOCK7 decreased the size of the MT aster, and, importantly, that co-expression of DOCK7 with TACC3 restored the MT aster size to that seen in control vector transfected cells (Figure 4.7). To test whether any of these manipulations affected MT nucleation, COS7 cells were treated with nocodazole (which depolymerizes MTs), and subsequently allowed to recover after drug washout. We observed that after a 5 min recovery period, most of the transfected cells in all groups showed a clear MT aster, indicating that MT nucleation was not affected. However, after 20 min of recovery, similar to the results in Figure 4.7a, DOCK7 and TACC3 expressing cells showed a smaller and larger MT aster, respectively, compared to control cells and cells co-expressing DOCK7 and TACC3 (Figure 4.8).

We then extended these studies to cortical neural progenitors. These cells display a MT “fork”-like structure which consists of two or more prominent MT bundles coupling the centrosome and the nucleus[76]. As expected, knockdown of TACC3 in cultured cortical

Figure 4.7

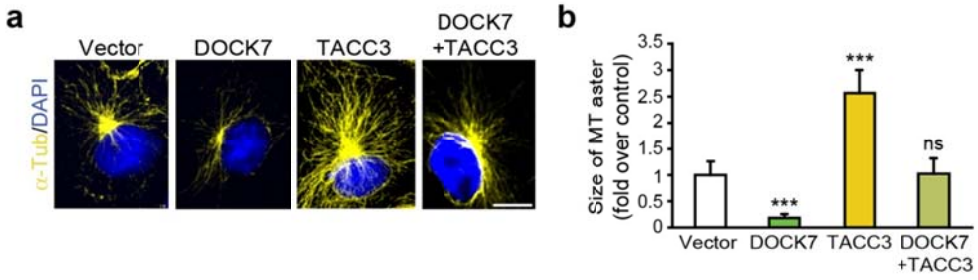

Figure 4.7. DOCK7 antagonizes the ability of TACC3 to increase the size of the MT aster in COS7 cells. (a) γ-tubulin immunostaining (yellow) of COS7 cells expressing FLAG-DOCK7 (DOCK7) and EGFP-TACC3 (TACC3) alone, or in combination. Cells were also co-immunostained for FLAG and EGFP (not shown), and counterstained with DAPI (blue). Scale bar, 10 μm. **(b)** Measurement of the size of the MT aster. The average size of the MT aster of control vector transfected cells was set as 1. Data are mean ± s.e.m.; *n* = 69-115 cells from 3 independent experiments for each condition. ****P* < 0.001; ns, not significant; one-way ANOVA.

Figure 4.8

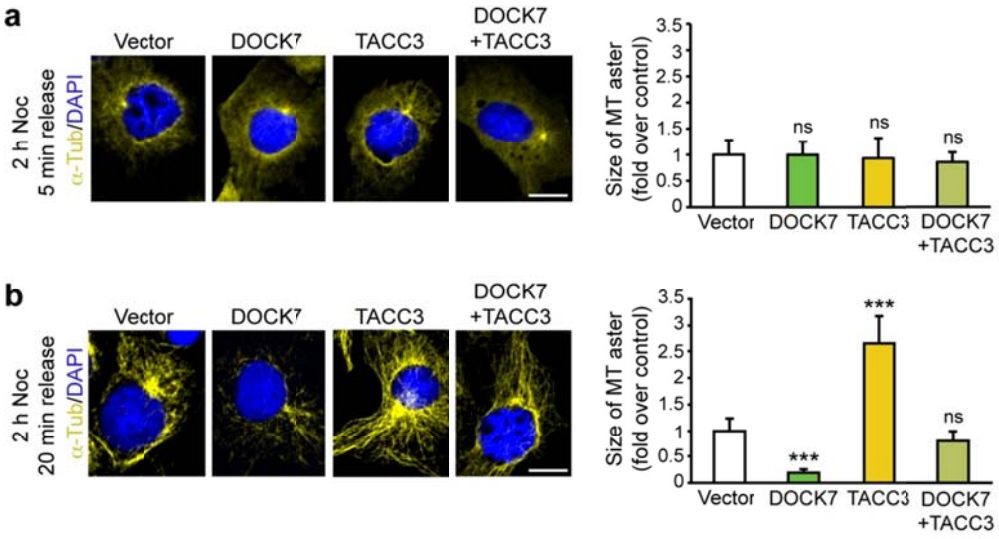

Figure 4.8. Neither DOCK7 nor TACC3 affects centrosomal microtubule nucleation. (a,b) COS7 cells were transfected with empty control vector (vector) or plasmids expressing FLAG-DOCK7 (DOCK7) and EGFP-TACC3 (TACC3) alone, or in combination. 3 days post-transfection, cells were treated with 5 μg/ml nocodazole (noc) for 2 hours. Following treatment, cells were washed with PBS and allowed to recover in nocodazole-free medium for 5 min (a) or 20 min (b). Left panels: γ-tubulin immunostaining (yellow) of transfected COS7. Cells were also co-immunostained for FLAG and EGFP (not shown), and counterstained with DAPI (blue). Scale bars, 10 μm. Right panels: Measurement of the MT aster size relative to that of control vector, which was set as 1. Data are shown as mean ± s.e.m. (a: n = 63-127 cells; b: n = 59-105 cells; from 3 independent experiments for each condition). ***P < 0.001; ns, not significant; one-way ANOVA.

Figure 4.9

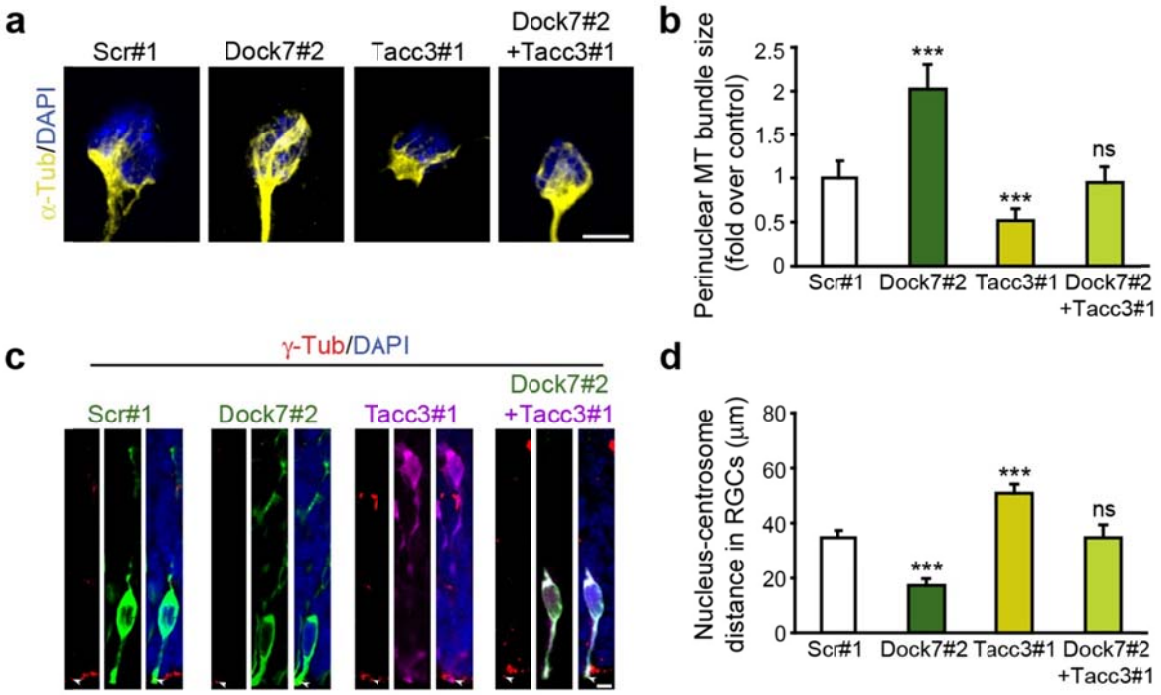

Figure 4.9. DOCK7 antagonizes the MT growth-promoting/stabilizing function of TACC3. **(a,b)** Simultaneous silencing of TACC3 prevents the enlargement of the MT "fork"-like structure caused by DOCK7 knockdown in cultured neocortical cells. Mouse neocortices were transfected via electroporation at E12.5 with plasmids co-expressing EGFP and scr#1 or Dock7#2 shRNA, RFP and Tacc3#1 shRNA, or both the Tacc3#1 and Dock7#2 shRNA-expressing plasmids, and dissociated at E13.5. Neocortical cells were cultured for 2 days and then immunostained for γ-tubulin (yellow), EGFP and/or RFP (not shown), and counterstained with DAPI (blue). (**c**) Representative images showing MT "fork"-like structure in transfected neocortical cells. Scale bar, 5 μm. **(b)** Measurement of perinuclear MT bundle size of the "fork"-like structure. The average MT bundle size of scr#1 shRNA transfected cells was set as 1. Data are mean ± s.e.m.; *n* = 77-103 cells from 3 independent experiments for each condition. ***$P < 0.001$; ns, not significant; one-way ANOVA. **(c,d)** Silencing of TACC3 rescues the decrease in nucleus-centrosome distance caused by DOCK7 knockdown in RGCs *in vivo*. Mouse embryos were electroporated at E13.5 as in c, and sacrificed at E15.5. Coronal brain slices were immunostained for γ-tubulin (red), EGFP (green) and/or RFP (purple), and counterstained with DAPI (blue). **(c)** Examples of transfected RGCs. Arrowheads indicate centrosomes of transfected cells. Scale bar, 5 μm. **(d)** Quantification of nucleus-centrosome distance. Data are mean ± s.e.m.; *n* = 215-371 cells from 3 animals for each condition. ***$P < 0.001$; ns, not significant; one-way ANOVA.

progenitors decreased the size of the MT “fork”-like structure, while knockdown of DOCK7 increased the overall size (Figure 4.8a,b). Importantly, simultaneous knockdown of TACC3 and DOCK7 restored the size of the MT “fork”-like structure to that seen in control cells (Figure 4.9a,b).

Finally, we measured the nucleus-centrosome distance in RGCs expressing Dock7#2 shRNA, Tacc3#1 shRNA or both, as this distance is affected by alterations in MT growth and integrity[76,153]. To this end, brain slices prepared from electroporated embryos were stained with γ-tubulin (centrosomal marker) and counterstained with DAPI (nuclear marker), and the nucleus-centrosome distance was measured. We found that in contrast to Tacc3#1 shRNA expressing RGCs, where the nucleus-centrosome distance was increased, this distance was significantly decreased in Dock7#2 shRNA expressing RGCs, which, importantly, could be restored to that seen for scr#1 expressing RGCs by co-expression of Tacc3#1 shRNA (Figure 4.9c,d). Combined with the above data, these findings indicate that DOCK7 antagonizes the MT growth-promoting/stabilizing function of TACC3. Of note, this effect of DOCK7 is independent of its DHR2 domain, as DOCK7ΔDHR2 was able to rescue the DOCK7 RNAi evoked decrease in nucleus-centrosome distance (Figure 4.10).

Figure 4.10

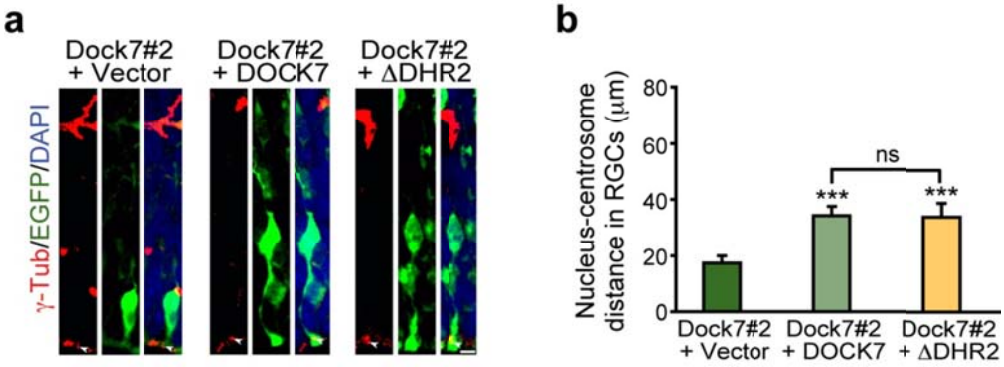

Figure 4.10. DOCK7ΔDHR2 rescues the decrease in nucleus-centrosome distance caused by DOCK7 knockdown in RGCs *in vivo*. Mouse embryos were electroporated at E13.5 with a plasmid co-expressing EGFP marker protein and Dock7 targeting shRNA (Dock7#2), together with an empty control vector (vector), a FLAG-DOCK7 WT (DOCK7) or a FLAG-DOCK7ΔDHR2 (ΔDHR2)-expressing plasmid, and sacrificed at E15.5. Coronal brain slices were co-immunostained for γ-tubulin (red) and EGFP (green), and counterstained with DAPI (blue). (**a**) Examples of transfected RGCs. Arrowheads indicate centrosomes of transfected cells. Scale bar, 5 μm. (**b**) Quantification of nucleus-centrosome distance. Data are mean ± s.e.m.; *n* = 257-323 cells; from 3 animals for each condition. ***$P < 0.001$; $P = 0.185$ between Dock7#2+DOCK7 and Dock7#2+ DOCK7ΔDHR2; ns, not significant; one-way ANOVA.

CHAPTER FIVE

Discussion and Prospective

Fundamental to the proper development of the mammalian cerebral cortex is the ability of RGCs to balance self-renewal with neuronal differentiation in an appropriate temporal manner. Disruption of this balance has been associated with several neurological and neuropsychiatric disorders, ranging from microcephaly to Schizophrenia[34,154]. Defects in *ASPM* (microcephaly)[155] and *DISC-1* (Schizophrenia)[156], for example, result in precocious generation of excess neurons that prematurely depletes the progenitor pool and leads to insufficient neurons at later stages, which then results in an abnormal brain structure development. Key determinants reported to influence RGC function during neurogenesis include cell polarity, cell cycle duration, and, more recently, INM[2,20,22,23,36], of which the latter remains less well understood. In this dissertation, I present evidence that DOCK7, a member of the DOCK180 family proteins, controls bl-to-ap INM by antagonizing the microtubule (MT) growth-promoting function of TACC3, and thereby controls the genesis of neurons from RGCs.

With the onset of neurogenesis, RGCs typically start switching from proliferative to differentiative neuron generating divisions. As such, the number of RGCs is maintained by self-renewal throughout the peak of neurogenesis, and meanwhile the population of neurons expanded[1,2,32,33,37]. The data shown in this thesis implicate a critical role of DOCK7 in the regulation of this switch. Knockdown of DOCK7 expanded the radial glial progenitor pool with favoring the maintenance of RGCs as cycling progenitors at the apical side of the VZ. Significantly, with the expansion of RGCs, generation of BPs and neurons was reduced, implying that neuronal differentiation was impaired at the RGC stage. Ectopic expression of

DOCK7, on the other hand, resulted in an increase in BP and neuron production, and a concomitant reduction in cycling RGCs, indicating accelerated differentiation of RGCs. These data indicate that DOCK7 plays a key role in the regulation of RGC proliferation versus differentiation and is required for the proper genesis of neurons from RGCs.

5.1 Non-redundant role of DOCK7 in INM and neurogenesis

DOCK7 belongs to the DOCK-C subfamily of DOCK180 superfamily, which consists of 11 members. Our findings indicate that other DOCK180 family members do not compensate for the function of DOCK7 in controlling INM and neurogenesis, as knockdown of DOCK7 alone is sufficient to cause defects in both processes (Figure 2.6, 2.11 and 2.12). This is perhaps not surprising, since the overall similarity among the DOCK180 family members is largely restricted to the DHR2 and DHR1 domains; none of which appears to be required for DOCK7 function in neurogenesis (Figure 4.2 and 4.6). Non-redundant functions for several of the DOCK180 family members have been previously reported, with for example DOCK1, DOCK2, and DOCK3 mutant mice displaying defects in myoblast fusion[112], lymphocyte migration/recirculation[113,115] and central axonal dystrophy[117], respectively.

It should be noted that recently mice carrying a nonsense mutation in the *Dock7* locus that originate from a chemical mutagenesis screen have been described[157]. These mice were not reported to exhibit gross neurological or behavioral abnormalities in tests probing innate and/or anxiety/stress related behavior[157]. The point mutation that disrupts the DOCK7 coding sequence, however, does still allow for expression of a truncated DOCK7 protein. Thus, it remains to be seen whether this is functional null. Furthermore, Blasius et al did not carry out any anatomical studies, and all the behavioral tests performed examined innate behavioral and/or anxiety/stress related behavior, all of which do not require training. It would be interesting to assess the mutant mice specifically for cognitive in puissant linked to cortical dysfunction, which DOCK7 defects would be expect to lead to.

5.2 DOCK7 controls bl-to-ap leg of INM

Our data demonstrated a central role for DOCK7 in the INM process, and support a model in which DOCK7 influences the mode of RGC division and genesis of neurons through its regulatory effects on bl-to-ap INM. We found that ectopic expression of DOCK7 impeded bl-to-ap INM of RGCs, without, importantly, affecting cell cycle progression (Figure 3.2, 3.3 and 2.10). This led to an extended residence of RGCs' nuclei at basal locations and occurrence of mitoses at ectopic sites away from the ventricular surface, producing daughter cells that likely differentiated into BPs and/or neurons, as the numbers of both were increased upon DOCK7 overexpression, while those of RGCs were decreased (Figure 2.7 and 2.11). In line with this, increased neurogenesis has been reported in other studies, in which INM was impaired upon knockdown of Cep120 or Hook3[75,76].

Conversely, knockdown of DOCK7 accelerated the movement of RGCs' nuclei from bl-to-ap positions, resulting in an extended apical residency of the RGCs' nuclei and occurrence of apical mitoses (Figure 3.3). This was associated with an increase in RGCs and reduction in BPs and neurons, implying that an extended nuclear residence at the apical side favors RGCs to divide symmetrically, with two RGCs as progeny (Figure 2.6 and 2.11). In concurrence with our model are reports indicating an enrichment of proliferative signals at the apical versus the basal axis of the neuroepithelium[20,22,68,74]. Thus, we posit that DOCK7 controls the bl-to-ap INM step and thereby influences RGC behavior and neurogenesis. Of note, our studies revealed that the progenitors undergo S phase at their normal basal position regardless of the levels of DOCK7 expression, consistent with a normal ap-to-bl basal migration of RGC nuclei during the G1 phase.

Importantly, we performed several experiments to determin that other properties of RGCs were not affected by altering the levels of DOCK7. First, Caspase-3 immunostaining revealed that DOCK7 overexpression did not trigger apoptosis of RGCs (Figure 2.8). Second,

BrdU experiments and Flow cytometry analysis revealed that DOCK7 knockdown did not affect cell cycle progression (Figure 2.10). Moreover, we found that RGC adhesion and polarity is not affected, as revealed by RGC coupling by adherens junctions to the apical side of the neuroepithelium (Figure 3.1). These results support our finding that DOCK7 exerts its function by controlling INM without interfering with other properties of RGCs.

5.3 DOCK7 exerts its effect on INM and neurogenesis by antagonizing TACC3 function

Although initially somewhat surprising given the reported role(s) of Rho GTPases in INM[48,158,159], we found that DOCK7's effects on INM and neurogenesis do not require its catalytic DHR2 domain, and, hence, are not mediated by DOCK7's GEF activity toward Rac/Cdc42 (Figure 4.6). Instead, evidence from our studies indicates that DOCK7 exerts its effects by antagonizing the centrosome-associated MT growth-promoting/stabilizing function of TACC3. Specifically, the two proteins exerted opposing effects on centrosomal MT growth, and on INM and neurogenesis (Figure 4.4, 4.7 and 4.9). Additionally, the phenotypes associated with DOCK7 knockdown, including MT growth, INM and genesis of neurons, were rescued by reducing TACC3 levels (Figure 4.5). Finally, a DOCK7 mutant defective in TACC3 binding failed to rescue the DOCK7 RNAi-evoked phenotypes (Figure 4.6). We posit that fine-tuned regulation of the MT-associated function of TACC3 by DOCK7 controls the growth and dynamics of MTs coupling the centrosome and nucleus. As such, gain or suppression of TACC3 function facilitates or impedes, respectively, the movement of the nucleus toward the centrosome. The translocation of the nucleus along the MTs likely involves the minus end-directed motor dynein and associated proteins, as previously reported[68,81,84]. Future studies will be required to determine the precise mechanism(s) by which DOCK7 antagonizes TACC3's MT-associated function and how DOCK7 itself is regulated, and whether DOCK7 acts on other MT-controlled cellular processes as well.

How could DOCK7 antagonize the TACC3 MT associated function in concurrence with the cell cycle to regulate bl-to-ap INM? Interestingly, TACC3 protein levels are tightly linked with cell cycle progression, with its levels elevating from S to G_2/M phases and declining during mitotic exit[150,160]. This oscillation of TACC3 levels through the cell cycle is regulated by a proteasome-dependent pathway[160]. Our data demonstrated a central role for DOCK7 in the bl-to-ap leg of INM, where the RGCs reside in the S-to-G_2 phase of the cell cycle, and that DOCK7 exerts its effects by antagonizing the function of TACC3. Thus, a possible scenario is that DOCK7 antagonizes TACC3's function by regulating the expression levels of TACC3 in synchrony with the cell cycle.

Alternatively or additionally, the TACC3 protein is associated with the centrosomal region and mitotic spindle during mitosis, and localizes to the cytoplasm and perinuclear region in interphase[149,150]. Thus, a possible scenario is that altered DOCK7 expression disturbs the localization of TACC3, and as such interferes with TACC3's MT-associated function.

What are the upstream regulators of DOCK7 in the bl-to-ap INM process (S/G2 phases of RGCs) but not the ap-to-bl INM process (G1 phase)? They should include intracellular cues that regulate the progression of cell cycle and extracellular cues that provide the localization information of RGCs within the VZ. The localization of DOCK7 at the centrosome, an organelle that serves as the microtubule organizing center (MTOC) as well as a regulator of cell-cycle progression, suggests a potential relationship between DOCK7 and cell cycle regulatory molecules. Moreover, the centrosome of RGC resides close to the ventricular surface and extends cilia into the lateral ventricle, suggesting a potential relationship between DOCK7 and extracellular cues. Thus far, the only reported upstream regulator of DOCK7 is ErbB2. DOCK7 was found to mediate ErbB2-induced Schwann cells migration. ErbB2 interacts with and phosphorylate DOCK7, leading to activation of Rac1/Cdc42 and downstream c-Jun kinase, leading to Schwann cell myelination and migration[104]. ErbB2 in the developing rat brain was

reported to be mainly expressed within the VZ, as determined by in situ hybridization[161]. While it will be interesting to test whether the phosphorylation of DOCK7 by ErbB2 is important for its function in RGCs, it should be noted that DOCK7 function in neurogenesis does not required its DHR2 domain, and Rac activation. Hence, the identification of additional DOCK7-interacting proteins will aid to fully understand when and how does DOCK7 initiate its influence to the INM of RGCs. ErbB2 mediated phosphorylation of DOCK7 could though be important for its function in migration (see below).

5.4 Multi-functional role of DOCK7 in the developing neocortex

Besides controlling the genesis of neurons, our data suggest an additional role for DOCK7 in the polarization and/or migration of IZ neurons. This is shown by an increased number of Tuj1-positive neurons in the IZ, but not in the CP, upon ectopic expression of DOCK7. Since DOCK7's GEF activity toward Rac/Cdc42 was shown to be required for axon formation of hippocampal neurons[103] and migration of Schwann cells[104], we envision the GEF activity of DOCK7 to be also important for the polarization and/or migration of IZ neurons. To further address the role of DOCK7 in the latter process, expressing DOCK7 shRNA and/or DOCK7 WT or DOCK7ΔDHR2 proteins in postmitotic neurons under a NeuroD promoter or DCX promoter, which only express in newly born neurons, will help us to elucidate DOCK7's function and the requirement of its DHR2 domain in the migration of cortical neurons.

5.5 Potential role of DOCK7 in the adult neurogenesis

In this study, we found that DOCK7 plays an important role in the regulation of RGC proliferation versus differentiation in the developing neocortex. As mentioned in chapter two, DOCK7 is highly expressed during cortical neurogenesis and its levels of expression gradually reduce at postnatal stages. Our lab recently initiated the assessment of DOCK7 expression in the adult mouse brain. Although expression of DOCK7 in adult mouse brain is relatively low or

undetectable in many brain regions, DOCK7 expression was clearly detected in the subgranular zone (SGZ) of the dentate gyrus (DG) in the hippocampus, the subventricular zone (SVZ) of the lateral ventricles, the rostral migratory stream (RMS) and the olfactory bulb. Interestingly, both the SGZ of the DG in the hippocampus and the SVZ of the lateral ventricles have been demonstrated to harbor self-renewing neural progenitor cells (NPCs) and the neurogenesis continuously occurs throughout life (for review, see Zhao et al. 2008[162]). Therefore, expression of DOCK7 in these regions in the adult mouse brain suggests that it might also be involved in adult neurogenesis.

Although INM has as yet been reported in adult NPCs during their self-renewing division, DOCK7 may still exert its effects on adult NPCs by antagonizing the function of TACC3. Knockdown of TACC3 by shRNA in cultured adult NPCs was reported to promote neuronal differentiation. In addition, a pharmacological compound (KHS101), which can bind to TACC3 protein and suppress its function, was reported to promote cell cycle exit of adult hippocampal neuronal progenitors and to accelerate neuronal differentiation by increasing the expression of $p21^{WAF}$, a cyclin-dependent kinase inhibitor[163]. Thus, the accelerated neuronal differentiation upon TACC3 depletion was suggested to occur by promotion of cell cycle exit and concomitant activation of a neuronal differentiation program in NPCs. Furthermore, a study using an inducible TACC3 shRNA revealed that TACC3 depletion increases the expression levels of $p21^{WAF}$, thereby inducing a $p21^{WAF}$-mediated G0/G1 phase cell arrest[164]. Interestingly, we observed ectopic expression of DOCK7 promoted cell cycle exit while knockdown of DOCK7 maintained cells in the cell cycle. Thus, it will be interesting to test a) whether the increased neuronal differentiation caused by TACC3 depletion can be rescued by DOCK7 shRNA and b) whether the cell cycle exit of adult NPCs is controlled by DOCK7 antagonistic effect on TACC3 function in regulating $p21^{WAF}$ levels.

Newborn neurons derived from NPCs within the adult SGZ primarily migrate into the adjacent granule cell layer of the dentate gyrus to differentiate into mature dentate granule cells. In the adult SVZ, newborn neurons migrate a long distance through the rostral migratory stream (RMS) and become granule neurons and periglomerular neurons in the olfactory bulb (for review, see Zhao et al. 2008[162] and Hsieh 2012[165]). As depicted in Figure 2.12, DOCK7 also plays a role in cortical neuron migration during development. Hence, it will be interesting to test whether DOCK7 is also involved in regulating the migration of the newly generated neurons in the adult niche. Interestingly, proliferation of adult NPCs increases after injury to the brain. This holds substantial promise for neural repair after injury by generating new neurons which following migration to the site of injury region can replace the damaged neurons[166]. Therefore, it will be interesting to test whether DOCK7 might also be involved in the migration process of newborn neurons after brain injury.

As described before, the only reported mice carrying a nonsense mutation in the *Dock7* locus do still allow for expression of a truncated DOCK7 protein, while so far no complete *Dock7*-null mouse strain is available. To further address the role of DOCK7 in cortical development, the use of a conditional DOCK7 knockout mouse could provide further insight. To this end, we plan to obtain the DOCK7 conditional knockout ES cells from EUCOMM (The European Conditional Mouse Mutagenesis Program) and generate DOCK7 conditional knockout mice. A Cre recombinase protein driven by a RGC specific promoter, i.e. *nestin* promoter, will be used to remove DOCK7 in embryonic brain. We expect that the overall thickness of neocortices will be thinner in these conditional DOCK7 knockout mice, as our finding indicated that loss of DOCK7 increases the proliferation of RGCs and decreases neuron production. It will be also interesting to perform several cognitive behavioral tests linked to cortical dysfunction, i.e. attention tests (multiple-choice serial-reaction task, go/no-go test) and learning/memory tests (object-discrimination test, eye-blink conditioning test)[167], when these mice are viable. To

assess the role of DOCK7 in the context of adult neurogenesis, a lentiviral vector expressing Cre recombinase could be delivered to the SVZ or DG of conditional DOCK7 knockout mouse brain by stereotactic injection to remove DOCK7 expression in NPCs in these regions. Subsequent to injection, neurogenesis and migration of DOCK7 knockout NPCs within these regions can be further followed up by consecutive BrdU incorporation method.

In summary (Figure 5.1), we show that DOCK7 controls bl-to-ap INM, and, importantly, the genesis of cortical neurons from RGCs, via interaction with the centrosome- and MT-associated protein, TACC3. As such, this study not only offers new insight into the function of DOCK7, but also sheds light on the INM process as it pertains to the regulation of RGC proliferation versus differentiation in the developing neocortex.

Figure 5.1

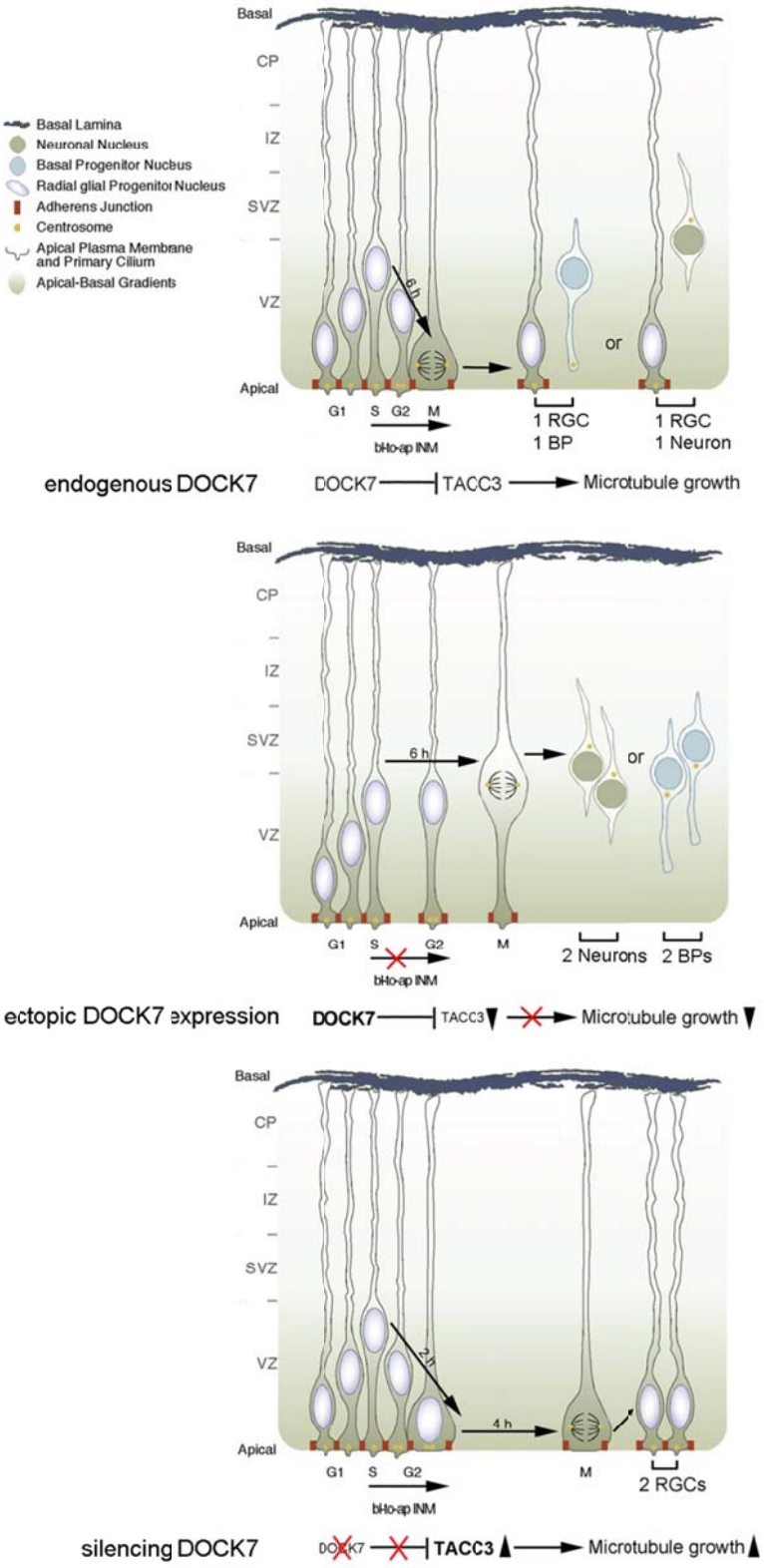

Figure 5.1 DOCK7 interacts with TACC3 to regulate interkinetic nuclear migration and genesis of neurons from cortical neuronal progenitors.

CHAPTER SIX

Materials and Methods

6.1 DNA constructs

cDNAs encoding full-length DOCK7 (pCAGGS-FLAG-DOCK7) and DOCK7ΔDHR2 (pCAGGS-FLAG-DOCK7ΔDHR2) were generated by pervious lab member M. Watabe-Uchida[103]. cDNAs encoding DOCK7Δ513-812 (DOCK7ΔDHR1), DOCK7Δ812-931 and DOCK7Δ933-1164 (DOCK7ΔTACC3) were subsequently cloned into pCAGGS[168] with the addition of an N-terminal FLAG epitope tag. The pEGFP-TACC3[76] plasmid was gift from L.-H. Tsai (MIT). pCAG-EGFP and pCAG-mKO2-F constructs were obtained by subcloning EGFP cDNA (Clontech) and mKO2-F cDNA[169] (provided by Dr. F. Matsuzaki, RIKEN) into pCAGGS, respectively. The yeast two-hybrid (YTH) constructs pGBD-DOCK7-R1, -R2, and -R3 were generated by insertion of cDNAs encoding amino acids 1-664 (R1), 506-1164 (R2) and 1030-1644 (R3) of DOCK7 into pPC97 (GAL4 DNA Binding Domain, GBD). pGAD-TACC3 full-length (FL) and pGAD-TACC3-TACC were obtained in YTH screen. The YTH constructs and screen were done by pervious laboratory member K. John. pGBD-Lamin, pGBD-H-Ras, pGAD-Lamin and pGAD-PI3KD were generated by subcloning cDNAs encoding Lamin, H-Ras and PI3-kinase delta into pPC86 (GAD) and pPC97(GBD), respectively. The GST-TACC3 construct was obtained by subcloning full-length mTACC3 cDNA into pGEX-4T-3 (GE Healthcare Biosciences). For RNAi knockdown experiments, previously described DNA fragments encoding short hairpin RNAs directed against 3'UTR of mouse DOCK7 mRNA (Dock7#2)[103] or mTACC3 mRNA (Tacc3#1)[76] were cloned into pSUPER (Oligoengine), a modified version of pSUPER in which

an EGFP, EGFP-NLS (nuclear localization signal) or a DsRed-NLS encoding sequence driven from the chicken β-actin promoter was inserted into the *XhoI* site of pSUPER, and in the case of Dock7#2 shRNA also into the pTRIPΔU3-EF1α-EGFP lentiviral vector[170]. cDNA encoding full-length DOCK6 (pCAGGS-FLAG-DOCK6) was generated by pervious lab member M. Watabe-Uchida. cDNA encoding full-length DOCK8 (pCA-FLAG-DOCK8) was generated from FLJ00346 clone (obtained from the Kazuza DNA Research Institute) with additional cDNA fragment encoding the N-terminal part of DOCK8 raised via cDNAs prepared from 293T cells.

6.2 Yeast two-hybrid screening

1×10^6 clones of a mouse fetal brain cDNA library in the pPC86 vector were screened using DOCK7-R1, -R2, or -R3 fragments cloned into pPC97 as baits in the PJ69a yeast reporter strain.

6.3 Cell culture and transfection/infection

HEK293, COS7, Neuro-2A, SK-N-BE and N1E115 cells were cultured in DMEM (Invitrogen) containing 10% fetal bovine serum (HyClone), 4 mM L-glutamine (Gibco BRL), 100 I.U./ml *penicillin* (Gibco BRL), and 100 μg/ml *streptomycin* (Gibco BRL). BaF3 cells were cultured in RPMI 1640 medium (Invitrogen) supplemented with 10% fetal bovine serum and 10% WEHI-3 conditioned medium as a source of interleulkin-3 (IL-3), kindly provided by Lab member J.Janas. Dissociated cortical progenitors were prepared from E12.5 or E13.5 cortices of CD1 mice embryos and cultured in Neurobasal medium (Gibco BRL) containing 20 ng/ml FGF2 (Promega), 10 ng/ml EGF, 2% B27 (v/v, Gibco BRL), 4 mM L-glutamine, 100 I.U./ml *penicillin*, and 100 μg/ml *streptomycin* as described[39]. HEK293 cells were transfected using the calcium phosphate co-precipitation method. COS7 cells were transfected using the transfection reagent Fugene 6 (Roche), as outlined by the manufacturer. Neuro-2A cells were infected with lentiviruses, which were generated as previously described[170]. SK-N-BE cells and dissociated cortical progenitors were transfected using the Amaxa Nucleofection system (Amaxa, Lonza) by

following manufacturer's instructions. 3-5 μg totals of the indicated plasmids were used per electroporation.

6.4 *In utero* electroporation and BrdU injections.

In utero electroporation was performed largely as described[41]. Specifically, a timed-pregnant CD1 mouse (Charles River) at 13.5 day of gestation was anesthetized by 2% Isoflurane and placed on a heating pad; the uterine horns were exposed by abdominal incision and rinsed with warm and sterilized phosphate-buffered saline (PBS). Plasmid DNA solution was prepared with molecular ratio for shRNA/cDNA constructs and pCA-EGFP plasmid at 5:1; and the final concentration of mixed DNA is 2μg/μl and is increased to 3μg/μl for simultaneous knockdown experiment. DNA solution was premixed with 0.1% non-toxic food dye, fast green (Sigma), allowed for the visualization of injection. Approximately 1 to 2 μl of plasmid DNA solution was injected manually into the lateral ventricles of each embryo using a pulled-glass, beveled and calibrated micropipette. The head of each embryo was placed between two 3mm custom-made tweezer electrode paddles, and five 50 ms pulses of 35 V with a 950 ms interval were delivered across the uterus (BTX, ECM830). After electroporation, the uterus was placed back in the abdominal cavity and the wound was surgically sutured (CP Medical, 493A Visorb® suture). For BrdU-labeling experiments, mouse embryos were electroporated at E13.5 and BrdU (150 mg per kg of body weight, Sigam B5002) was injected at E15.5. Animals were sacrificed at indicated time points following BrdU injection. All animal care protocols were approved by Cold Spring Harbor Laboratory.

6.5 Immunohistochemistry and immunocytochemistry.

For immunostaining of tissue sections, whole embryos (E9.5 and E10.5) or brains of embryos were fixed in 4% paraformaldehyde (PFA) in PBS for 1h at room temperature (RT; whole embryos) or overnight at 4°C (brains of embryos). Whole embryos and brains were

subjected to cyrosection or microtome section. For cyrosection, whole embryos and brains were cryoprotected in 30 % sucrose in PBS at 4°C for 12-24 h and cut, after embedding in Tissue-Tek O.C.T compound (Skura Finetek), into 16 μm thick coronal sections on a Leica CM3050S *cryostat. For microtome section, fixed brains were embedded in 3% low melting agarose and* sectioned into 40 μm thick coronal sections using a Vibratome (Leica VT1000S). Cyrostat sections (12 μm) were rehydrated in PBS at room temperature (RT) for 20 min and subjected to blocking and permeabilization as prepared for microtome sections. Brain sections were blocked and permeabilized with 10% normal goat serum (NGS) and 0.3% Triton X-100 in PBS for 1 h at RT, followed by incubation with primary antibodies diluted in 3% NGS and 0.2% Triton X-100 in PBS at 4°C overnight at concentrations indicated below.

For immunostaining of COS7, SK-N-BE, and dissociated neocortical cells, the cells were fixed for 4 min with 100% methanol at -20°C. Fixed cells were blocked and permeabilized with 10% normal goat serum (NGS) and 0.1% Triton X-100 in PBS for 10 min at RT, followed by incubation with primary antibodies diluted in 5% NGS/PBS at 4°C overnight at concentrations indicated below.

The following primary antibodies were used: anti-DOCK7[103] (rabbit, 1:500); anti-nestin (mouse, 1:200, Chemicon); anti-Tuj1 (mouse 1:1,500, Covance); anti-γ-tubulin (mouse, 1:2,000, Sigma); anti-GFP (chicken, 1:500 Aves Labs); anti-BrdU (rat, 1:500, AbD Serotec); anti-PH3 (rabbit, 1:1,000, Millipore); anti-Ki67 (rabbit, 1:250, Vector Laboratories); anti-Pax6 (rabbit, 1:500, Covance); anti-Tbr2 (rabbit, 1:300, Abcam); anti-RFP (rabbit, 1:500, Rockland); anti-pericentrin (mouse, 1:1,000, BD Biosciences); anti-TACC3 (mouse, 1:300, Santa Cruz); anti-α-tubulin (mouse, 1:2,000, Sigma); anti-ZO-1 (mouse, 1:100, Invitrogen); anti-GFAP (chicken, 1:500 Aves Labs). Of note, for BrdU staining, brain sections were incubated in 2N HCl solution for 30 min at 37°C to unmask the antigen, followed by a neutralization step with 0.1 M sodium tetraborate and three washes in PBS. Brain sections were also subjected to immunostaining

using primary antibodies against GFP due to its natural fluorescence was impaired by HCl treatment. For Pax6 and Tbr2 staining, brain sections were incubated in antigen retrieval solution (10% (V/V) glycerol in 10mM sodium citrate, pH 6.0) for 1 h at 65°C and allowed to cool down for 20 min at RT. Sections were permeabilized with 0.3% Triton X-100 in PBS for 30 min, quenched with 0.1M glycine-Tris pH7.4 for 30 min, and incubated with blocking solution (0.3% Trition X-100 and 0.2% gelatin in a 3:7 mixture of 1M NaCl and PBS) for 30min followed by incubation with anti-Pax6 or anti-Tbr2 antibody diluted in 3% NGS and 0.2% Triton X-100 in PBS[171].

The secondary antibodies used were: Alexa Fluor 488, 594, or 647 goat anti-mouse, rabbit, rat, or chicken (1:500 for immunohistochemistry and 1:1,000 for immunocytochemistry, Molecular Probes). Nuclei were counterstained with 0.3 µg/ml 4',6-diamidino-2-phenylindole (DAPI, Sigma) in PBS for 10 min. Of note, all brain slices were counterstained with DAPI; images depicting DAPI staining were not always included for reasons of clarity. Images of brain sections and cells were acquired using a spinning disk confocal microscope (Perkin-Elmer) with 20x, 40x (brain sections) or 60X (cells) objective.

6.6 Cell cycle analysis

Neuro-2A cells were infected with lentiviral vectors co-expressing EGFP and Dock7#2 shRNA (Dock7#2) or scr#1 shRNA (scr#1). Cells were harvested 3-4 days post-infection and a single-cell suspension was prepared in PBS buffer for each smaple. Cells were counted and re-suspended at 0.5-1 X 10^6 cells/ml. 1ml of cell suspension was added into a non-stick microfuge tube and fixed with 0.5% PFA overnight at 4°C. Cells were washed once with 1ml PBS containing 1%BSA and re-suspended with 1 ml ice-cold 75% ethanol in PBS overnight at 4°C. Cells were subjected to stain with 100µg/ml RNAse containing propidium iodide (50 µg/ml) for 30min at 37°C. Profiles of DNA content were then determined by flow cytometry analysis with the number of EGFP-positive cells in each phase of the cell cycle being quantified.

6.7 Slice culture and time-lapse imaging.

Time-lapse imaging of brain slices was largely performed as previously described[169]. In brief, mouse embryos at E13.5 were electroporated with plasmids expressing indicated shRNAs or cDNAs together with EGFP and mKO2-F expressing plasmids. The electroporated embryos were dissected 48 hours later in freshly made, 5% CO_2/ 95% O_2 bubbled and ice-cold artificial cerebral spinal fluid (ACSF: 125mM NaCl, 2.5mM KCl, 1 mM $MgCl_2$, 2mM $CaCl_2$, 1.25mMNaH_2PO_4, 25mM $NaHCO_3$, 25mM glucose. The solution would be approximately 310mOsm, pH7.4 after bubbling). Brains were isolated, embedded in 4% Low-melting agarose in ACSF and cut into 300 μm thick coronal slices using a Vibratom. Slices were transferred to a cell culture membrane insert (Millicell, 0.4μm pore size, 30 mm diameter) and incubated with slice culture medium (DMEM/F-12, 5% horse serum (v/v), 5% fetal bovine serum (v/v), N2 supplement (1:100, Invitrogen), B27 supplement without retinoic acid (1:50, Invitrogen), 100 U/ml penicillin/streptomycin, 10 ng/ml epidermal growth factor, and 10 ng/ml basic fibroblast growth factor) for about 3 hours at 37°C. Subsequently, slices were immersed in 200 μl of type Ia collagen (Cellmatrix, Nitta Gelatin) for 1 hour at 37°C, and inserts containing the slices were placed in a glass bottom microwell imaging dish (MatTek). The sample was observed with an inverted spinning disk confocal microscope (Perkin-Elmer) equipped with an environmental chamber (37°C, moisturized 5% CO_2). The brain regions in which there were EGFP/mKO2-F-expressing cell with complete radial glia morphology were imaged. The pictures were taken at 10 min intervals with 20–25 Z sections (4 μm intervals). The time-lapse data were assembled and analyzed by ImageJ (NIH) and Volocity software (Improvision).

6.8 GST pull-down assays, co-immunoprecipitation and Western blot analysis.

For GST pull-down assays, GST-TACC3 fusion protein and GST alone were expressed in BL21(DE3) bacteria strain and immobilized onto Glutathione-Sepharose beads (GE Healthcare Biosciences). Mouse E13.5 cortices and HEK293 cells expressing FLAG-DOCK7,

FLAG-DOCK7Δ513-812, FLAG-DOCK7Δ812-931, or FLAG-DOCK7Δ933-1164 fusion proteins, or empty control vector, were homogenized using Micropestles (Eppendorf) in lysis buffer (50 mM Tris pH 7.5, 1 % Triton X-100, 150 mM NaCl, 5% glycerol, 5 mM NaF, 1 mM Na_3VO_4 and protease inhibitors), centrifuged for 15 min, 4°C, 12,000g and the supernatants were collected. Equal amounts of total lysates were incubated with GST-TACC3 fusion protein or GST on a rocking plate for 1 hour at 4°C. The precipitates were washed four times with lysis buffer, resuspended and boiled in 2×SDS sample loading buffer. Immunoblots were probed with anti-DOCK7 or anti-FLAG polyclonal antibody (Sigma).

For co-immunoprecipitations, HEK293 cells expressing EGFP-TACC3 and FLAG-DOCK7, or empty control vector, were homogenized in lysis buffer. Total lysates were incubated with anti-FLAG M2-agarose beads (Sigma) overnight at 4°C. Beads were washed 6 times with lysis buffer. Immunoprecipitates were then resolved by SDS-PAGE and immunoblotted with anti-EGFP (Invitrogen) and anti-FLAG (Sigma) polyclonal antibodies.

For Western blots in Figure 2.3a, mouse cortices (E11-P3) were homogenized using Micropestles in 75 mM Tris-HCl (pH 6.8), 3.8% SDS, 4 M urea, and 20% glycerol and subjected to Western blot analysis with anti-DOCK7 antibody, and anti-γ-tubulin as a loading control. In Figure 2.4, mouse cortical progenitors transfected with indicated plasmids were homogenized using Micropestles in lysis buffer and subjected to Western blot analysis with anti-DOCK7 antibody, anti-FLAG polyclonal antibody. Anti-γ-tubulin antibody was also used as a loading control. In Figure 2.5, N1E 115 cells, BaF3 Cells, HEK-293 cells transfected with FLAG-DOCK6, FLAG-DOCK7 or FLAG-DOCK8 plasmids and mouse cortical progenitors transfected with Scr#1 or Dock7#2 plasmids were homogenized using Micropestles in lysis buffer and subjected to Western blot analysis with anti-DOCK7; anti-DOCK6 (rabbit, 1:1,000, MBL); and anti-DOCK8[123] (rabbit, 1:1,000, provided by P. Aspenström).

6.9 Analysis of microtubules (MTs).

COS7 cells transfected with indicated plasmids were fixed 2 days later with ice-cold 100% methanol for 5 min and immunostained with antibodies against EGFP and FLAG (to identify transfected cells) and α-tubulin (to visualize MTs), and counterstained with DAPI. For nocodazole treatment, COS7 cells were transfected with indicated constructs. Three days later, cells were incubated with 5 μg/ml nocodazole for 2 hours. Afterwards, nocodazole-containing medium were removed, washed with PBS buffer for 3 times and replaced with non-nocodazole normal medium. After a 5 min or a 20 min recovery period, cells were immediately fixed with ice-cold 100% methanol for 5 min and followed by immunostaning procedure described above. Images were acquired using a Perkin-Elmer spinning disk confocal microscope. The area of the MT aster emanating from the centrosome was measured using ImageJ software (NIH). Dissociated neocortical cells were prepared from E13.5 neocortices 1 day post-electroporation with indicated plasmids as described[76]. Cells were plated on coverslips precoated with poly-D-lysine (40 μg/ml) and laminin (2.5 μg/ml), and cultured for 2 day before fixation, immunostaining with antibodies against EGFP, RFP and α-tubulin, and counterstaining with DAPI. Confocal images were acquired and the area occupied by MT bundles around the nucleus was measured by ImageJ. Several *Z*-series confocal images of transfected cells were merged to show the entire MT "fork"-like structure.

6.10 Quantitative analysis of electroporated neocortices.

All the quantification studies were carried out on transfected cells localized within the dorsolateral cortex. To score images, the GFP or RFP channel was first judged independently, followed by judgments of the other markers. A total of 3-6 brain sections were analyzed per animal by taking up to three 10-20 μm *z* stack images to cover the electroporated VZ, SVZ and/or CP of each coronal section with a 20x or a 40x objective and comparing them with

equivalent sections in littermate counterparts. $BrdU^+$, $PH3^+$, $Ki67^+$, $Pax6^+$, $Tbr2^+$ or $Tuj1^+$ transfected cells were quantified using Volocity 6.0.1 software (Improvision). The number of $BrdU^+$ and/or $PH3^+$ or $Ki67^+$ transfected (EGFP- NLS^+ and/or RFP-NLS^+) cells within the VZ, and of $Pax6^+$ or $Tbr2^+$ transfected cells within the VZ and SVZ, were quantified and calculated as the percentage of total transfected cells. Note, for quantification of $Pax6^+$ and $Tbr2^+$ transfected cells, fluorescence intensities of $Pax6^+$ and $Tbr2^+$ were measured, and only cells with Pax6 or Tbr2 fluorescence intensity above the mean plus 1.5 times the standard deviation of background intensity were counted as $Pax6^+$ or $Tbr2^+$. Small puncta or signals that were not compliant with the EGFP-NLS^+ and/or RFP-NLS^+ nuclear labeling were ignored. Divisions at apical and basal positions were defined as those located less than and more than 20 μm, respectively, from the ventricular surface. Quantification of the distribution of transfected cells across the neocortical layers and of the number of transfected neurons were performed on single optical sections by quantifying all $EGFP^+$, and $EGFP^+$ $Tuj1^+$ cells, respectively, and dividing by the number of $EGFP^+$ cells in a radial stripe comprising all cortical layers. Transfected cells were scored as neurons only when Tuj1 immunostaining clearly surrounded a DAPI-positive nucleus in the $EGFP^+$ and/or RFP^+ cell. The interkinetic nuclear migration was measured by quantifying the number of $BrdU^+$ transfected cells in each bin, 15 min, 2 hour, 4 hour and 6 hour after a single BrdU injection (a bin was defined as a 20-μm-thick stripe parallel to the ventricle surface). The centrosome to nucleus distance in transfected RGCs was determined by measuring the distance from the centrosome to the lower edge of the nucleus. To measure the velocity of bl-to-ap nuclear migration, brain slices were imaged as previously described in time-lapse imaging section. The distance traveled by individual nuclei of transfected RGCs from the position at which they started migrating apically to the position where they reach the ventricular surface (control and Dock7#2 hp) or to the position where they divide (DOCK7) was measured with Volocity software. The change in apico-basal distance was

then divided by the time that each nucleus was imaged yielding an average velocity measurement of μm/hr.

6.11 Statistical analysis.

Data were presented as mean ± s.e.m. from at least three independent experiments. Direct comparisons were made using Student's *t*-test and multiple group comparisons were made using one-way analysis of variance (ANOVA). Statistical significance was defined as $P < 0.05$, 0.01 or 0.001 (indicated as *, ** or ***, respectively). P values ≥ 0.05 were considered not significant.

References

1. McConnell, S.K. Constructing the cerebral cortex: neurogenesis and fate determination. *Neuron* **15**, 761-768 (1995).
2. Gotz, M. & Huttner, W.B. The cell biology of neurogenesis. *Nature reviews. Molecular cell biology* **6**, 777-788 (2005).
3. Kriegstein, A., Noctor, S. & Martinez-Cerdeno, V. Patterns of neural stem and progenitor cell division may underlie evolutionary cortical expansion. *Nature reviews. Neuroscience* **7**, 883-890 (2006).
4. Rakic, P. Specification of cerebral cortical areas. *Science* **241**, 170-176 (1988).
5. Hosoya, T. Elucidating the brain's neural network. *Riken Research* **4**(2009).
6. Dehay, C. & Kennedy, H. Cell-cycle control and cortical development. *Nature reviews. Neuroscience* **8**, 438-450 (2007).
7. Nadarajah, B. & Parnavelas, J.G. Modes of neuronal migration in the developing cerebral cortex. *Nature reviews. Neuroscience* **3**, 423-432 (2002).
8. Malatesta, P., Hartfuss, E. & Gotz, M. Isolation of radial glial cells by fluorescent-activated cell sorting reveals a neuronal lineage. *Development* **127**, 5253-5263 (2000).
9. Noctor, S.C., Flint, A.C., Weissman, T.A., Dammerman, R.S. & Kriegstein, A.R. Neurons derived from radial glial cells establish radial units in neocortex. *Nature* **409**, 714-720 (2001).
10. Haubensak, W., Attardo, A., Denk, W. & Huttner, W.B. Neurons arise in the basal neuroepithelium of the early mammalian telencephalon: a major site of neurogenesis. *Proc Natl Acad Sci U S A* **101**, 3196-3201 (2004).
11. Noctor, S.C., Martinez-Cerdeno, V., Ivic, L. & Kriegstein, A.R. Cortical neurons arise in symmetric and asymmetric division zones and migrate through specific phases. *Nature neuroscience* **7**, 136-144 (2004).
12. Angevine, J.B., Jr. & Sidman, R.L. Autoradiographic study of cell migration during histogenesis of cerebral cortex in the mouse. *Nature* **192**, 766-768 (1961).
13. Marin-Padilla, M. Cajal-Retzius cells and the development of the neocortex. *Trends in neurosciences* **21**, 64-71 (1998).
14. Rakic, P. Mode of cell migration to the superficial layers of fetal monkey neocortex. *The Journal of comparative neurology* **145**, 61-83 (1972).
15. Kriegstein, A.R. & Noctor, S.C. Patterns of neuronal migration in the embryonic cortex. *Trends in neurosciences* **27**, 392-399 (2004).
16. Huttner, W.B. & Brand, M. Asymmetric division and polarity of neuroepithelial cells. *Current opinion in neurobiology* **7**, 29-39 (1997).
17. Bittman, K., Owens, D.F., Kriegstein, A.R. & LoTurco, J.J. Cell coupling and uncoupling in the ventricular zone of developing neocortex. *The Journal of neuroscience : the official journal of the Society for Neuroscience* **17**, 7037-7044 (1997).
18. Miyata, T. Development of three-dimensional architecture of the neuroepithelium: role of pseudostratification and cellular 'community'. *Development, growth & differentiation* **50 Suppl 1**, S105-112 (2008).

19. Chenn, A., Zhang, Y.A., Chang, B.T. & McConnell, S.K. Intrinsic polarity of mammalian neuroepithelial cells. *Molecular and cellular neurosciences* **11**, 183-193 (1998).
20. Latasa, M.J., Cisneros, E. & Frade, J.M. Cell cycle control of Notch signaling and the functional regionalization of the neuroepithelium during vertebrate neurogenesis. *The International journal of developmental biology* **53**, 895-908 (2009).
21. Sauer, F.C. Mitosis in the neural tube. *The Journal of comparative neurology* **62**, 337-405 (1935).
22. Willardsen, M.I. & Link, B.A. Cell biological regulation of division fate in vertebrate neuroepithelial cells. *Developmental dynamics : an official publication of the American Association of Anatomists* **240**, 1865-1879 (2011).
23. Taverna, E. & Huttner, W.B. Neural progenitor nuclei IN motion. *Neuron* **67**, 906-914 (2010).
24. Caviness, V.S., Jr., Takahashi, T. & Nowakowski, R.S. Numbers, time and neocortical neuronogenesis: a general developmental and evolutionary model. *Trends in neurosciences* **18**, 379-383 (1995).
25. Bentivoglio, M. & Mazzarello, P. The history of radial glia. *Brain research bulletin* **49**, 305-315 (1999).
26. Cameron, R.S. & Rakic, P. Glial cell lineage in the cerebral cortex: a review and synthesis. *Glia* **4**, 124-137 (1991).
27. Tamamaki, N., Nakamura, K., Okamoto, K. & Kaneko, T. Radial glia is a progenitor of neocortical neurons in the developing cerebral cortex. *Neuroscience research* **41**, 51-60 (2001).
28. Takahashi, T., Nowakowski, R.S. & Caviness, V.S., Jr. The leaving or Q fraction of the murine cerebral proliferative epithelium: a general model of neocortical neuronogenesis. *The Journal of neuroscience : the official journal of the Society for Neuroscience* **16**, 6183-6196 (1996).
29. Noctor, S.C., Martinez-Cerdeno, V. & Kriegstein, A.R. Distinct behaviors of neural stem and progenitor cells underlie cortical neurogenesis. *The Journal of comparative neurology* **508**, 28-44 (2008).
30. Miyata, T.*, et al.* Asymmetric production of surface-dividing and non-surface-dividing cortical progenitor cells. *Development* **131**, 3133-3145 (2004).
31. Attardo, A., Calegari, F., Haubensak, W., Wilsch-Brauninger, M. & Huttner, W.B. Live imaging at the onset of cortical neurogenesis reveals differential appearance of the neuronal phenotype in apical versus basal progenitor progeny. *PloS one* **3**, e2388 (2008).
32. Farkas, L.M. & Huttner, W.B. The cell biology of neural stem and progenitor cells and its significance for their proliferation versus differentiation during mammalian brain development. *Current opinion in cell biology* **20**, 707-715 (2008).
33. Miyata, T., Kawaguchi, D., Kawaguchi, A. & Gotoh, Y. Mechanisms that regulate the number of neurons during mouse neocortical development. *Current opinion in neurobiology* **20**, 22-28 (2010).
34. Manzini, M.C. & Walsh, C.A. What disorders of cortical development tell us about the cortex: one plus one does not always make two. *Current opinion in genetics & development* **21**, 333-339 (2011).
35. Walsh, C.A. Genetic malformations of the human cerebral cortex. *Neuron* **23**, 19-29 (1999).
36. Doe, C.Q. Neural stem cells: balancing self-renewal with differentiation. *Development* **135**, 1575-1587 (2008).
37. Johansson, P.A., Cappello, S. & Gotz, M. Stem cells niches during development--lessons from the cerebral cortex. *Current opinion in neurobiology* **20**, 400-407 (2010).
38. Konno, D.*, et al.* Neuroepithelial progenitors undergo LGN-dependent planar divisions to maintain self-renewability during mammalian neurogenesis. *Nature cell biology* **10**, 93-101 (2008).

39. Kim, W.Y.*, et al.* GSK-3 is a master regulator of neural progenitor homeostasis. *Nature neuroscience* **12**, 1390-1397 (2009).
40. Lange, C., Huttner, W.B. & Calegari, F. Cdk4/cyclinD1 overexpression in neural stem cells shortens G1, delays neurogenesis, and promotes the generation and expansion of basal progenitors. *Cell stem cell* **5**, 320-331 (2009).
41. Bultje, R.S.*, et al.* Mammalian Par3 regulates progenitor cell asymmetric division via notch signaling in the developing neocortex. *Neuron* **63**, 189-202 (2009).
42. Wang, X.*, et al.* Asymmetric centrosome inheritance maintains neural progenitors in the neocortex. *Nature* **461**, 947-955 (2009).
43. Schwamborn, J.C., Berezikov, E. & Knoblich, J.A. The TRIM-NHL protein TRIM32 activates microRNAs and prevents self-renewal in mouse neural progenitors. *Cell* **136**, 913-925 (2009).
44. Rakic, P. Less is more: progenitor death and cortical size. *Nature neuroscience* **8**, 981-982 (2005).
45. Costa, M.R., Wen, G., Lepier, A., Schroeder, T. & Gotz, M. Par-complex proteins promote proliferative progenitor divisions in the developing mouse cerebral cortex. *Development* **135**, 11-22 (2008).
46. Chenn, A. & Walsh, C.A. Regulation of cerebral cortical size by control of cell cycle exit in neural precursors. *Science* **297**, 365-369 (2002).
47. Lien, W.H., Klezovitch, O., Fernandez, T.E., Delrow, J. & Vasioukhin, V. alphaE-catenin controls cerebral cortical size by regulating the hedgehog signaling pathway. *Science* **311**, 1609-1612 (2006).
48. Cappello, S.*, et al.* The Rho-GTPase cdc42 regulates neural progenitor fate at the apical surface. *Nature neuroscience* **9**, 1099-1107 (2006).
49. Imai, F.*, et al.* Inactivation of aPKClambda results in the loss of adherens junctions in neuroepithelial cells without affecting neurogenesis in mouse neocortex. *Development* **133**, 1735-1744 (2006).
50. Zetterberg, A., Larsson, O. & Wiman, K.G. What is the restriction point? *Current opinion in cell biology* **7**, 835-842 (1995).
51. Cunningham, J.J. & Roussel, M.F. Cyclin-dependent kinase inhibitors in the development of the central nervous system. *Cell growth & differentiation : the molecular biology journal of the American Association for Cancer Research* **12**, 387-396 (2001).
52. Lukaszewicz, A.*, et al.* G1 phase regulation, area-specific cell cycle control, and cytoarchitectonics in the primate cortex. *Neuron* **47**, 353-364 (2005).
53. Lukaszewicz, A., Savatier, P., Cortay, V., Kennedy, H. & Dehay, C. Contrasting effects of basic fibroblast growth factor and neurotrophin 3 on cell cycle kinetics of mouse cortical stem cells. *The Journal of neuroscience : the official journal of the Society for Neuroscience* **22**, 6610-6622 (2002).
54. Glucksmann, A. Cell death in normal development. *Archives de biologie* **76**, 419-437 (1965).
55. Saunders, J.W., Jr. Death in embryonic systems. *Science* **154**, 604-612 (1966).
56. Thomaidou, D., Mione, M.C., Cavanagh, J.F. & Parnavelas, J.G. Apoptosis and its relation to the cell cycle in the developing cerebral cortex. *The Journal of neuroscience : the official journal of the Society for Neuroscience* **17**, 1075-1085 (1997).
57. Haydar, T.F., Kuan, C.Y., Flavell, R.A. & Rakic, P. The role of cell death in regulating the size and shape of the mammalian forebrain. *Cereb Cortex* **9**, 621-626 (1999).
58. Kuida, K.*, et al.* Decreased apoptosis in the brain and premature lethality in CPP32-deficient mice. *Nature* **384**, 368-372 (1996).
59. Kuida, K.*, et al.* Reduced apoptosis and cytochrome c-mediated caspase activation in mice lacking caspase 9. *Cell* **94**, 325-337 (1998).

60. Yang, X*., et al.* Notch activation induces apoptosis in neural progenitor cells through a p53-dependent pathway. *Developmental biology* **269**, 81-94 (2004).
61. Depaepe, V*., et al.* Ephrin signalling controls brain size by regulating apoptosis of neural progenitors. *Nature* **435**, 1244-1250 (2005).
62. Berger, J*., et al.* Conditional activation of Pax6 in the developing cortex of transgenic mice causes progenitor apoptosis. *Development* **134**, 1311-1322 (2007).
63. Artavanis-Tsakonas, S., Rand, M.D. & Lake, R.J. Notch signaling: cell fate control and signal integration in development. *Science* **284**, 770-776 (1999).
64. Justice, N.J. & Jan, Y.N. Variations on the Notch pathway in neural development. *Current opinion in neurobiology* **12**, 64-70 (2002).
65. Bergemann, A.D*., et al.* Ephrin-B3, a ligand for the receptor EphB3, expressed at the midline of the developing neural tube. *Oncogene* **16**, 471-480 (1998).
66. Klein, R. Eph/ephrin signaling in morphogenesis, neural development and plasticity. *Current opinion in cell biology* **16**, 580-589 (2004).
67. Meyer, E.J., Ikmi, A. & Gibson, M.C. Interkinetic nuclear migration is a broadly conserved feature of cell division in pseudostratified epithelia. *Current biology : CB* **21**, 485-491 (2011).
68. Del Bene, F., Wehman, A.M., Link, B.A. & Baier, H. Regulation of neurogenesis by interkinetic nuclear migration through an apical-basal notch gradient. *Cell* **134**, 1055-1065 (2008).
69. Grosse, A.S*., et al.* Cell dynamics in fetal intestinal epithelium: implications for intestinal growth and morphogenesis. *Development* **138**, 4423-4432 (2011).
70. Sauer, M.E. & Walker, B.E. Radioautographic study of interkinetic nuclear migration in the neural tube. *Proc Soc Exp Biol Med* **101**, 557-560 (1959).
71. Tamai, H*., et al.* Pax6 transcription factor is required for the interkinetic nuclear movement of neuroepithelial cells. *Genes to cells : devoted to molecular & cellular mechanisms* **12**, 983-996 (2007).
72. Chenn, A. & McConnell, S.K. Cleavage orientation and the asymmetric inheritance of Notch1 immunoreactivity in mammalian neurogenesis. *Cell* **82**, 631-641 (1995).
73. Miyata, T., Kawaguchi, A., Okano, H. & Ogawa, M. Asymmetric inheritance of radial glial fibers by cortical neurons. *Neuron* **31**, 727-741 (2001).
74. Murciano, A., Zamora, J., Lopez-Sanchez, J. & Frade, J.M. Interkinetic nuclear movement may provide spatial clues to the regulation of neurogenesis. *Molecular and cellular neurosciences* **21**, 285-300 (2002).
75. Ge, X., Frank, C.L., Calderon de Anda, F. & Tsai, L.H. Hook3 interacts with PCM1 to regulate pericentriolar material assembly and the timing of neurogenesis. *Neuron* **65**, 191-203 (2010).
76. Xie, Z*., et al.* Cep120 and TACCs control interkinetic nuclear migration and the neural progenitor pool. *Neuron* **56**, 79-93 (2007).
77. Schenk, J., Wilsch-Brauninger, M., Calegari, F. & Huttner, W.B. Myosin II is required for interkinetic nuclear migration of neural progenitors. *Proc Natl Acad Sci U S A* **106**, 16487-16492 (2009).
78. Reiner, O., Sapir, T. & Gerlitz, G. Interkinetic nuclear movement in the ventricular zone of the cortex. *Journal of molecular neuroscience : MN* **46**, 516-526 (2012).
79. Kosodo, Y. Interkinetic nuclear migration: beyond a hallmark of neurogenesis. *Cellular and molecular life sciences : CMLS* (2012).
80. Spear, P.C. & Erickson, C.A. Interkinetic nuclear migration: a mysterious process in search of a function. *Development, growth & differentiation* **54**, 306-316 (2012).
81. Tsai, J.W., Chen, Y., Kriegstein, A.R. & Vallee, R.B. LIS1 RNA interference blocks neural stem cell division, morphogenesis, and motility at multiple stages. *J Cell Biol* **170**, 935-945 (2005).

82. Kosodo, Y., *et al.* Regulation of interkinetic nuclear migration by cell cycle-coupled active and passive mechanisms in the developing brain. *The EMBO journal* **30**, 1690-1704 (2011).
83. Zhang, X., *et al.* SUN1/2 and Syne/Nesprin-1/2 complexes connect centrosome to the nucleus during neurogenesis and neuronal migration in mice. *Neuron* **64**, 173-187 (2009).
84. Tsai, J.W., Lian, W.N., Kemal, S., Kriegstein, A.R. & Vallee, R.B. Kinesin 3 and cytoplasmic dynein mediate interkinetic nuclear migration in neural stem cells. *Nature neuroscience* **13**, 1463-1471 (2010).
85. Gambello, M.J., *et al.* Multiple dose-dependent effects of Lis1 on cerebral cortical development. *The Journal of neuroscience : the official journal of the Society for Neuroscience* **23**, 1719-1729 (2003).
86. Cappello, S., Monzo, P. & Vallee, R.B. NudC is required for interkinetic nuclear migration and neuronal migration during neocortical development. *Developmental biology* **357**, 326-335 (2011).
87. Cote, J.F. & Vuori, K. Identification of an evolutionarily conserved superfamily of DOCK180-related proteins with guanine nucleotide exchange activity. *Journal of cell science* **115**, 4901-4913 (2002).
88. Meller, N., Merlot, S. & Guda, C. CZH proteins: a new family of Rho-GEFs. *Journal of cell science* **118**, 4937-4946 (2005).
89. Cote, J.F. & Vuori, K. GEF what? Dock180 and related proteins help Rac to polarize cells in new ways. *Trends in cell biology* **17**, 383-393 (2007).
90. Hasegawa, H., *et al.* DOCK180, a major CRK-binding protein, alters cell morphology upon translocation to the cell membrane. *Molecular and cellular biology* **16**, 1770-1776 (1996).
91. Kiyokawa, E., *et al.* Activation of Rac1 by a Crk SH3-binding protein, DOCK180. *Genes & development* **12**, 3331-3336 (1998).
92. Kiyokawa, E., Hashimoto, Y., Kurata, T., Sugimura, H. & Matsuda, M. Evidence that DOCK180 up-regulates signals from the CrkII-p130(Cas) complex. *The Journal of biological chemistry* **273**, 24479-24484 (1998).
93. Schmidt, A. & Hall, A. Guanine nucleotide exchange factors for Rho GTPases: turning on the switch. *Genes & development* **16**, 1587-1609 (2002).
94. Van Aelst, L. & D'Souza-Schorey, C. Rho GTPases and signaling networks. *Genes & development* **11**, 2295-2322 (1997).
95. Hoffman, G.R., Nassar, N. & Cerione, R.A. Structure of the Rho family GTP-binding protein Cdc42 in complex with the multifunctional regulator RhoGDI. *Cell* **100**, 345-356 (2000).
96. Schmidt, V.A., *et al.* IQGAP2 functions as a GTP-dependent effector protein in thrombin-induced platelet cytoskeletal reorganization. *Blood* **101**, 3021-3028 (2003).
97. Burridge, K. & Wennerberg, K. Rho and Rac take center stage. *Cell* **116**, 167-179 (2004).
98. Meller, N., Irani-Tehrani, M., Kiosses, W.B., Del Pozo, M.A. & Schwartz, M.A. Zizimin1, a novel Cdc42 activator, reveals a new GEF domain for Rho proteins. *Nature cell biology* **4**, 639-647 (2002).
99. Lin, Q., Yang, W., Baird, D., Feng, Q. & Cerione, R.A. Identification of a DOCK180-related guanine nucleotide exchange factor that is capable of mediating a positive feedback activation of Cdc42. *The Journal of biological chemistry* **281**, 35253-35262 (2006).
100. Miyamoto, Y., Yamauchi, J., Sanbe, A. & Tanoue, A. Dock6, a Dock-C subfamily guanine nucleotide exchanger, has the dual specificity for Rac1 and Cdc42 and regulates neurite outgrowth. *Experimental cell research* **313**, 791-804 (2007).
101. Hiramoto, K., Negishi, M. & Katoh, H. Dock4 is regulated by RhoG and promotes Rac-dependent cell migration. *Experimental cell research* **312**, 4205-4216 (2006).

102. Nishikimi, A.*, et al.* Zizimin2: a novel, DOCK180-related Cdc42 guanine nucleotide exchange factor expressed predominantly in lymphocytes. *FEBS letters* **579**, 1039-1046 (2005).
103. Watabe-Uchida, M., John, K.A., Janas, J.A., Newey, S.E. & Van Aelst, L. The Rac activator DOCK7 regulates neuronal polarity through local phosphorylation of stathmin/Op18. *Neuron* **51**, 727-739 (2006).
104. Yamauchi, J., Miyamoto, Y., Chan, J.R. & Tanoue, A. ErbB2 directly activates the exchange factor Dock7 to promote Schwann cell migration. *J Cell Biol* **181**, 351-365 (2008).
105. Kulkarni, K., Yang, J., Zhang, Z. & Barford, D. Multiple factors confer specific Cdc42 and Rac protein activation by dedicator of cytokinesis (DOCK) nucleotide exchange factors. *The Journal of biological chemistry* **286**, 25341-25351 (2011).
106. Yang, J., Zhang, Z., Roe, S.M., Marshall, C.J. & Barford, D. Activation of Rho GTPases by DOCK exchange factors is mediated by a nucleotide sensor. *Science* **325**, 1398-1402 (2009).
107. Brugnera, E.*, et al.* Unconventional Rac-GEF activity is mediated through the Dock180-ELMO complex. *Nature cell biology* **4**, 574-582 (2002).
108. Cote, J.F., Motoyama, A.B., Bush, J.A. & Vuori, K. A novel and evolutionarily conserved PtdIns(3,4,5)P3-binding domain is necessary for DOCK180 signalling. *Nature cell biology* **7**, 797-807 (2005).
109. Kanai, A.*, et al.* Identification of DOCK4 and its splicing variant as PIP3 binding proteins. *IUBMB life* **60**, 467-472 (2008).
110. Kunisaki, Y.*, et al.* DOCK2 is a Rac activator that regulates motility and polarity during neutrophil chemotaxis. *J Cell Biol* **174**, 647-652 (2006).
111. Lu, M.*, et al.* A Steric-inhibition model for regulation of nucleotide exchange via the Dock180 family of GEFs. *Current biology : CB* **15**, 371-377 (2005).
112. Laurin, M.*, et al.* The atypical Rac activator Dock180 (Dock1) regulates myoblast fusion in vivo. *Proc Natl Acad Sci U S A* **105**, 15446-15451 (2008).
113. Fukui, Y.*, et al.* Haematopoietic cell-specific CDM family protein DOCK2 is essential for lymphocyte migration. *Nature* **412**, 826-831 (2001).
114. Reif, K. & Cyster, J. The CDM protein DOCK2 in lymphocyte migration. *Trends in cell biology* **12**, 368-373 (2002).
115. Jiang, H.*, et al.* Deletion of DOCK2, a regulator of the actin cytoskeleton in lymphocytes, suppresses cardiac allograft rejection. *The Journal of experimental medicine* **202**, 1121-1130 (2005).
116. Chen, Q., Chen, T.J., Letourneau, P.C., Costa Lda, F. & Schubert, D. Modifier of cell adhesion regulates N-cadherin-mediated cell-cell adhesion and neurite outgrowth. *The Journal of neuroscience : the official journal of the Society for Neuroscience* **25**, 281-290 (2005).
117. Chen, Q.*, et al.* Loss of modifier of cell adhesion reveals a pathway leading to axonal degeneration. *The Journal of neuroscience : the official journal of the Society for Neuroscience* **29**, 118-130 (2009).
118. de Silva, M.G.*, et al.* Disruption of a novel member of a sodium/hydrogen exchanger family and DOCK3 is associated with an attention deficit hyperactivity disorder-like phenotype. *Journal of medical genetics* **40**, 733-740 (2003).
119. Yajnik, V.*, et al.* DOCK4, a GTPase activator, is disrupted during tumorigenesis. *Cell* **112**, 673-684 (2003).
120. Ueda, S., Fujimoto, S., Hiramoto, K., Negishi, M. & Katoh, H. Dock4 regulates dendritic development in hippocampal neurons. *Journal of neuroscience research* **86**, 3052-3061 (2008).
121. Vives, V.*, et al.* The Rac1 exchange factor Dock5 is essential for bone resorption by osteoclasts. *Journal of bone and mineral research : the official journal of the American Society for Bone and Mineral Research* **26**, 1099-1110 (2011).

122. Shaheen, R.*, et al.* Recessive mutations in DOCK6, encoding the guanidine nucleotide exchange factor DOCK6, lead to abnormal actin cytoskeleton organization and Adams-Oliver syndrome. *American journal of human genetics* **89**, 328-333 (2011).
123. Ruusala, A. & Aspenstrom, P. Isolation and characterisation of DOCK8, a member of the DOCK180-related regulators of cell morphology. *FEBS letters* **572**, 159-166 (2004).
124. Takahashi, K.*, et al.* Homozygous deletion and reduced expression of the DOCK8 gene in human lung cancer. *International journal of oncology* **28**, 321-328 (2006).
125. Griggs, B.L., Ladd, S., Saul, R.A., DuPont, B.R. & Srivastava, A.K. Dedicator of cytokinesis 8 is disrupted in two patients with mental retardation and developmental disabilities. *Genomics* **91**, 195-202 (2008).
126. Randall, K.L.*, et al.* Dock8 mutations cripple B cell immunological synapses, germinal centers and long-lived antibody production. *Nature immunology* **10**, 1283-1291 (2009).
127. Zhang, Q.*, et al.* Combined immunodeficiency associated with DOCK8 mutations. *The New England journal of medicine* **361**, 2046-2055 (2009).
128. Lambe, T.*, et al.* DOCK8 is essential for T-cell survival and the maintenance of CD8+ T-cell memory. *European journal of immunology* **41**, 3423-3435 (2011).
129. Kuramoto, K., Negishi, M. & Katoh, H. Regulation of dendrite growth by the Cdc42 activator Zizimin1/Dock9 in hippocampal neurons. *Journal of neuroscience research* **87**, 1794-1805 (2009).
130. Gadea, G., Sanz-Moreno, V., Self, A., Godi, A. & Marshall, C.J. DOCK10-mediated Cdc42 activation is necessary for amoeboid invasion of melanoma cells. *Current biology : CB* **18**, 1456-1465 (2008).
131. Yelo, E.*, et al.* Dock10, a novel CZH protein selectively induced by interleukin-4 in human B lymphocytes. *Molecular immunology* **45**, 3411-3418 (2008).
132. Van Aelst, L. Two-hybrid analysis of Ras-Raf interactions. *Methods Mol Biol* **84**, 201-222 (1998).
133. Daub, H., Gevaert, K., Vandekerckhove, J., Sobel, A. & Hall, A. Rac/Cdc42 and p65PAK regulate the microtubule-destabilizing protein stathmin through phosphorylation at serine 16. *The Journal of biological chemistry* **276**, 1677-1680 (2001).
134. Wittmann, T., Bokoch, G.M. & Waterman-Storer, C.M. Regulation of microtubule destabilizing activity of Op18/stathmin downstream of Rac1. *The Journal of biological chemistry* **279**, 6196-6203 (2004).
135. Yamauchi, J.*, et al.* The atypical Guanine-nucleotide exchange factor, dock7, negatively regulates schwann cell differentiation and myelination. *The Journal of neuroscience : the official journal of the Society for Neuroscience* **31**, 12579-12592 (2011).
136. Tabata, H. & Nakajima, K. Efficient in utero gene transfer system to the developing mouse brain using electroporation: visualization of neuronal migration in the developing cortex. *Neuroscience* **103**, 865-872 (2001).
137. Borrell, V., Yoshimura, Y. & Callaway, E.M. Targeted gene delivery to telencephalic inhibitory neurons by directional in utero electroporation. *Journal of neuroscience methods* **143**, 151-158 (2005).
138. Ayala, R., Shu, T. & Tsai, L.H. Trekking across the brain: the journey of neuronal migration. *Cell* **128**, 29-43 (2007).
139. Gupta, A., Tsai, L.H. & Wynshaw-Boris, A. Life is a journey: a genetic look at neocortical development. *Nature reviews. Genetics* **3**, 342-355 (2002).
140. Mochida, G.H. & Walsh, C.A. Genetic basis of developmental malformations of the cerebral cortex. *Archives of neurology* **61**, 637-640 (2004).
141. Solecki, D.J., Govek, E.E., Tomoda, T. & Hatten, M.E. Neuronal polarity in CNS development. *Genes & development* **20**, 2639-2647 (2006).
142. Tsai, L.H. & Gleeson, J.G. Nucleokinesis in neuronal migration. *Neuron* **46**, 383-388 (2005).

143. Tewari, M.*, et al.* Yama/CPP32 beta, a mammalian homolog of CED-3, is a CrmA-inhibitable protease that cleaves the death substrate poly(ADP-ribose) polymerase. *Cell* **81**, 801-809 (1995).
144. Scholzen, T. & Gerdes, J. The Ki-67 protein: from the known and the unknown. *Journal of cellular physiology* **182**, 311-322 (2000).
145. Gotz, M., Stoykova, A. & Gruss, P. Pax6 controls radial glia differentiation in the cerebral cortex. *Neuron* **21**, 1031-1044 (1998).
146. Englund, C*., et al.* Pax6, Tbr2, and Tbr1 are expressed sequentially by radial glia, intermediate progenitor cells, and postmitotic neurons in developing neocortex. *The Journal of neuroscience : the official journal of the Society for Neuroscience* **25**, 247-251 (2005).
147. Takahashi, T., Nowakowski, R.S. & Caviness, V.S., Jr. Cell cycle parameters and patterns of nuclear movement in the neocortical proliferative zone of the fetal mouse. *The Journal of neuroscience : the official journal of the Society for Neuroscience* **13**, 820-833 (1993).
148. Still, I.H., Vince, P. & Cowell, J.K. The third member of the transforming acidic coiled coil-containing gene family, TACC3, maps in 4p16, close to translocation breakpoints in multiple myeloma, and is upregulated in various cancer cell lines. *Genomics* **58**, 165-170 (1999).
149. Gergely, F*., et al.* The TACC domain identifies a family of centrosomal proteins that can interact with microtubules. *Proc Natl Acad Sci U S A* **97**, 14352-14357 (2000).
150. Piekorz, R.P*., et al.* The centrosomal protein TACC3 is essential for hematopoietic stem cell function and genetically interfaces with p53-regulated apoptosis. *The EMBO journal* **21**, 653-664 (2002).
151. Gergely, F., Draviam, V.M. & Raff, J.W. The ch-TOG/XMAP215 protein is essential for spindle pole organization in human somatic cells. *Genes & development* **17**, 336-341 (2003).
152. Peset, I. & Vernos, I. The TACC proteins: TACC-ling microtubule dynamics and centrosome function. *Trends in cell biology* **18**, 379-388 (2008).
153. Tanaka, T*., et al.* Lis1 and doublecortin function with dynein to mediate coupling of the nucleus to the centrosome in neuronal migration. *J Cell Biol* **165**, 709-721 (2004).
154. Barenz, F., Mayilo, D. & Gruss, O.J. Centriolar satellites: busy orbits around the centrosome. *European journal of cell biology* **90**, 983-989 (2011).
155. Thornton, G.K. & Woods, C.G. Primary microcephaly: do all roads lead to Rome? *Trends in genetics : TIG* **25**, 501-510 (2009).
156. Ishizuka, K*., et al.* DISC1-dependent switch from progenitor proliferation to migration in the developing cortex. *Nature* **473**, 92-96 (2011).
157. Blasius, A.L*., et al.* Mice with mutations of Dock7 have generalized hypopigmentation and white-spotting but show normal neurological function. *Proc Natl Acad Sci U S A* **106**, 2706-2711 (2009).
158. Minobe, S*., et al.* Rac is involved in the interkinetic nuclear migration of cortical progenitor cells. *Neuroscience research* **63**, 294-301 (2009).
159. Liu, X., Hashimoto-Torii, K., Torii, M., Ding, C. & Rakic, P. Gap junctions/hemichannels modulate interkinetic nuclear migration in the forebrain precursors. *The Journal of neuroscience : the official journal of the Society for Neuroscience* **30**, 4197-4209 (2010).
160. Jeng, J.C., Lin, Y.M., Lin, C.H. & Shih, H.M. Cdh1 controls the stability of TACC3. *Cell Cycle* **8**, 3529-3536 (2009).
161. Kornblum, H.I., Yanni, D.S., Easterday, M.C. & Seroogy, K.B. Expression of the EGF receptor family members ErbB2, ErbB3, and ErbB4 in germinal zones of the developing brain and in neurosphere cultures containing CNS stem cells. *Developmental neuroscience* **22**, 16-24 (2000).
162. Zhao, C., Deng, W. & Gage, F.H. Mechanisms and functional implications of adult neurogenesis. *Cell* **132**, 645-660 (2008).
163. Wurdak, H*., et al.* A small molecule accelerates neuronal differentiation in the adult rat. *Proc Natl Acad Sci U S A* **107**, 16542-16547 (2010).

164. Schneider, L*., et al.* TACC3 depletion sensitizes to paclitaxel-induced cell death and overrides p21WAF-mediated cell cycle arrest. *Oncogene* **27**, 116-125 (2008).
165. Hsieh, J. Orchestrating transcriptional control of adult neurogenesis. *Genes & development* **26**, 1010-1021 (2012).
166. Scharfman, H.E. & Hen, R. Neuroscience. Is more neurogenesis always better? *Science* **315**, 336-338 (2007).
167. Rodriguiz, R.M. & Wetsel, W.C. Assessments of Cognitive Deficits in Mutant Mice. in *Animal Models of Cognitive Impairment* (eds. Levin, E.D. & Buccafusco, J.J.) (Boca Raton (FL), 2006).
168. Tokui, M*., et al.* Intramuscular injection of expression plasmid DNA is an effective means of long-term systemic delivery of interleukin-5. *Biochem Biophys Res Commun* **233**, 527-531 (1997).
169. Shitamukai, A., Konno, D. & Matsuzaki, F. Oblique radial glial divisions in the developing mouse neocortex induce self-renewing progenitors outside the germinal zone that resemble primate outer subventricular zone progenitors. *The Journal of neuroscience : the official journal of the Society for Neuroscience* **31**, 3683-3695 (2011).
170. Janas, J., Skowronski, J. & Van Aelst, L. Lentiviral delivery of RNAi in hippocampal neurons. *Methods in enzymology* **406**, 593-605 (2006).
171. Arai, Y*., et al.* Neural stem and progenitor cells shorten S-phase on commitment to neuron production. *Nature communications* **2**, 154 (2011).